Francisella Tularensis infection uncovers a link between neutrophil metabolism and apoptosis

Krysa, Samantha Jo

Krysa, S. J. (2022). Francisella Tularensis infection uncovers a link between neutrophil metabolism and apoptosis [University of Iowa]. https://doi.org/10.25820/etd.006524

FRANCISELLA TULARENSIS INFECTION UNCOVERS A LINK BETWEEN NEUTROPHIL METABOLISM AND APOPTOSIS

by

Samantha Jo Krysa

A thesis submitted in partial fulfillment
of the requirements for the
Doctor of Philosophy
degree in Biomedical Science (Molecular Medicine) in the
Graduate College of
The University of Iowa

August 2022

Thesis Committee: Lee-Ann H. Allen, Thesis Advisor
Jason Barker
Anil Chauhan
Hasem Habelhah
Matthew Potthoff

To my espresso machine and Fluoxetine. None of this would've been possible without either.

“If you want sense, you’ll have to make it yourself.”
Norton Juster
The Phantom Tollbooth

ACKNOWLEDGMENTS

My proudest achievement isn't the PhD itself, but the incredible community of colleagues, mentors, scientists, and friends I have built during my time in Iowa and beyond. I can't wait to support you all in your future accomplishments, and I hope that you will continue to support me as well. I would first like to thank my advisor, Dr. Lee-Ann Allen, for everything she has done to make me the scientist that I am today. Thank you for introducing me to the coolest cells ever (neutrophils!! More on them later!!) and for entrusting me with a project that taught me so many new things and enabled me to learn so many cool techniques. Thank you for taking me to so many scientific conferences and introducing me to so much cool science and amazing scientists, I am so grateful for all the opportunities you have given me. I truly would not be even half the scientist I am today without you. I would also like to thank the members, past and present, of the Allen lab. You made my time in lab a true joy and I will greatly miss working with all of you. Having you all by my side down in the trenches of the day-to-day lab work made me love coming to work and I am so grateful for how much you all contributed to my development as a scientist and a good lab citizen. To Allan Prichard, I'm so glad we joined the lab together, and that you have become one of my best friends. To Kara Wuchter, thank you for always helping me draw blood at my crazy timepoints, for always being there for me, and for being such a great listener. To Stephanie Silva-Del Toro, thank you for being my comps editor, lab mentor, shoulder to cry on and FRIEND! To Adam Fitzsimmons, thank you for always being your positive, wholesome, Dad vibin' self, and for being my espressBRO AKA my go-to contact for all things espresso-related. To Lisa Khuu, thank you for making the lab such a fun place to be and for always being down to go for boba. To Sydney, thank you for carrying on the Franny T torch!! I could not think of a better, or more capable scientist for the job. To Dr. Laura Whitmore, for

helping me brainstorm about my project and for being a wonderful role model in the lab. To Dr. Lauren Kinkead, for passing your *Francisella* knowledge on to me and for helping me get my project off the ground. I also want to thank Dr. Mary Wilson and the members of her laboratory for so graciously taking me in following Lee-Ann's move to Missouri. Thank you for adopting me and for providing additional mentorship, community and support during the final two years of my graduate work.

To my crazy, amazing family: thank you for letting me be such a smart, opinionated, independent, weird little girl, and for enabling me to grow up to be such a smart, opinionated, independent, weird woman. Mom and Dad, thank you for always supporting my education and career goals, and for helping me move all over the Midwest for the last 10 years. Thank you for the words of encouragement, the motivational Dunkin Donuts gift cards, the many wonderful family meals, and your inexhaustible, unflinching support. To Brini, I am so lucky to have a sister who is also my best friend. In many ways, you were more of a big sister to me than I was to you because I have always depended on you and admired your strength. Thank you for bringing me McDonald's on the weekend when I'm too tired (lol), for always visiting me, for listening to me, for letting me vent, and for being my best friend. Thank you, Mom, Dad and Brini for always being happy for me and proud of me throughout my accomplishments in life. I also want to thank my extended family, grandparents, and all my partner's family for their endless support these past 5 years, as well. I love you all and thank you all for everything you have done and continue to do for me.

I must also recognize all the wonderful friends I have made during my time in Iowa. To my Super Science Sisters™, Gillian, Lucy and Gabby, this PhD really put us through it in some *unexpected* ways, and the trials and tribulations of this process were only possible because you

were all there for me. From the late-night homework sessions during our first year, the monumental stress of our comprehensive exams, the losses, the failures, the wins, the happy hours, the EVERYTHING, you were all there by my side, making my awful days bearable and my amazing days that much more amazing. I am so proud of all of you, and I love you so much. To my Dungeons and Dragons group, Anthony, Chris, Chandler, Allan and Derek, thank you for being the biggest nerds I have ever met (and probably ever will meet) and for not judging the actions of the incredibly cursed and evil characters I always build (I hope I haven't increased the frequency of your nightmares too much these past several years). Thank you for being the funniest, weirdest, craziest group of murder hobos I could ever hope to be a part of (and apologies to the imaginary village of Tia for the fire damage you suffered at our hands). To my high school and college friends, Ashlee, Hannah, Gio, Emma, Christina (aka Tina), Hask and Lauren, thank you for your continual friendship and love and support. I feel so lucky and overcome with gratitude that I have been friends with y'all for 10-20+ years (can you believe?!).

I would also like to thank my committee for their guidance, feedback, and mentorship. I hope that I will become a scientist that you will be proud to call your mentee. I also owe a huge thanks to the University of Iowa Inflammation program. Thank you for providing such an enriching, collaborative environment for me to learn and grow. I would especially like to thank Sonya Pugh for being such a great administrator and advocate for me. You significantly improved the quality of my lab life by always ensuring that we got our reagents, reimbursements, and any other administrative thing you could think of on time. I can't wait to see your annual Halloween decorations for many years to come!

Finally, I must also thank my two rocks in life: my cat, Medusa, and my partner, Derek. I can't picture my time here in Iowa without these 2 by my side, and I cannot thank them enough

for being there for me every day (I know it's odd to be including Medusa in this section so prevalently when she clearly will not be reading this, but these are my acknowledgements and I want to acknowledge her!). Derek, I marvel at the life we are building together every day, and while it is bittersweet that we are bringing our Iowa chapter to a close, I can't wait to see where life takes us next. Anytime I feel anxious about the future, just remembering that you will be there by my side makes me feel at ease. Thank you for supporting me in achieving my career goals, thank you for listening to me, thank you for being goofy and making me laugh, thank you for just being there with me through all my low days, thank you for letting me be my skeptical, cynical self, while also showing me the beauty in optimism, thank you for adding so much joy to my life, thank you. I love and appreciate you so much.

Thank you all.

ABSTRACT

Francisella tularensis is the etiological agent of tularemia, one of the most infectious pathogens known and one of few pathogens capable of infecting host neutrophils (polymorphonuclear leukocytes; PMNs). PMNs are vital innate immune cells that undergo constitutive apoptosis 24 hours after entering circulation, and disruption of this tightly regulated process leads to an impaired immune response that is incapable of resolving infection. Our laboratory discovered that *Francisella tularensis* delays human PMN apoptosis by inhibiting the intrinsic, extrinsic, and phagocytosis-induced cell death pathways, but the mechanisms by which this is achieved are not fully understood.

We demonstrate here that metabolic reprogramming of neutrophils, including induction of glycolysis, is an important and previously unappreciated aspect of neutrophil longevity. Specifically, our data indicate that *Francisella*-infected PMNs released significantly more lactate and upregulated expression of genes encoding glucose transporters and 10 of 11 glycolytic enzymes. Direct measurements made using a Seahorse XF analyzer demonstrate that glycolysis (measured as the extracellular acidification rate) nearly quadrupled, and glycolytic capacity doubled by 12 hours after *Francisella* infection. Inhibition of glycolysis or glucose uptake using 2-deoxy-D-glucose or WZB-117 blocked the ability of *Francisella tularensis* to delay PMN apoptosis, thus confirming that these processes are mechanistically linked. Intriguingly, *Francisella*-infected PMNs also contained significantly more glycogen than their uninfected counterparts. Furthermore, inhibition of glycogen breakdown with the glycogen phosphorylase inhibitor CP-91149 was sufficient to delay uninfected PMN apoptosis and significantly enhanced the apoptosis delay in *Francisella*-infected PMNs. Finally, we show that treating PMNs with the

pan-caspase inhibitor Q-VD-OPH not only caused delayed apoptosis, but also significantly upregulated glycolysis and glycogen content, further supporting the hypothesis that PMN metabolism and lifespan are fundamentally linked.

p38 mitogen-associated protein kinase (MAPK) and class IA phosphoinositide-3 kinase (PI3K) influence PMN lifespan in a stimulus-specific manner, and also have established roles as glycolytic regulators. Our laboratory demonstrated that inhibition of p38 MAPK or PI3K signaling blocks *Francisella*-mediated apoptosis delay, and we hypothesize that *Francisella*-mediated glycolytic upregulation is mechanistically linked to extension of PMN lifespan by host p38 MAPK and PI3K signaling.

PUBLIC ABSTRACT

Many kinds of bacteria invade the human body every day and the immune system protects the body against infection or illness from these bacteria. The immune system is composed of various types of cells, and one important cell type for preventing infections is the neutrophil. Neutrophils are on the front lines defending the body, meaning they are one of the first cells to recognize invading bacteria. Neutrophils eat and kill the bacteria with toxic compounds, and once they have fulfilled this function, neutrophils die and are subsequently eaten by another type of immune cell, the macrophage. Macrophages consume neutrophils after they die to prevent the toxic compounds contained inside neutrophils from leaking out and damaging the body's tissues.

However, some bacteria that are eaten by neutrophils are able to avoid being killed, which prevents neutrophils from fulfilling their function, ultimately preventing the neutrophils from dying and hindering resolution of the infection. *Francisella tularensis* is one of few bacteria capable of blocking neutrophil function, preventing neutrophils from dying, surviving and hiding inside neutrophils to avoid detection from other immune cells.

We believe that infection with *Francisella tularensis* may be changing how certain components inside the neutrophil are interacting with each other, a process referred to as "signaling". We also believe that infection changes neutrophil metabolism, and the combined changes in signaling and metabolism are extending neutrophil lifespan. The goal of this research is to understand how *Francisella tularensis* prevents neutrophils from dying by examining how the signaling and metabolism inside the neutrophil changes following infection. This work establishes that signaling and metabolism are both altered in neutrophils infected with *Francisella tularensis*, and these changes are required for the neutrophils to be able to live

longer. These data provide insight into the mechanism by which *Francisella*-infected neutrophils evade death, and are among some of the first to establish that neutrophil metabolism and lifespan are intimately linked.

TABLE OF CONTENTS

LIST OF TABLES

LIST OF FIGURES

LIST OF ABBREVIATIONS

1,5AG: 1,5-anhydroglucitol

1,5AGP: 1,5-anhydroglucitol-6-phosphate

2-DG: 2-Deoxy-D-Glucose

3-MPA: 3-Mercaptopicolinic acid

3PO: 3-(3-pyridinyl)-1-(4-pyridinyl)-2-propen-1-one

6-PGD: 6-Phosphogluconate dehydrogenase

6PGLS: 6-phosphogluconolactonase

A1: BCL2-related protein A1

A20: Tumor necrosis factor-α-induced protein 3

AEBSF: 4-(2-Aminoethyl)benzenesulfonyl fluoride hydrochloride

ALDOA: Aldolase

AKT: Akt strain transforming, also known as protein kinase B

ANOVA: Analysis of variance

APC: Allophycocyanin

ASCT2: Neutral amino acid transporter 2

ATP: Adenosine triphosphate

AV: Annexin-V

BCA: Bicinchoninic assay

BCL2: B-cell lymphoma 2

BHI: Brain heart infusion

BLP: Bacterial lipoprotein

BSL-2: Biosafety level 2

BSL-3: Biosafety level 3

C5a: Complement component 5a

CA: Chlorogenic acid

CD: Cluster of differentiation

CDC: Centers for Disease Control and Prevention

cDNA: Complementary deoxyribonucleic acid

cFLIP: FLICE-like inhibitory protein

CHAB: Cysteine heart agar supplemented with 9% defibrinated sheep blood

cIAP2: Inhibitor of apoptosis protein 2

cIAP3: Inhibitor of apoptosis protein 3

CM: Conditioned media

CREB: Cyclic AMP response element-binding protein

CXCL8: Chemokine (C-X-C motif) ligand 8, also known as IL-8

ddH_2O: Double distilled water

DMSO: Dimethyl sulfoxide

DNA: Deoxyribonucleic acid

DPBS: Dulbecco's phosphate buffered saline

ECAR: Extracellular acidification rate

EDTA: Ethylenediaminetetraacetic acid

EEA-1: Early endosome antigen-1

ENO1: Enolase 1

ERK: Extracellular signal-regulated kinase

FACS: flow cytometry staining

Fas: First apoptosis signal

FasL: Fas ligand

FATP2: Fatty acid transport protein 2

FITC: Fluorescein isothiocyanate

fMLF: N-Formyl-L-methionyl-L-leucyl-L-phenylalanine

F-6-P: Fructose-6-phosphate

FPI: *Francisella* pathogenicity island

FSC: Forward scatter

Ft: *Francisella tularensis*

G-6-P: Glucose-6-phosphate

G6PDH: Glucose-6-phosphate dehydrogenase

G6PT: Glucose-6-phosphate translocase

Ga3P: Glyceraldehyde-3-phosphate

GADD45B: Growth arrest and DNA-damage-inducible beta

GAPDH: Glyceraldehyde-3-phosphate dehydrogenase

GBE1: Glycogen branching enzyme 1

GC-MS: Gas chromatography-mass spectrometry

G-CSF: Granulocyte colony-stimulating factor

GLUT: Glucose transporter

GM-CSF: Granulocyte-macrophage colony-stimulating factor

GMI: Geometric mean intensity

GPCR: G-protein coupled receptor

GPI: Glucose-6-phosphate isomerase

GSK3β: Glycogen synthase kinase 3 β

GYS1: Glycogen synthase 1

HBSS: Hank's balanced salt solution

HEPES: N-2-hydroxyethylpiperazine-N-2-ethane sulfonic acid

HIF: Hypoxia-inducible factor

HK2: Hexokinase-2

HMS: Hexose monophosphate shunt

hpi: Hours post infection

HRP: Horse radish peroxidase

HSP27: Heat shock protein 27

HTRA2: Serine protease HTRA2 mitochondrial

IKK: IkB (inhibitor of nuclear factor kappa B) kinase

IL: Interleukin

IMS: Inner membrane space

iPMN: Infected neutrophil

JNK: c-Jun N-terminal kinase

KEGG: Kyoto Encyclopedia of Genes and Genomes

kg: Kilogram

LAMP-1: Late endosome membrane protein-1

LDH/LDHA: Lactate dehydrogenase

LPS: Lipopolysaccharide

LTB4: Leukotriene B4

LVS: Live vaccine strain

mAb: Monoclonal antibody

MAPK: Mitogen-activated protein kinase

MCL1: Myeloid leukemia 1

MCL-1: Induced myeloid leukemia differentiation protein

MEK: Mitogen-activated protein kinase kinase

MFI: Mean fluorescence intensity

MIP: Macrophage inflammatory protein

MK2: MAP kinase-activated protein kinase 2

MKK: Dual specificity mitogen-activated protein kinase kinase

MMP: Matrix metalloproteinase

MnSOD: Manganese-dependent superoxide dismutase

MOI: Multiplicity of infection

MPC: Mitochondrial pyruvate carrier

mRNA: messenger ribonucleic acid

MSK: Ribosomal protein S6 kinase alpha-5

mTOR: Mammalian target of rapamycin

NADPH: Nicotinamide adenine dinucleotide phosphate, reduced form

NET: Neutrophil extracellular trap

NF-kB: Nuclear factor kappa B

NF-kB AI: NF-kB activation inhibitor

NP-40: Nonidet P-40

OD_{600}: Optical density measured at 600 nm

OMM: Outer mitochondrial membrane

pAb: Polyclonal antibody

PAMP: Pathogen-associated molecular pattern

PBMC: Peripheral blood mononuclear cell

PDK1: 3-phoshoinositide dependent protein kinase-1

PE: Phycoerythrin

PFKFB3: 6-phosphofructo-2-kinase/fructose-2,6-bisphosphatase

PFKFB4: 6-Phosphofructo-2-Kinase/Fructose-2,6-Biphosphatase 4

PFK/PFKL: Phosphofructokinase

PGK1: Phosphoglycerate kinase 1

PGM: phosphoglucomutase

PI: Propidium iodide

PI3K: Phosphoinositide-3-kinase

PICD: Phagocytosis-induced cell death

PIK3CA: Phosphatidylinositol-4,5-bisphosphate 3-kinase catalytic subunit alpha

PIM2: Proto-oncogene serine/threonine kinase-2

PKC: Protein kinase C

PKM2: Pyruvate kinase M2

PMN: Polymorphonuclear leukocyte; neutrophil

PMSF: Phenylmethanesulfonyl fluoride

PPP: Pentose phosphate pathway

PS: Phosphatidylserine

qRT-PCR: Quantitative reverse transcriptase polymerase chain reaction

Rac: Ras-related C3 botulinum toxin substrate

RNA: Ribonucleic acid

ROS: Reactive oxygen species

RPIA: Ribose-5-phosphate isomerase

RPMI-1640: Roswell Park Memorial Institute medium 1640

RSK: Ribosomal s6 kinase

RT: Room temperature

SDS-PAGE: Sodium dodecyl sulfate polyacrylamide gel electrophoresis

SEM: Standard error of the mean

SILAC: Stable isotope labelling with amino acids in cell culture

SMAC: Second mitochondria-derived activator of caspases

SSC: Side scatter

ssp: Subspecies

TAN: Tumor-associated neutrophil

TCA cycle: Tricarboxylic acid cycle

TGFβ: Transforming growth factor beta

TIGAR: TP53 Induced Glycolysis Regulatory Phosphatase

TLR: Toll-like receptor

TNF: Tumor necrosis factor

TPI1: Triosephosphate Isomerase 1

UGP2: UDP-glucose pyrophosphorylase 2

UQCRB: Ubiquinol-cytochrome c reductase binding protein

VDAC: Voltage-dependent anion channel

VEGF: Vascular endothelial growth factor

WHO: World Health Organization

wt: Wild-type

XIAP: X-Linked Inhibitor Of Apoptosis

CHAPTER 1: INTRODUCTION

Francisella tularensis

Francisella tularensis is a Gram-negative, intracellular coccobacillus and the causative agent of the zoonotic disease tularemia (1). *Francisella tularensis* was initially identified in ground squirrels in Tulare County, California (from which the pathogen's name is partially derived) in 1911 and described as a "plague-like illness", while the first human infection with this pathogen was reported in 1914 (2-4). Initially named *Bacterium tularense*, Dr. Edward Francis was the first to characterize the clinical presentation of infection with this organism and ultimately named the disease tularemia (1). The organism was designated a genus of its own in 1947, *Francisella*, to honor the innumerable contributions to our understanding of tularemia symptoms, epidemiology, and clinical features by Dr. Francis (5).

Francisella tularensis is one of three known species within the *Francisella* genus and comprises three subspecies: *tularensis*, *holarctica* and *mediastatica* (6-8) though subspecies *mediastatica* is seldom studied due to its relatively low virulence and the extreme rarity of human infections by this subspecies (6, 8). *Francisella tularensis* subspecies (ssp) *tularensis* (type A) is almost completely restricted to North America, while *Francisella tularensis* ssp *holarctica* (type B) is distributed throughout the entire Northern Hemisphere (6, 7). Type A organisms require biosafety level 3 (BSL-3) containment, are the most virulent, with fewer than 10 bacteria being sufficient to cause life-threatening illness, and underlie the majority of lethal cases of tularemia. Type B organisms are less virulent, incurring milder infections that are seldom fatal, though the type B strain still requires BSL-3 containment (9). A commonly studied, human-attenuated strain of *Francisella tularensis* ssp *holarctica* is the live vaccine strain (LVS)

(9). Despite its name, LVS has not been approved for use as a vaccine in the United States because its exact mode of attenuation is unknown (10). Developed by the former Soviet Union and obtained by the United States in the 1950s, LVS induces many of the same phenotypes as the fully virulent organisms in cell culture and is safe to use in a BSL-2 laboratory (10, 11). As such, LVS has become a widely studied model organism for tularemia research.

Francisella infects a remarkably broad range of hosts including over 200 species of mammals, fish, birds, amoebae, ticks and other arthropod vectors (1, 12-14). While ticks act as a permanent reservoir for *Francisella tularensis* in the environment, rabbits are a prominent source of human infection, garnering tularemia the nickname "rabbit fever" (15). Humans have proven to be highly vulnerable to tularemia, despite being considered accidental hosts of *Francisella tularensis*, with human outbreaks often mirroring outbreaks in other animals (16). Those most at risk include landscapers, farmers, hunters, butchers, and any other individuals in frequent contact with potentially infected wildlife or insects.

Francisella is transmitted to humans most frequently through direct contact with the tissues or bodily fluids of an infected animal or being bitten by an infected arthropod vector (13). This results in ulceroglandular tularemia, which comprises ~80% of the clinical manifestations of the disease (13). Individuals suffering from ulceroglandular tularemia typically present with an ulcer at the infection site and bacteria can disseminate to, and causes extensive swelling of, the draining lymph nodes (17). While ulceroglandular tularemia is not the most immediately dangerous manifestation of this infection, bacterial egress from the lymph nodes can occur in untreated infections, allowing the bacteria to enter the circulation and disseminate to the lungs, spleen, and liver. Transmission can also occur through ingestion of meat from an infected animal, or other contaminated food or fluids, which causes oropharyngeal tularemia. Entry

through the eyes via contaminated fluid is also a possible route of transmission and results in oculoglandular tularemia, though both oropharyngeal and oculoglandular tularemia are less common. The most dangerous mode of infection is entry through the respiratory route, where inhalation of as few as 10 aerosolized Type A organisms can culminate in a rapidly fatal pneumonic tularemia, with mortality rates nearing 60% in untreated infections (13, 17, 18). Pneumonic tularemia features rapid expansion of the pulmonary infection followed by bacterial dissemination to the spleen and liver, with patients usually succumbing to significant damage to their lung tissue (1, 18, 19). However, lethality and clinical presentation of tularemia is contingent on the infective strain and transmission route, and the average mortality rate for all cases of untreated tularemia is 5-15% (1).

The capacity of type A *Francisella tularensis* to cause rapid onset of severe disease, combined with its highly infectious nature and ability to aerosolize and enter via the respiratory route make it a potential candidate for bioweapon development. Several countries, Japan, the former Soviet Union, and the United States weaponized *Francisella tularensis* during the Cold War, with the Soviet Union reportedly continuing *Francisella* bioweapon development well into the 1990s (20). It is estimated that release of 50 kg of dried *Francisella tularensis* over a metropolitan area containing 5 million people would culminate in approximately 250,000 cases of disease and nearly 20,000 deaths, as assessed by the World Health Organization (WHO) (20). The United States Centers for Disease Control and Prevention (CDC) estimate that the economic burden of an attack with *Francisella tularensis* would cost over $5 billion per 100,000 people exposed (9). As such, the CDC have classified virulent strains of *Francisella tularensis* as Tier 1 Select Agents, a classification reserved for potential bioweapons.

Modern tularemia research has focused primarily on vaccine development, but there is still much to learn about the etiological agent, *Francisella tularensis*, particularly its immune evasion strategies, and this work seeks to address that gap in understanding. *Francisella tularensis* wields a devastating potential that demands our further understanding to mitigate the threat of fatal disease and to guide tularemia vaccine development.

Francisella tularensis can infect neutrophils, macrophages, dendritic cells, epithelial cells, and the intracellular lifecycle of this organism in each cell type is similar, though this process has mostly been studied in human and murine macrophages (21-25). These studies established that *Francisella*-containing phagosomes appear to successfully start the digestion process as they recruit early endosome antigen 1 (EEA1), late endosome membrane protein (LAMP)-1 and CD63 (cluster of differentiation 63) (21-23, 25). However, assembly of the nicotinamide adenine dinucleotide phosphate (NADPH) oxidase is impaired, severely limiting production of reactive oxygen species (ROS) (26, 27). Furthermore, *Francisella*-containing phagosomes fail to acquire the vacuolar proton ATPase and lysosomal enzymes, preventing sufficient acidification of the phagosome. In fact, these phagosomes are typically only acidified to pH 6.7, which is incidentally the approximate optimal pH for growth of *Francisella tularensis*, though there is no evidence indicating that this organism can replicate within the phagosome. This effectively precludes phagosome maturation, trafficking to lysosomes, and ultimately elimination of the bacteria. *Francisella* then escapes from the phagosome, though the process of phagosomal egress is still not well understood, and replicates in the cytosol (21-23, 25). Several genes in the *Francisella* pathogenicity island (FPI), *iglI* and *iglJ*, and their regulators MigR and FevR, have been identified as required for phagosomal escape and intracellular replication (28-32). *Francisella tularensis* replicates tremendously in macrophages and epithelial cells, though

macrophages are infected more frequently and are the typical replicative niche (13). One notable aspect of the infection strategy of *Francisella tularensis* is that it is one of extremely few pathogens capable of infecting and parasitizing neutrophils (**Figure 1**).

Neutrophils

Neutrophils, also known as polymorphonuclear leukocytes (PMNs), comprise the majority of white blood cells in human circulation, with the body producing approximately 100 billion neutrophils each day (33, 34). Truly a professional phagocyte, neutrophils are incredibly adept at recognizing and eliminating a wide variety of pathogens (35). Almost immediately following infection, neutrophils sense chemotactic factors produced by the host and/or invading organism, extravasate from the bloodstream towards the infection source, and are usually the first immune cell to reach the infection (33, 36). Neutrophils contain a vast repertoire of antipathogen armaments including ROS produced by the NADPH oxidase, antimicrobial peptides, and cytotoxic granules, which empower neutrophils to be incredibly efficient at killing and degrading an array of microbes (35, 37). Within seconds of pathogen binding, neutrophils undergo a powerful respiratory burst and mobilize their granules against the microbe; one feature of many that distinguishes neutrophils from other immune cells.

Another distinctive feature of neutrophils is their short, tightly-regulated lifespan. Approximately 24 hours after entering circulation, neutrophils undergo constitutive (spontaneous) apoptosis wherein they are inherently programmed to die, and strict control of neutrophil turnover is fundamental to disease resolution, as well as maintenance of homeostasis (38). Phagocytosis prompts neutrophils to die earlier than they are programmed to, in a process known

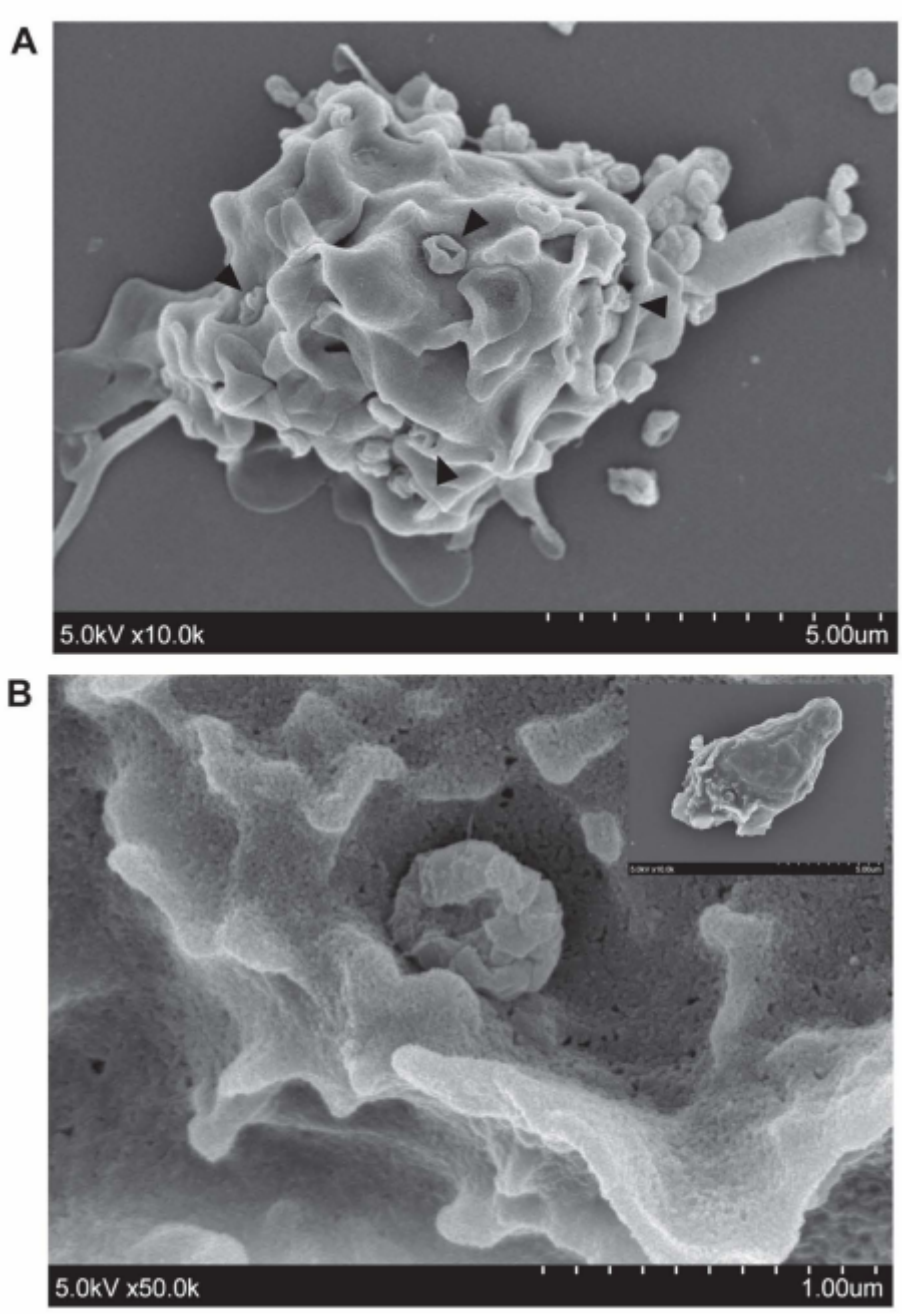

Figure 1. *Francisella tularensis* is one of few pathogens capable of infecting neutrophils.

Scanning electron micrograph of *Francisella tularensis*-infected neutrophils 24 hours post infection (hpi). **(A)** Arrowheads emphasize several associated bacteria. **(B)** One bacterium being engulfed by the neutrophil. Inset: view of the whole neutrophil. Images captured by Dr. Lauren Kinkead in the Allen laboratory.

as phagocytosis-induced cell death (PICD) (39). PICD is a complex pathway that precipitates downregulation of proinflammatory factors to prevent the release of cytotoxic components from the neutrophil and ultimately promotes the clearance of spent neutrophils by macrophages and homeostasis restoration.

Neutrophil apoptosis

Neutrophil fate decisions occur when the balance of apoptosis regulators shifts in favor of either the pro-apoptotic factors or the anti-apoptotic factors. This shift is regulated by intracellular signaling and global transcriptional changes referred to as an “apoptosis differentiation program" (40-42). The onset of apoptosis is distinguished by specific morphological and biochemical changes including accumulation of externalized phosphatidylserine on the plasma membrane, nuclear condensation, DNA fragmentation, membrane blebbing and fragmentation into apoptotic bodies. Neutrophils employ three main cell death mechanisms: PICD, the extrinsic apoptosis pathway, and the intrinsic apoptosis pathway, which all rely on varying combinations of caspase-3, caspase-8 and caspase-9 activity (39). As mentioned, phagocytic events typically precipitate neutrophil death in a process known as PICD, wherein expression of the proapoptotic protein, BAX, increases and the surge in NADPH oxidase-derived ROS promotes release of cathepsins from granules, which activate caspase-8 (41, 43-46). Extracellular signals, such as FasL or TNF, activate the extrinsic apoptosis pathway via formation of receptor signaling complexes which leads to caspase-8 activation (44, 45). Mitochondria are a key regulator of neutrophil lifespan, as they mediate both PICD and the intrinsic apoptosis pathway. Mitochondrial apoptosis is also linked to the extrinsic pathway by tBID for essential amplification in PMNs. Permeabilization of the outer mitochondrial membrane

(OMM) is an early apoptotic event that is thought to irrevocably commit cells to apoptosis (38, 47, 48). OMM pores are formed when oligomerized BAX is activated by tBID at the mitochondria, enabling BAX to insert into the OMM (49). The generation of OMM pores disrupts mitochondrial membrane potential and allows for release of cytochrome c and other proapoptotic proteins which trigger caspase-9 activation. It is critical that neutrophil apoptosis is tightly controlled spatially and temporally in order to effectively eliminate infection in a manner that limits discharge of cytotoxic components and minimizes destruction of host tissues (42, 50, 51). Disruption of neutrophil turnover promotes tissue necrosis and aberrant inflammation that serves to sustain, rather than eradicate, the infection (43, 51).

Modulation of neutrophil lifespan during *Francisella tularensis* infection

Infection resolution generally follows the same general steps wherein neutrophils are rapidly mobilized to the infection site where they phagocytose the invading pathogen, kill and degrade the microbe intracellularly, undergo cell death, and are subsequently cleared by macrophages (**Figure 2**) (52). Strict control of this process is critical for resolution of disease and disruption of any of these steps can derail the inflammatory response. Of particular importance are pathogen killing and the timely progression of neutrophils through the appropriate cell death pathway. It is nearly impossible for pathogens to avoid death by neutrophils, but some have evolved mechanisms enabling them to not only avoid intracellular killing, but to also escape the phagosome, replicate intracellularly and manipulate neutrophil lifespan (53, 54). Several pathogens that achieve this are *Coxiella burnetii*, *Chlamydia pneumoniae*, *Leishmania major*, *Anaplasma phagocytophilum*, and *Francisella tularensis*. Each pathogen subverts neutrophil apoptosis via a distinct mechanism involving modulation of host apoptosis regulators and at least

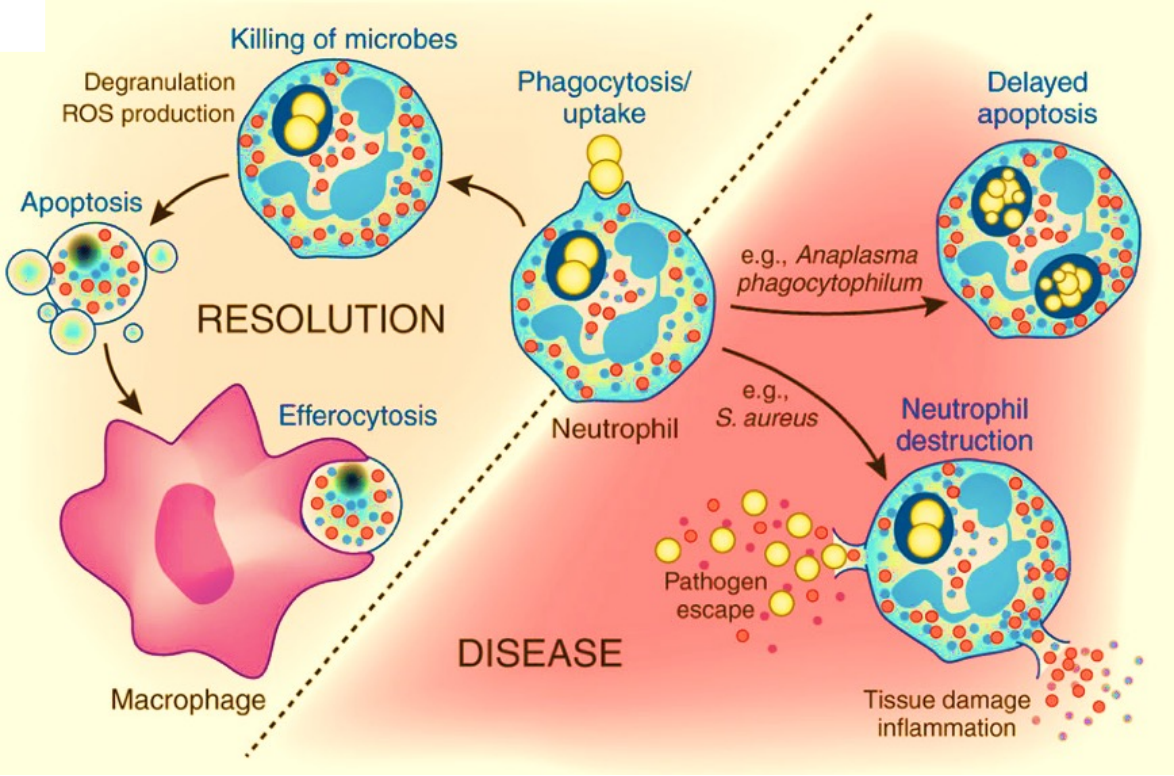

Figure 2. Neutrophil-pathogen interactions and outcomes.

Infection resolution depends on phagocytosis, intracellular killing of microbes using reactive oxygen species (ROS) and granule components, neutrophil apoptosis, and subsequent clearance of dead neutrophils by macrophages. Pathogen subversion of this process can manipulate neutrophil lifespan leading to neutrophil destruction, pathogen escape and dissemination. Alternatively, delay of neutrophil apoptosis provides a potential replication site for pathogens and results in an accumulation of infected neutrophils. Manipulation of neutrophil lifespan in either direction promotes tissue damage, inflammation, and exacerbated disease. Reprinted under Creative Commons license from Rigby et al 2012 (52).

one survival signaling pathway, but the outcome is similar in that it enables all these pathogens to replicate freely while remaining relatively hidden from other immune cells (53, 54).

As mentioned, *Francisella tularensis* is one such pathogen capable of dysregulating neutrophil apoptosis pathways, effectively extending neutrophil lifespan and rendering the neutrophils dysfunctional (55). Studies by our laboratory have revealed that *Francisella tularensis*-infected neutrophils exhibit significant decreases in the processing, activation and activity of caspase-3, caspase-8, and caspase-9 (56). These data, combined with the discovery that assembly of the NADPH oxidase at *Francisella*-containing phagosomes is blocked, effectively inhibiting PICD, established that all three cell death pathways in neutrophils are inhibited by this infection. We have also observed that *Francisella*-infected neutrophils feature increased mitochondrial stabilization, sustained mitochondrial membrane potential and organelle integrity, which are mediated by downregulation of *BAX* mRNA, decreased BAX translocation to mitochondria and diminished BID processing to tBID (57, 58). Beyond pro- and anti-apoptosis factors, neutrophil cell death is governed by coordinated changes in gene expression which comprise an "apoptosis differentiation program" (36, 40, 41). Our work has demonstrated that *Francisella tularensis* LVS reshapes the transcriptional landscape of infected neutrophils during the first 24 hours of infection, ultimately manipulating the expression of ~3,500 neutrophil genes, 365 of which are involved in apoptosis and survival (59). Upregulated among these genes were *BIRC3* and *BIRC4*, which encode the anti-apoptotic proteins cIAP2 (baculoviral IAP repeat-containing protein 3) and XIAP (X-linked inhibitor of apoptosis protein), respectively (57). These proteins promote survival by inhibiting caspases and XIAP, which specifically inhibits caspase-3 and caspase-9, is the strongest caspase inhibitor found in neutrophil cytosol (60). Calpain is a lysosomal cysteine protease that degrades XIAP during apoptosis, however *Francisella tularensis*

also hinders calpain through upregulation of *CAST*, which encodes calpastatin, an endogenous inhibitor of calpain (57, 58). A final notable change observed in *Francisella*-infected neutrophils is the sustained expression of MCL-1 (57, 58). MCL-1 promotes neutrophil survival by binding to BAX to prevent the formation of pores in the outer mitochondrial membrane (OMM), and continual expression of MCL-1 is a requirement of neutrophil survival (46, 61). Intriguingly, *MCL1* gene expression is reduced in *Francisella*-infected neutrophils and the mechanisms by which MCL-1 protein levels are maintained have yet to be determined (57).

The role of neutrophils in tularemia pathogenesis

Tight regulation of neutrophil lifespan is vital for homeostasis maintenance and resolution of disease (36, 37). As *Francisella tularensis* aberrantly extends neutrophil lifespan, accumulation of infected neutrophils at the nidus is a prominent feature of tularemia (62). Studies of non-human primates infected with *Francisella tularensis* aerosols in the 1970s demonstrated that neutrophils contribute to host tissue destruction and tularemia progression (63-67). Neutrophils were highly abundant in the lungs, which culminated in the presence of necrotic debris, and granulomas comprising infected neutrophils and viable bacteria (63-67). In mouse models of pulmonary *Francisella* infection, alveolar macrophages are the most highly infected cell type on day one, but by day three the majority of infected cells are neutrophils (68, 69). Matrix metalloproteinase-9 (MMP9) has been identified as a key mediator of leukocyte recruitment during *Francisella* infection, and induction of this protease correlates with increased bacterial burden, more predominant histopathology characterized by neutrophil infiltration, increased morbidity, and increased mortality (62). Notably, loss of MMP9 in mice effectively blocked neutrophil migration into the lungs following aerosol infection with *Francisella*

tularensis, which enhanced host resistance to the infection and improved morbidity and mortality of the mice (62). Complementary experiments were also done demonstrating that conditions which induce neutrophilia significantly exacerbate tularemia severity (70, 71). Similar data were obtained from rabbits and rats infected with *Francisella tularensis* (72), and these animals, as well as many humans, succumb to pneumonic infections with *Francisella tularensis* (64, 67). This high mortality rate can be attributed, in part, to the overwhelming accumulation of infected neutrophils in the airway, precipitating the release of cytotoxic components, the presence of necrotic debris, and immense host tissue damage, which can lead to death so quickly, it often occurs before the adaptive immune cells are able to mobilize against the infection (69, 73, 74). In fact, the overwhelming necrosis of infected tissues that characterizes tularemia directly correlates to neutrophil density. These data taken together highlight that neutrophils contribute distinctly to tularemia disease progression, rather than conferring protection to the host.

Immunometabolism & the metabolic control of neutrophil function

Immunometabolism is a rapidly expanding field of study, which seeks to understand how metabolism regulates immune cell function. Improving our understanding of how immune cells fuel effective responses, and how their metabolic pathways may be reprogrammed during infection or other disease states, could provide new avenues for therapeutic intervention. While immunometabolism research has increased remarkably in recent years, most studies have focused on T lymphocytes and macrophages, and the few that have investigated neutrophil metabolism utilized murine neutrophils, which are metabolically quite different from mature, human neutrophils (75-81).

Seminal studies by Niels Borregaard established neutrophils as metabolically distinctive due to their reliance on glycolysis for ATP generation (82). Since then, the other major metabolic pathways in mature, human neutrophils that have been identified are the tricarboxylic acid (TCA) cycle, the pentose phosphate pathway (PPP), fatty acid oxidation and synthesis, and glycogen metabolism (**Figure 3**) (75-79, 83, 84). Interestingly, developing, immature neutrophils rely primarily on oxidative phosphorylation for energy production, but following maturation and release into circulation, human neutrophils perform very little oxidative phosphorylation (76, 77). While glycolysis yields much fewer ATP than oxidative phosphorylation, glycolysis occurs approximately 100 times more quickly than oxidative phosphorylation, and thus can ultimately generate more ATP at a faster rate (85, 86). In neutrophils, which must rapidly expend huge portions of their energy stores to fuel immune responses, glycolysis allows for faster ATP production. Glycolysis is also a more advantageous mode of energy production from a competition standpoint, as glycolysis-using cells will more rapidly consume glucose from the environment, effectively starving and outcompeting cells which rely on oxidative phosphorylation (85). In addition to the thermodynamic advantages, glycolysis endows cells with a degree of flexibility, in that it enables cells to produce ATP in the absence of oxygen (87). Neutrophils must survive and function in varying nidi, in which oxygen and nutrient availability are unreliable, and glycolysis empowers these cells to be a flexible and competitive component of the immune response. Further metabolic flexibility is imparted on neutrophils by their ability to access three separate pools of glucose: 1) extracellular glucose, 2) cytosolic glycogen, a branched glucose polymer surrounding a glycogenin core, and 3) glucose-6-phosphate stored in the endoplasmic reticulum.

However, in certain disease contexts, such as cancer, neutrophils are metabolically

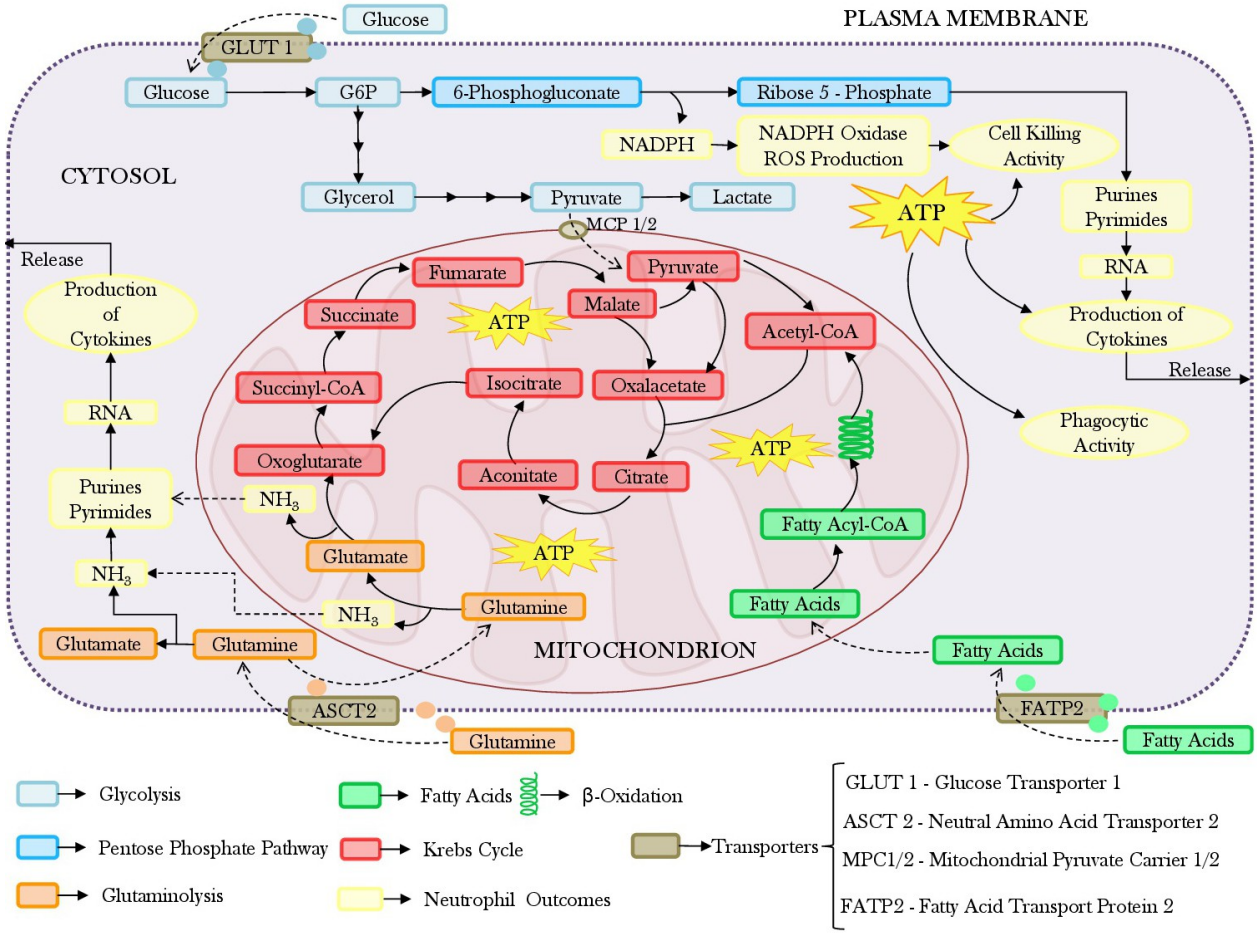

Figure 3. The major metabolic pathways in human neutrophils.

Reprinted under Creative Commons license from Curi et al 2020 (76).

adapted, and metabolic alterations have significant effects on neutrophil function which directly impact disease progression (88). Tumor-associated neutrophils (TANs) exhibit a more immature phenotype, which is demonstrated in part by their reliance on oxidative phosphorylation and renders the cells functionally incapable of resolving the disease (88). Emerging evidence suggests that shifts in neutrophil metabolism are stimulus- and context-dependent, with at least seven distinctive metabolic states described thus far: 1) immature, bone marrow-localized neutrophils and tumor-associated neutrophils, 2) mature PMNs under homeostasis, 3) migrating neutrophils, 4) canonically-activated neutrophils, 5) neutrophils undergoing degranulation, 6) NET-releasing neutrophils, and 7) apoptosing neutrophils (77, 78, 88, 89). Specifically, immature and tumor-associated PMNs rely on fatty acid oxidation, TCA cycle and oxidative phosphorylation, whereas resting mature cells utilize glycolysis and actively phagocytosing cells activate glycogenolysis. Glycolysis and mitochondrial purinergic signaling fuel chemotaxis, while NET formation requires glycolysis and PPP. Canonical activation is characterized by glycolysis, glycogenolysis, PPP, TCA and glutaminolysis, and apoptosing cells selectively downregulate glycolysis and glycogenesis (42, 77, 78). These studies highlight metabolism as a key regulator of neutrophil function, but there is a lack of data evaluating the role of neutrophil metabolism as a regulator of neutrophil lifespan.

Summary

Francisella tularensis is one of few pathogens capable of surviving neutrophil killing and one aspect of this pathogen's infection strategy is inhibition of neutrophil apoptosis. While this phenotype has been extensively characterized by our laboratory, the mechanisms by which *Francisella*-infected neutrophils are able to commandeer the highly conserved, tightly-regulated

pathways that dictate neutrophil survival to ultimately evade death are unclear. *Francisella tularensis* infection causes global changes in the neutrophil transcriptome, including dysregulation of over 800 metabolism-associated genes, but the role of neutrophil metabolism during infection has barely been explored (59). It is established that neutrophil lifespan and function are intimately linked, but the role of metabolism in regulating lifespan or is unknown. In addition to being distinctly short-lived, human neutrophils are also metabolically unique in that they rely primarily on glycolysis for energy production (76-78, 82). Thus, it is attractive to predict that infection with *Francisella tularensis* may reprogram neutrophil metabolism, and that metabolic reprogramming may be linked to the observed apoptosis delay. The research described herein will advance our understanding of neutrophil metabolism and determine the role of metabolism in regulation of neutrophil lifespan.

Hypothesis and specific aims

The research described herein endeavored to characterize the metabolic and signaling reprogramming that occurs in human neutrophils following infection with *Francisella tularensis*. This work sought to advance previous findings from our laboratory, which established that *Francisella* infection significantly delays neutrophil apoptosis, but the mechanism by which these cells commandeer the strictly regulated pathways governing cell lifespan are not fully characterized. We hypothesize that *Francisella*-infected neutrophils feature reprogramming of their metabolism, which promotes induction of survival signaling and subsequent extension of neutrophil lifespan. This research will establish, for the first time, a comprehensive understanding of the kinetics and mechanisms of metabolic reprogramming of human neutrophils infected with *Francisella tularensis*. These studies will also determine the role of metabolism in regulation of neutrophil lifespan. This work will have a broad impact by improving our comprehension of, and ultimately our capacity to treat, inflammatory diseases characterized by dysregulation of neutrophil apoptosis. This thesis comprises the following specific aims:

I. Determine the pro-survival signaling pathways required for apoptosis inhibition in human neutrophils infected with *Francisella tularensis*.

II. Characterize the metabolic reprogramming of human neutrophils infected with *Francisella tularensis*.

III. Define the extent to which metabolic reprogramming of human neutrophils contributes to apoptosis inhibition.

CHAPTER 2: NEUTROPHIL SURVIVAL SIGNALING DURING *FRANCISELLA TULARENSIS* INFECTION

Introduction

Neutrophils are critical innate immune cells that are among the first cells recruited to a site of an infection. These cells comprise the majority of the white blood cells in circulation and are turned over on the order of 10^{11} cells per day (34). Notably, these phagocytes are essential for innate host defense and utilize a combination of ROS, antimicrobial peptides, and proteolytic enzymes to kill invading microorganisms (35).

Neutrophils have an intrinsically short lifespan of less than 24 hours in the bloodstream and undergo constitutive apoptosis, an active, tightly regulated form of cell death that is essential for homeostasis (49, 54, 90). Various stimuli can alter the rate of constitutive apoptosis including cytokines, microbial molecular patterns, and phagocytosis (37, 54). In particular, phagocytosis and ROS production typically accelerate neutrophil cell death and lead to efficient engulfment of dying cells by macrophages (52). Not only does this process aid in pathogen elimination, it also reprograms macrophages to a pro-resolving, anti-inflammatory phenotype that is essential for resolution of the inflammatory response (37, 52).

Neutrophil apoptosis occurs when the levels of numerous proapoptotic factors outweigh the levels of antiapoptotic factors in the cell. Constitutive apoptosis is governed by the intrinsic pathway, and at the core of this pathway are mitochondria. Outer mitochondrial membrane (OMM) permeabilization is one of the early events in the intrinsic apoptotic pathway (54) and is mediated by two major proapoptotic factors of the BCL-2 family, BAX and BAK. These proteins oligomerize and insert into the OMM, thus disrupting membrane potential and mediating release

of inner membrane space (IMS) proteins cytochrome *c*, Smac, and HtrA2 which initiate apoptosis via caspase-9 and the apoptosome (54, 59). Antiapoptotic factors such as MCL-1 and A1 prevent OMM disruption and are present in excess in healthy neutrophils but diminish in abundance as cells age (54, 91). Additional regulation is mediated by cellular inhibition of apoptosis proteins such XIAP, which acts downstream of mitochondria and inhibits caspase-9 and caspase-3 by direct binding (92).

To avert apoptosis, neutrophils must receive one or more survival cues that are robust enough to sustain an excess of pro-survival/antiapoptotic regulators that control cell lifespan. The major pro-survival pathways in neutrophils are overlapping and interconnected and include signaling cascades mediated by phosphoinositide 3-kinase (PI3K)/AKT, MEK/ERK and p38 MAP kinases (MAPKs) and NF-κB which are differentially activated by growth factors, ligation of β2 integrins, inflammatory mediators such as IL-8 and C5a and microbial products and pathogens (60, 90, 92).

Several pathogenic microbes have evolved strategies to circumvent neutrophil antimicrobial mechanisms and promote neutrophil survival to maintain a site for replication and immune evasion inside the host (53, 54). This group of pathogens includes, but is not restricted to, *Anaplasma phagocytophilum*, *Chlamydia pneumoniae*, *Leishmania major* and *Coxiella burnetii*. Each of these microbes utilizes a specific mechanism of apoptosis inhibition that involves manipulation of anti-apoptosis regulators and one or more of the survival signaling cascades (54, 93-97).

Francisella tularensis is a Gram-negative, facultative intracellular bacterium and the causative agent of the zoonosis tularemia. *F. tularensis,* subspecies *tularensis* (type A), and subspecies *holarctica* (type B) differ in geographic distribution and account for nearly all human

infections with this organism (20). Inhalation of as few as ten bacteria can result in a severe bronchopneumonia that is coupled to bacterial dissemination to the liver, spleen and other organs and has a mortality rate of approximately 30-60% if untreated (98). *F. tularensis* utilizes a variety of strategies to modulate the innate immune response and its effectors and infects several cell types, including macrophages and neutrophils (55). We demonstrated previously that both type A and type B *F. tularensis* strains modulate the major apoptotic pathways in neutrophils and significantly delay apoptosis (56, 58, 59). This delay involves inhibition of caspase processing and activation and sustained mitochondrial membrane integrity that coincides with impaired BAX translocation, and increased expression of genes encoding antiapoptotic factors such as XIAP, A20, FLIP, cIAP2 and calpastatin (56, 58, 59).

Despite prior studies, the molecular mechanisms of *F. tularensis*-mediated neutrophil apoptosis inhibition are incompletely defined. The objective of this study was to elucidate the pro-survival signaling pathways that are required to extend neutrophil lifespan during this infection. As NF-κB controls expression of many anti-apoptosis factor genes, we hypothesized that activity of this transcription factor would be essential. On the other hand, we also hypothesized that pathways linked to growth factor signaling and IL-8 (CXCL8) would be dispensable, as our studies utilize a serum-free infection model and because *F. tularensis*-infection does not elicit PMN IL-8 secretion (56). Herein, we demonstrate that survival of *F. tularensis*-infected human neutrophils is specifically dependent on the activity of NF-κB, PI3Kα and p38 MAPK, but not MEK/ERK, AKT or other Class I PI3K isoforms.

Materials and Methods

Isolation of human neutrophils.

Heparinized venous blood was obtained from healthy adult volunteers with no history of tularemia in accordance with protocols approved by the Institutional Review Board for Human Subjects at the University of Iowa (201609850 and 200307026). Neutrophils were isolated using a sequential dextran sedimentation, density-gradient separation with Ficoll-Hypaque (GE Healthcare, Little Chalfont, UK) and hypotonic erythrocyte lysis as previously described (99). Using this method, purity was >95% PMNs. PMNs were suspended in Hank's balanced salt solution (HBSS) without divalent cations (Fisher Scientific, Hampton, NH) enumerated, and diluted to $2x10^7$/ml. In all cases, replicate experiments were performed using PMNs from different donors.

Bacterial strains and growth conditions.

F. tularensis LVS has been previously described (26, 56, 59). Bacteria were inoculated onto Difco cysteine heart agar (BD Biosciences, San Jose, CA) supplemented with 9% defibrinated sheep blood (Remel, Lenexa, KS) (CHAB) and grown for 48 hours at 37°C in 5% CO_2. Unless otherwise stated, cultures of LVS were started at an OD_{600} of 0.01 in Bacto brain heart infusion (BD Biosciences) (BHI) broth and incubated overnight (14-18 hours), shaking at 200 rpm. Overnight cultures were diluted to an OD_{600} = 0.200 in BHI broth and incubated at 37°C in 5% CO_2, shaking at 200 rpm, for 2-4 hours. Mid-exponential growth phase bacteria were harvested and washed once with HBSS containing divalent cations (Fisher Scientific).

Infection and culture of neutrophils.

Washed bacteria were quantified by measurement of absorbance at 600 nm. Unless otherwise stated, PMNs ($5x10^6$/ml) were diluted in HEPES-buffered RPMI-1640 containing L-glutamine and phenol red (Lonza, Walkersville, MD) in the absence of serum and infected with LVS as previously described (58). Cultures (1-2 ml each) were incubated in 14 ml polypropylene snap-cap tubes at 37°C with humidity and 5% CO_2 for 0-24 hours.

Phospho-MAPK Dot Blots.

The Proteome Profiler™ human phospho-MAPK slide array kits (R&D Systems Inc., Minneapolis, MN) were used for detection of 24 different MAPK proteins in PMNs. Whole-cell lysates were prepared according to the manufacturer's instructions. Briefly, neutrophils were left untreated or were infected with LVS, and 10 hours later neutrophils were pelleted by centrifugation at 250 *g*. Cell pellets were resuspended in lysis buffer containing aprotinin, leupeptin, PMSF, AEBSF, levamisole, bestatin, E-64, and pepstatin A (Sigma Aldrich), supplemented with the Pierce Halt™ phosphatase inhibitor cocktail (sodium fluoride, sodium orthovanadate, sodium pyrophosphate and β-glycerophosphate) (Thermo Fisher Scientific, Waltham, MA). Protein concentrations were determined by performing a Pierce bicinchoninic acid (BCA) protein assay (Thermo Fisher Scientific), according to the manufacturer's instructions. Array dot blots were processed according to the manufacturer's protocol.

Assessment of neutrophil apoptosis.

Neutrophil apoptosis was measured by flow cytometric analysis of phosphatidylserine (PS) externalization using an Accuri C6 flow cytometer (BD Biosciences, Franklin Lakes, NJ).

PMNs ($5x10^5$) were co-stained with Annexin V-FITC (BioVision, Milpitas, CA) and propidium iodide (PI) (BioVision) in binding buffer (10mM HEPES pH 7.4, 140mM NaCl, 2.5mM $CaCl_2$) according to the manufacturer's instructions. PI staining was used to differentiate early apoptotic from late apoptotic/necrotic PMNs. For each sample, approximately ten thousand events were collected, and the data were analyzed using cFlow software (BD Biosciences).

Inhibition of signaling pathways.

All inhibitors were resuspended from powder in tissue culture-grade dimethyl sulfoxide (DMSO) (Sigma Aldrich, St. Louis, MO). Neutrophils were pretreated with various inhibitors of survival signaling (**Table 1**) at 37°C with 5% CO_2 for 30-60 min, as indicated, after which *F. tularensis* LVS was added to corresponding cultures. Neutrophil apoptosis was measured by Annexin V-FITC/PI staining and flow cytometry, as described above, after further incubation at 37°C for 4, 10, 18, and 24 hours.

Detection of phosphorylated, intracellular proteins via flow cytometry.

Neutrophils were left untreated, infected with LVS as described above or stimulated with N-formyl-L-methionyl-L-leucyl-L-phenylalanine (fMLF) (Sigma Aldrich) for 3 minutes. PI3K activity was inhibited using 100 μM LY294002 (Cell Signaling Technology, Danvers, MA) and phosphorylation of its downstream target, AKT was assessed. At the indicated time points, PMNs were fixed in IC fixation buffer (eBioscience, Waltham, MA) for 30 minutes at room temperature. Following fixation, cells were pelleted by centrifugation at 250 *g* and permeabilized in 100% ice-cold methanol for 30 minutes on ice. After two washes in blocking buffer (Dulbecco's phosphate-buffered saline (DPBS) without divalent cations (Fisher Scientific)

Inhibitor	Target	[Final]	Pre-treatment	Supplier
Afuresertib (GSK2110183)	AKT1/2/3	10 μM	60 min	SelleckChem, Houston, TX
GDC-0941 Pictilisib	PI3Kα,δ	20 μM	60 min	Cayman Chemical, Ann Arbor, MI
HS-173	PI3Kα	10 μM	60 min	SelleckChem
IC-87114	PI3Kβ, γ, δ*	1 μM	60 min	SelleckChem
LY294002	Pan PI3K	50 μM	30 min	Cell Signaling Technology, Danvers, MA
MK-2206	AKT1/2/3	1 μM	30 min	SelleckChem
NF-κB AI	NF-κB	20 μM	60 min	Calbiochem, San Diego, CA
PD98059	MEK1/2	50 μM	30 min	Calbiochem
PIK-294	PI3Kβ, γ, δ*	1 μM	60 min	Calbiochem
SB203580	p38 MAPK	30 μM	60 min	Calbiochem
SB202474	SB03580 negative control	30 μM	30 min	Calbiochem
TGX-221	PI3Kβ*, γ, δ	100 μM	30 min	Cayman Chemical

*preferentially inhibited

Table 1. List of inhibitors used in this study.

supplemented with 0.5% bovine serum albumin (Sigma Aldrich)), neutrophils were resuspended in blocking buffer at a concentration of 10^7 cells/ml. Aliquots of neutrophils (10^6) were mixed with purified human Fc binding inhibitor and either mouse anti-human phospho-AKT (S473)-APC (clone SDRNR, #17-9715) or phospho-p38 MAPK (T180/Y182)-APC (clone 4NIT4KK, #17-9078-42) (all from eBioscience). After incubation for 30 minutes at room temperature, stained cells were washed twice in blocking buffer and resuspended in DPBS without divalent cations for analysis on an Accuri C6 flow cytometer.

Statistical analyses.

Data are presented as the mean ± standard error of the mean (SEM) and were analyzed by two-way ANOVA followed by Tukey's multiple comparisons post-tests. All analyses were performed using GraphPad Prism version 7or 8 software (GraphPad, San Diego, CA). *p*-values less than 0.05 were considered statistically significant.

Results

p38 MAPK is activated and required for prolonged survival of *F. tularensis*-infected neutrophils.

MAPK signaling can be triggered by many stimuli that engage distinct cell surface receptors, including lipopolysaccharide (LPS) and other toll-like receptor (TLR) agonists, growth factors, and cytokines (49). MEK/ERK MAPK and p38 MAPK pathways can act separately or together to modulate neutrophil apoptosis in response to specific stimuli (54, 60, 97, 100-102). To elucidate possible effects of *F. tularensis* on activation of MAPK signaling, we initially utilized phospho-MAPK dot blot arrays to survey intermediates in several MAPK cascades. To this end, dot blots were probed with lysates prepared from control neutrophils and their LVS-

infected counterparts after 10 hours at 37ºC. These data show that infection triggered increased phosphorylation of p38α MAPK and to a lesser extent ERK2 (**Figure 4A**). The dot blot spot map is shown in **Figure 5**.

To examine the possible significance of these pathways in neutrophil apoptosis inhibition by *F. tularensis* we utilized first the p38 MAPK inhibitor SB203580 and included the related compound SB202474 as a negative control (102). Specifically, neutrophils were left in medium alone or pretreated with 30 μM inhibitor prior to infection with LVS, and apoptosis was quantified 4, 10, 18 and 24 hours later using Annexin V-FITC/PI staining and flow cytometry as we previously described (58, 103). In all cases, uninfected/untreated cells were included as an additional control. Our data show that inhibition of p38 MAPK markedly accelerated apoptosis of infected PMNs by 18 hours post-infection (hpi) and completely eliminated the ability of LVS to extend neutrophil lifespan by 24 hpi, whereas the rate of apoptosis of uninfected neutrophils was unchanged (**Figure 4B**). Specificity for p38 MAPK is indicated by the lack of effect of the negative control compound, SB202474. DMSO, the diluent/vehicle control for all drugs used in this study, was also without effect (**Figure 6**). Next, we utilized intracellular antigen staining and flow cytometry to define the kinetics of p38 MAPK activation (**Figure 4C**). By this assay, phosphorylation, and activation of p38 MAPK was low or absent in early infection, was elevated 6-12 hpi, and returned to baseline by 24 hpi.

In marked contrast to the data obtained for p38 MAPK, inhibition of MEK1/2 signaling using 50 μM PD98059 did not significantly alter the rate of PMN apoptosis in the presence or absence of LVS (**Figure 4D**). Taken together, these data indicate that both p38 MAPK and MEK/ERK signaling are activated in infected PMNs, but only p38 MAPK is required for *F. tularensis* to extend cell lifespan.

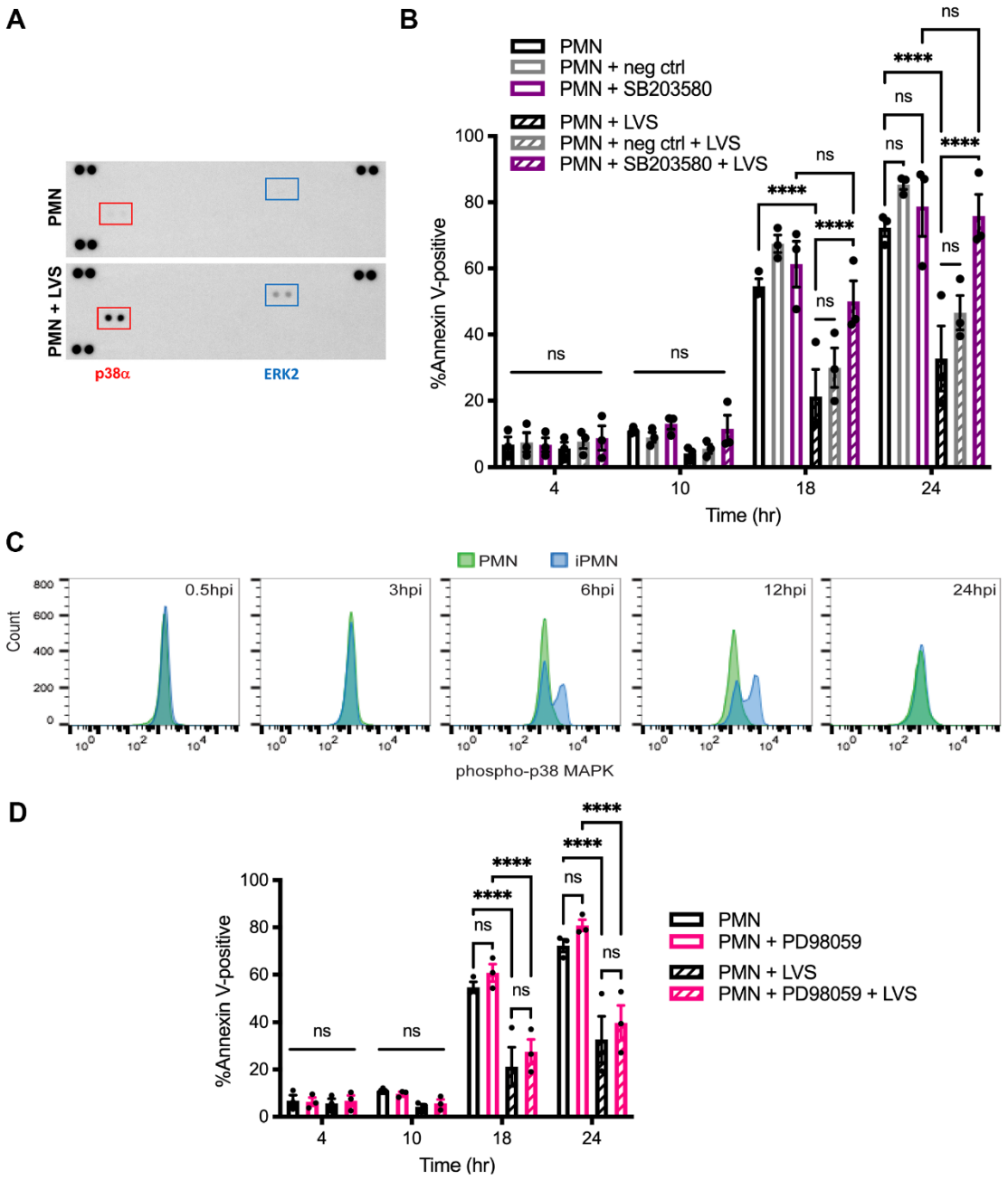
A
PMN
PMN + LVS
p38α
ERK2
B
PMN
PMN + neg ctrl
PMN + SB203580
PMN + LVS
PMN + neg ctrl + LVS
PMN + SB203580 + LVS
%Annexin V-positive
Time (hr)
ns
****
C
PMN
iPMN
0.5hpi
3hpi
6hpi
12hpi
24hpi
Count
phospho-p38 MAPK
D
PMN
PMN + PD98059
PMN + LVS
PMN + PD98059 + LVS
%Annexin V-positive
Time (hr)

Figure 4. Infected neutrophil survival requires p38 MAPK but not MEK/ERK activity.

(A) Dot blot arrays show increased phosphorylation of p38α and ERK2 10 hours after LVS infection. Corner spots are positive and negative controls. Data shown are representative of three independent determinations. These data are shared by Dr. Lauren C. Kinkead. **(B)** Effects of the p38 MAPK inhibitor SB203580 and its negative control SB202474 on apoptosis of control and LVS-infected neutrophils was quantified using Annexin V-FITC/PI staining and flow cytometry at 4, 10, 18 and 24 hours. Data are the mean ± SEM of three independent experiments. ns, not significant. ****$p < 0.0001$, as indicated. **(C)** Kinetics of p38 phosphorylation determined by intracellular straining and flow cytometry. Control cell data are in green and LVS-infected cell data (iPMNs) are shown in blue. Representative of three determinations. **(D)** Similar to (B) except cells were treated with PD98059 to inhibit MEK. Data are the mean ± SEM of three independent experiments. ns, not significant and ****$p < 0.0001$, as indicated.

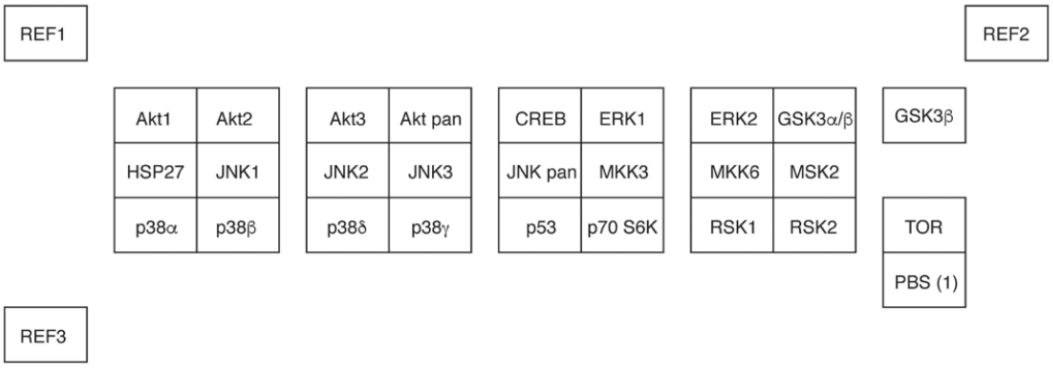

Figure 5. Key for Phospho-MAPK Dot Blots.

Spot map for R&D Systems human phospho-MAPK slide arrays. Each box contains two spots. Corner spots are positive (REF1-3) and negative (lower right) controls.

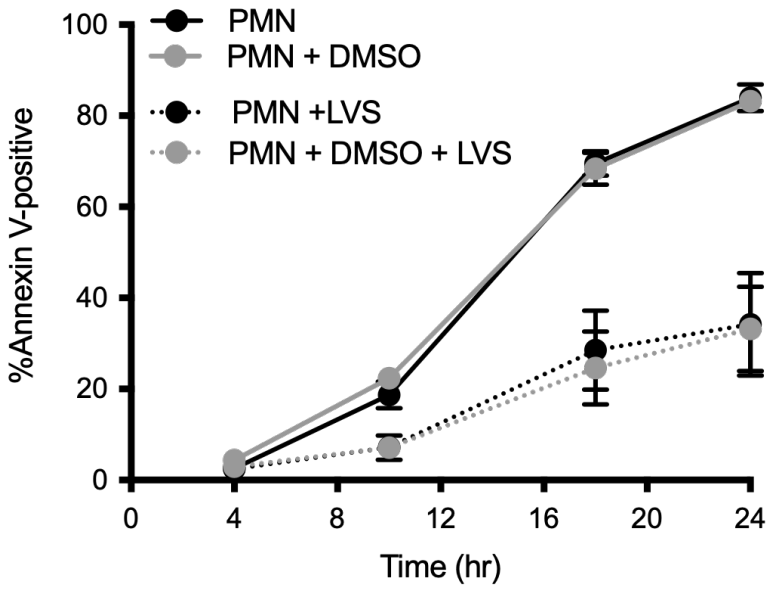

Figure 6. DMSO does not alter the kinetics of neutrophil apoptosis.

Control and LVS-infected neutrophils were incubated in medium with and without DMSO as the diluent control for the indicated amounts of time prior to analysis by Annexin V-FITC/Propidium Iodide co-staining and flow cytometry. Data show the percentage of Annexin V-FITC-positive cells at each time point and are the mean $\pm$ standard error of the mean, n=3.

PI3K activity is required for survival of both infected and uninfected neutrophils.

Class I PI3Ks catalyze conversion of $PI(4,5)P_2$ to $PI(3,4,5)P_3$ and have been extensively studied (104-106). Class IA PI3K isoforms (PI3Kα, PI3Kβ, and PI3Kδ) are important for growth and survival of many types of cells and in neutrophils and macrophages play additional roles in regulation of phagocytosis, cell adhesion, priming and NADPH oxidase activation. On the other hand, the lone Class IB PI3K isoform (PI3Kγ) is activated by heterotrimeric G-protein coupled receptors (GPCRs) and plays a specific role in regulating neutrophil migration to sites of infection and inflammation.

LY294002 is a competitive, reversible pan-Class I PI3K inhibitor (107, 108) and we show here that pretreatment of neutrophils with this drug markedly accelerated constitutive apoptosis of control, uninfected PMNs as indicated by Annexin V-FITC/PI staining at 10 hours, and remained significantly elevated at 18 hours (**Figure 7**). Apoptosis of LVS-infected cell was also profoundly accelerated by LY294002 at 10, 18 and 24 hpi (**Figure 7**). These data demonstrate that PI3K activity is required for delayed apoptosis of *F. tularensis*-infected neutrophils and also regulates constitutive apoptosis of the uninfected controls.

PI3Kα plays a specific role in extended survival of *F. tularensis*-infected neutrophils

Our next objective was to determine if a specific Class IA PI3K isoform was required for longevity of *F. tularensis*-infected neutrophils. To this end, we took advantage of inhibitors that have been designed to target PI3K isoforms individually or in combination (**Table 1**). Specifically, we pretreated neutrophils with 10 μM HS-173, a specific PI3Kα inhibitor, 20 μM of the PI3Kα/PI3Kδ-selective inhibitor GDC-0941 (also called Pictilisib), 1 μM of the PI3Kδ-selective inhibitors IC-87114 and PIK-294, or 100 μM of the PI3Kβ-selective inhibitor TGX-221

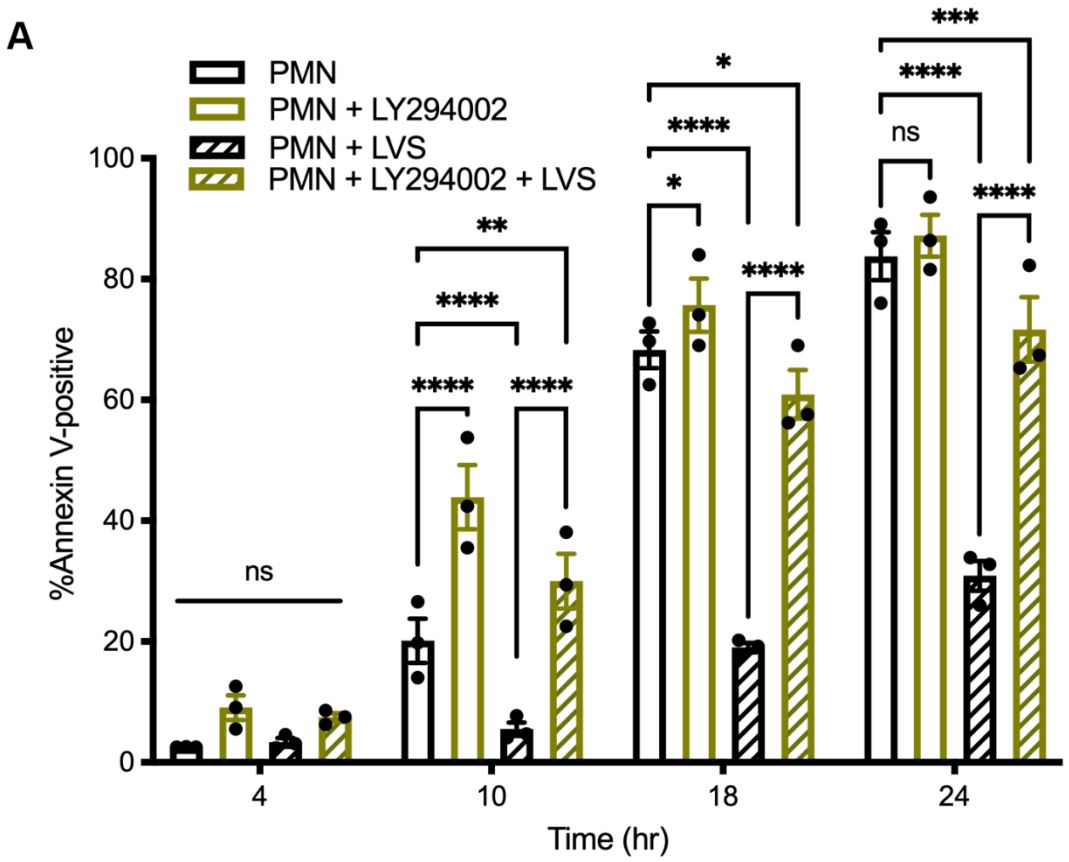

Figure 7. The pan-PI3K inhibitor LY294002 accelerates neutrophil death.

The effect of LY294002 on apoptosis of control and LVS-infected neutrophils was assessed at 4, 10, 18, and 24 hours using Annexin V-FITC/PI staining and flow cytometry. Data are the mean ± SEM of three independent experiments. Ns, not significant. *$p < 0.05$, **$p < 0.01$, ***$p < 0.001$, ****$p < 0.0001$, as indicated.

(108-111) (**Table 1**) and monitored apoptosis over the course of 24 hours in the presence and absence of LVS.

Our data demonstrate that HS-173 had no effect on apoptosis at 4 or 10 hours. Thereafter, apoptosis of the LVS-infected cells was markedly accelerated, whereas death of the uninfected control cells was significantly reduced (**Figure 8A**). On the other hand, treatment with the selective PI3Kα/PI3Kδ inhibitor GDC-0941 significantly increased apoptosis of both control and LVS-infected PMNs at 10, 18 and 24 hours (**Figure 8B**). Based on these data, we conclude that the Class I PI3K isoforms required to prevent apoptosis of control and infected PMNs are distinct. Specifically, the data demonstrate that inhibition of PI3Kα is sufficient to trigger apoptosis after *F. tularensis* infection. In contrast, inhibition of both PI3Kα and PI3Kδ is required for accelerated apoptosis of the uninfected controls.

In another series of experiments, PMNs were treated with 1 μM IC-87114 or 1 μM PIK-294, both of which preferentially inhibit PI3Kδ but have some activity against PI3Kβ and PI3Kγ. Neither of these drugs altered the rate of apoptosis of control or LVS-infected PMNs (**Figures 9A-B**). In our final series of PI3K experiments we tested TGX-221, which preferentially inhibits PI3Kβ, but has some activity against PI3Kδ and PI3Kγ. We now show that 100 μM TGX-221 profoundly diminished apoptosis of uninfected PMNs at 18 and 24 hours, yet had no significant effect on LVS-infected cells at any of the time points examined (**Figure 9C**).

Based on these data, we conclude that Class I PI3Ks play complex roles in PMN survival and death. In particular, we identify PI3Kα activity as critical for survival of neutrophils infected with *F. tularensis* whereas inhibition of PI3Kβ enhanced survival of the uninfected controls. The data also indicate that simultaneous inhibition of PI3Kα and PI3Kδ, but not specific or selective

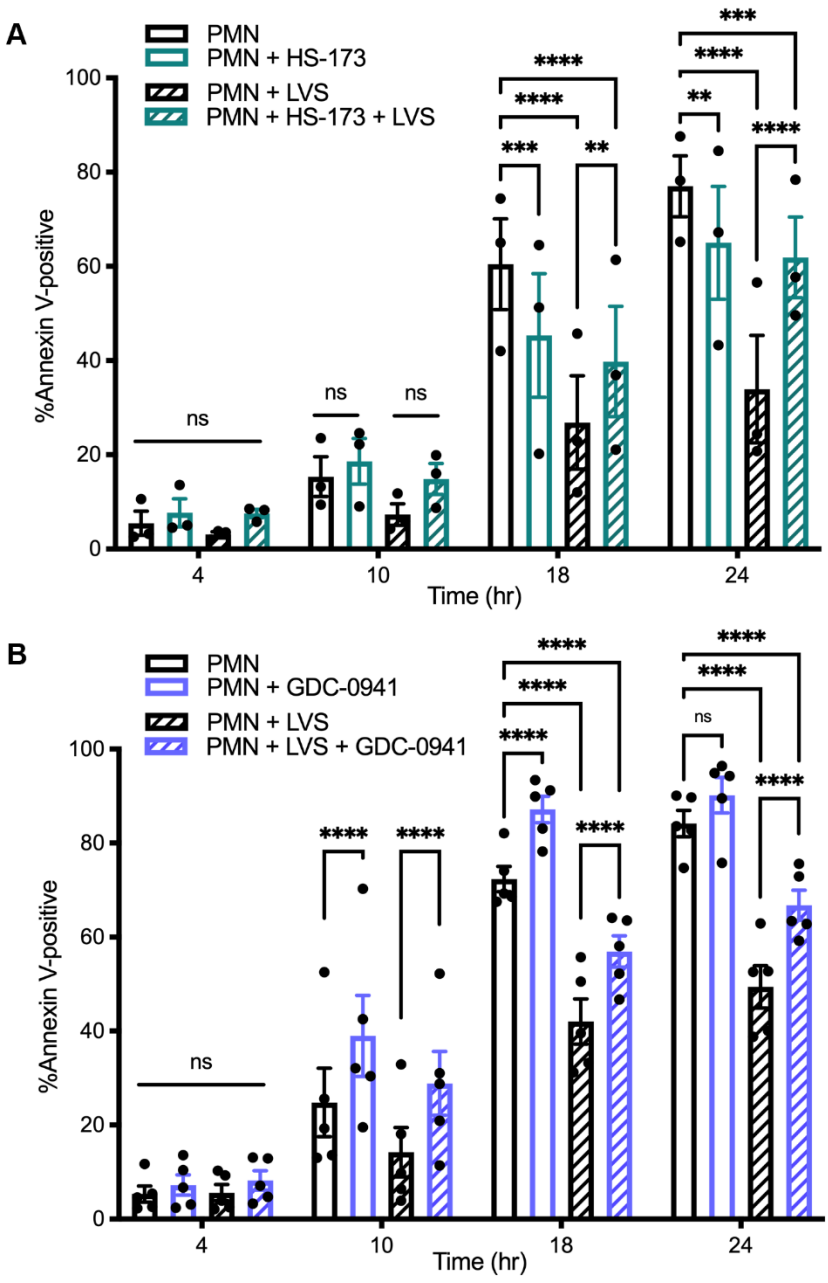

Figure 8. Class IA PI3Kα activity is required for survival after *F. tularensis* infection.

PMNs were treated with HS-173 **(A)** or GDC-0941 **(B)** and then incubated for up to 24 hours in the presence and absence of LVS. Apoptosis was assessed at 4, 10, 18, and 24 hours using Annexin V-FITC/PI staining and flow cytometry. Data are the mean ± SEM of three independent experiments. Ns, not significant. $^{**}p < 0.01$, $^{***}p < 0.001$, $^{****}p < 0.0001$, as indicated.

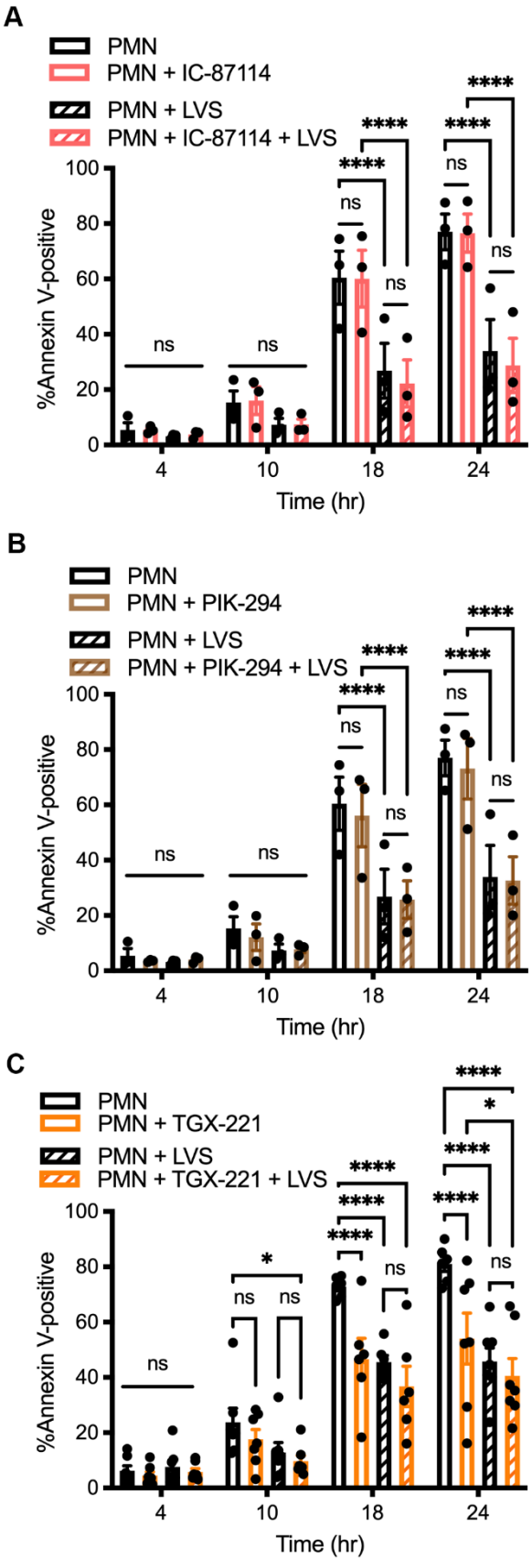
A
PMN
PMN + IC-87114
PMN + LVS
PMN + IC-87114 + LVS
%Annexin V-positive
Time (hr)
B
PMN
PMN + PIK-294
PMN + LVS
PMN + PIK-294 + LVS
%Annexin V-positive
Time (hr)
C
PMN
PMN + TGX-221
PMN + LVS
PMN + TGX-221 + LVS
%Annexin V-positive
Time (hr)

Figure 9. Inhibition of Class I PI3K isoforms PI3Kβ, PI3Kδ, and PI3Kγ does not prevent neutrophil apoptosis inhibition by *F. tularensis*.

PMNs were left in medium alone or treated with IC-87114 **(A)** or PIK-294 **(B)** or TGX-221 **(C)** prior to further incubaction in the presence and absence of LVS. Apoptosis was quantified at 4, 10, 18, and 24 hours using Annexin V-FITC/PI staining and flow cytometry. Data are the mean ± SEM of three independent experiments. Ns, not significant. *$p < 0.05$, ****$p < 0.0001$, as indicated.

inhibition of either isoform alone significantly accelerates PMN apoptosis in the absence of infection.

AKT activity is dispensable for infected neutrophil survival

One of the major downstream effectors of Class I PI3Ks is AKT, also known as protein kinase B. There are three isoforms of AKT, and AKT1 and AKT2 are expressed in neutrophils (112). To determine if AKT played a role in modulating neutrophil apoptosis, we treated cells with the allosteric pan-AKT inhibitor MK-2206 (113). In our hands, pretreatment of neutrophils 1 μM MK-2206 had no discernible effect on the rate of neutrophil apoptosis in the presence or absence of LVS (**Figure 10A**). As the effects of MK-2206 can be transient (114, 115), we also tested the newer and more potent AKT inhibitor, Afuresertib (113). Consistent with the aforementioned data, pretreatment with 10 μM Afuresertib had no significant effect on the lifespan of neutrophils infected with LVS, but significantly reduced the rate of apoptosis of the uninfected cells at 18 and 24 hours (**Figure 10B**).

Notably, our dot blot arrays did not detect AKT phosphorylation in resting or infected cells at 10 hours (**Figures 4A and 5**). As an alternative approach for detection of active AKT we also utilized flow cytometry. In this case, cells were stained with antibodies specific for AKT phosphorylated at S473 and were treated with fMLF for 3 minutes as a positive control. As shown in **Figure 10C** (*left panel*), fMLF enhanced phosphorylation of AKT above baseline, as indicated by an increase in MFI, and this was sensitive to inhibition by LY294002. Conversely, AKT phosphorylation appeared unchanged at 1, 3 and 6 hpi with LVS as compared with the uninfected controls (**Figure 10C**, right panels). At 12 hours, phospho-AKT was slightly lower in the infected PMNs yet was slightly higher than the controls at 24 hpi.

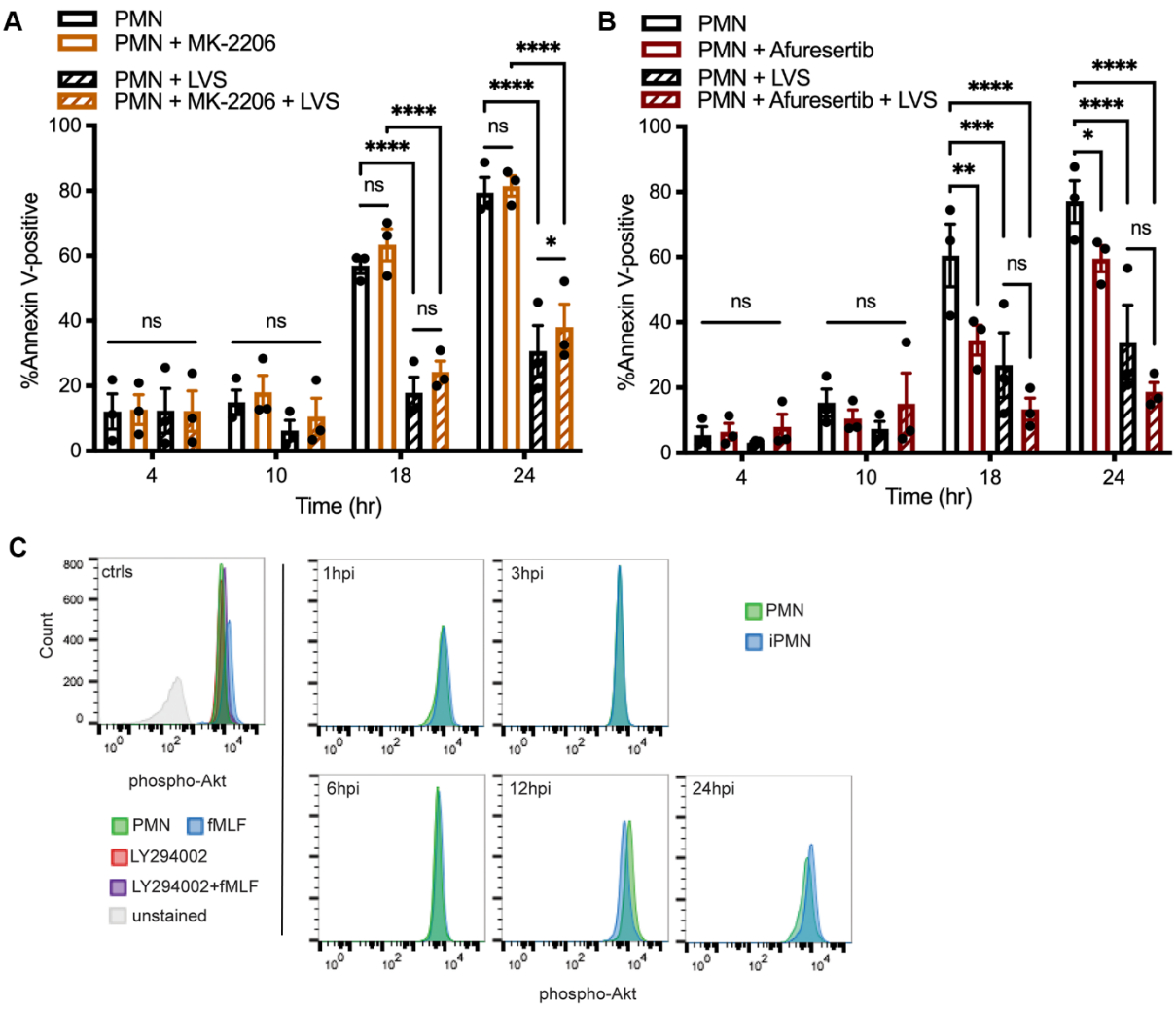
A
PMN
PMN + MK-2206
PMN + LVS
PMN + MK-2206 + LVS
%Annexin V-positive
Time (hr)
B
PMN
PMN + Afuresertib
PMN + LVS
PMN + Afuresertib + LVS
%Annexin V-positive
Time (hr)
C
ctrls
Count
phospho-Akt
PMN
fMLF
LY294002
LY294002+fMLF
unstained
1hpi
3hpi
6hpi
12hpi
24hpi
PMN
iPMN
phospho-Akt

Figure 10. AKT activity is not required for neutrophil survival.

(A-B) Neutrophils were treated with MK-2206 for 30 minutes (A) or Afuresertib for 60 minutes (B)6prior to further incubation in the presence or absence of LVS. Apoptosis was assessed at 4, 10, 18, and 24 hours using Annexin V-FITC/PI staining and flow cytometry. Data are the mean ± SEM of three independent experiments. Ns, not significant. *$p < 0.05$, **$p < 0.01$, ***$p < 0.001$, ****$p < 0.001$, as indicated. **(C)** Detection of intracellular phospho-AKT by flow cytometry. Neutrophils were left in medium alone (PMN), stimulated with fMLF for 3 minutes, treated with LY294002 for 30 minutes, or treated with LY294002 prior to stimulation with fMLF (*left panel*) or were incubated for 1, 3, 6, 12, and 24 hours in the absence (PMN) or presence (iPMN) of LVS (*right panels*). Data shown are representative of three determinations.

Based on these data, we conclude that AKT does not play a significant role in regulating apoptosis of neutrophils during *F. tularensis* infection.

F. tularensis requires NF-κB activation to prolong neutrophil lifespan.

NF-κB plays an important role in neutrophil survival during infection and inflammation by controlling expression of genes that encode important anti-apoptotic regulatory factors (59). We have shown that several NF-κB target genes are significantly differentially expressed during LVS infection, including *BCL2A1, BIRC3, BIRC4, TNFAIP3, CFLAR* and *CAST*, which encode A1, cIAP2, XIAP, A20, FLIP and calpastatin, respectively (116). Thus, we predicted that NF-κB activity may be essential in our system for infected cell survival. To test this hypothesis, we utilized NF-κB AI (NF-κB Activation Inhibitor) (117). The data in **Figure 11** clearly show that NF-κB AI significantly accelerated apoptosis of LVS-infected PMNs at all time points examined. Moreover, at both 4 and 10 hpi, 26.5% and 39.5% of the NF-κB AI-treated cells that were infected with LVS had already undergone apoptosis as compared with only 5.5% and 15.4% of the uninfected, untreated controls (**$p < 0.01$). In sharp contrast, inhibition of NF-κB did not significantly alter the rate of apoptosis of uninfected PMNs, confirming published data (118). We therefore conclude that NF-κB is essential for viability of *F. tularensis*-infected neutrophils and for the ability of this bacterium to delay apoptosis and extend PMN lifespan.

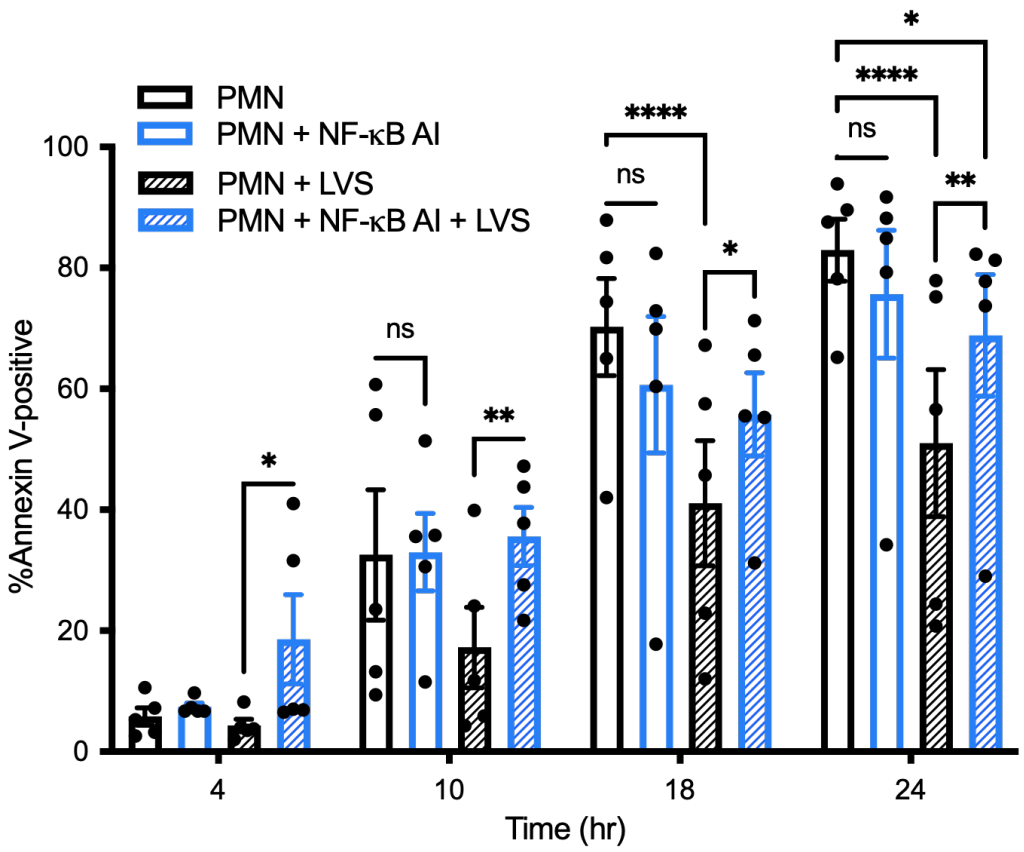

Figure 11. Inhibition of NF-κB selectively accelerates death of *F. tularensis*-infected neutrophils.

PMNs were pretreated with NF-κB AI for 30 minutes and then incubated for up to 24 hours in the presence and absence of LVS. Apoptosis was assessed at 4, 10, 18, and 24 hours using Annexin V-FITC/PI staining and flow cytometry. Data are the mean ± SEM of three independent experiments. Ns, not significant. $^{**}p < 0.01$, $^{***}p < 0.001$, $^{****}p < 0.0001$, as indicated.

Discussion

The ability of MAPKs, Class I PI3Ks and NF-kB to influence diverse neutrophil functions including migration, phagocytosis, oxidant production, cytokine secretion and lifespan is unequivocal. At the same time, a majority of studies have focused on responses to individual receptor ligands of host or microbial origin, such as GM-CSF or LPS. Much less is known about responses to whole microbes or other complex stimuli, and in most studies roles for enzyme isoforms were not interrogated. The results of this study demonstrate specific roles for p38 MAPK, PI3Kα and NF-kB in PMN apoptosis inhibition by *F. tularensis* and identify a distinct requirement for PI3Kα and PI3Kδ in regulation of human neutrophil lifespan in the absence of infection. The results of this study are summarized in **Figure 12**.

MEK/ERK signaling is activated in neutrophils in response to growth factors such as G-CSF and GM-CSF, LPS, hypoxia, or host inflammatory mediators such as IL-8, C5a, and LTB4 (49, 60, 119, 120). The central mechanisms of ERK-mediated apoptosis inhibition are phosphorylation of caspase-9, which curtails its activity, and phosphorylation of BAD at S112 which favors its sequestration in the cytosol, thereby helping to sustain mitochondrial outer membrane integrity (121, 122). We show here that although ERK2 phosphorylation was enhanced in neutrophils 10 hours after infection with *F. tularensis*, inhibition of ERK1/2 with PD90859 did not alter the rate of PMN apoptosis in the presence or absence of infection. This is likely due to redundant mechanisms of apoptosis inhibition in our system. For example, PIM2 can also phosphorylate BAD, and we have shown that *PIM2* expression is upregulated by LVS infection (59, 123). In addition, MCL-1 and A1 are abundant in LVS-infected neutrophils and sustain mitochondrial integrity by binding and sequestering BAX and BAK, which are generally believed to play a greater role in disrupting neutrophil mitochondria than BAD (54, 58, 59).

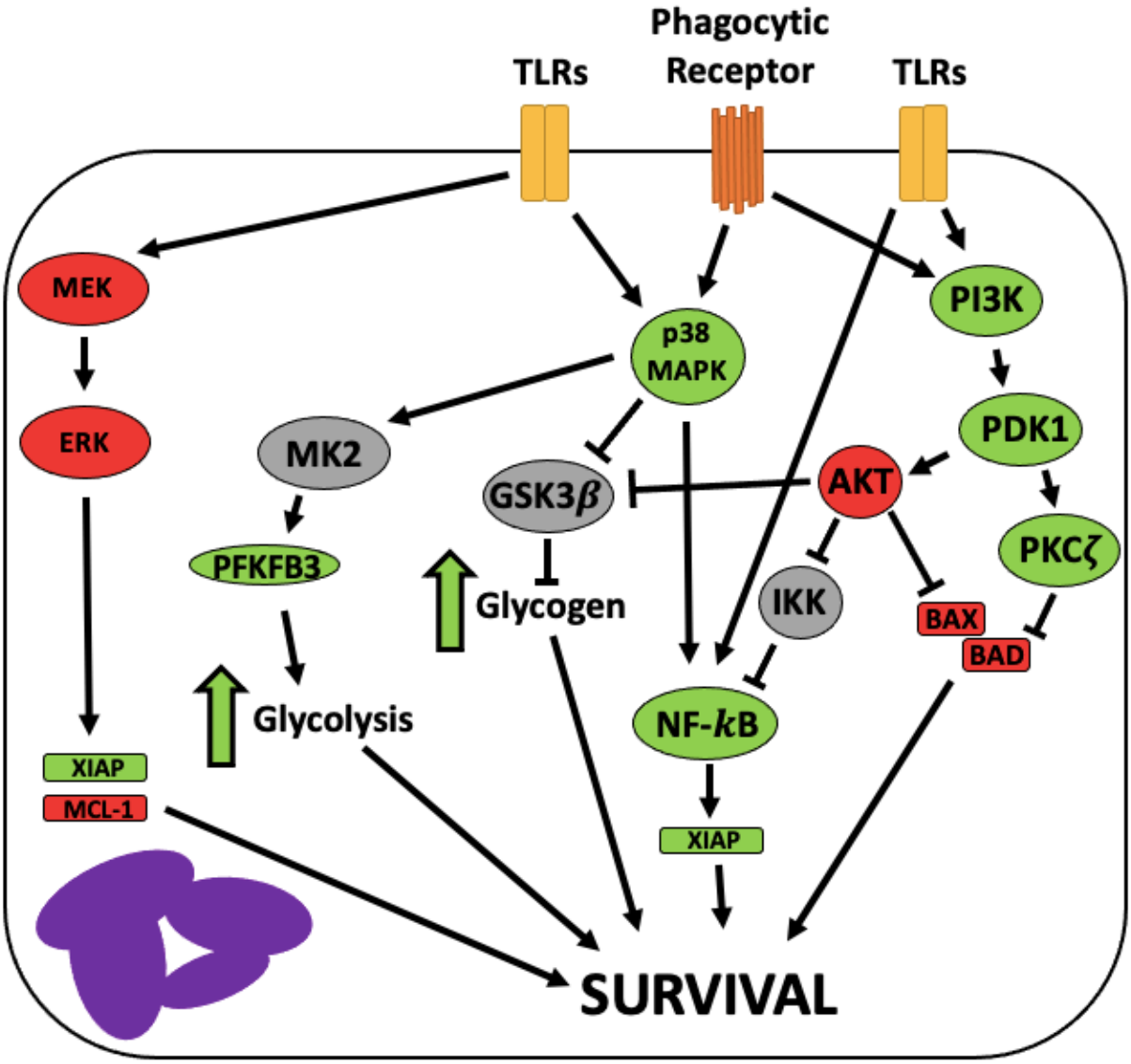

Figure 12. Simple schematic of survival signaling in human neutrophils.

See discussion for details.

Finally, XIAP is an inhibitor of apoptosis protein that binds directly to caspase-9 and caspase-3 to block their catalytic activity and also inhibits processing of the respective proenzymes to their mature, active forms (59, 60). XIAP is maintained at high levels in LVS-infected PMNs via increased expression of the *BIRC4* gene and by upregulation of calpastatin (*CAST*), which prevents calpain-mediated XIAP degradation in healthy cells and during LVS infection (54, 58, 59, 124).

p38 MAPK is of interest as it can enhance, inhibit, or have no effect on PMN apoptosis in a context-specific manner (54, 60, 124). In neutrophils, the pro-death effects of p38 MAPK are commonly linked to phosphorylation of $p47^{phox}$, NADPH oxidase activation and toxic oxidant production, whereas constitutive apoptosis of PMNs at rest is p38-independent (60, 120, 124, 125) (**Figure 4B**). In this regard it is of interest that *F. tularensis* uses multiple strategies to disrupt NADPH oxidase assembly and activity in PMNs, and phosphorylation $p47^{phox}$ is significantly diminished (26, 55). A role for p38 MAPK in prolonging PMN survival has been demonstrated in hypoxia, exposure to dexamethasone or IL-32γ and during infection with *Coxiella burnetii*, and we extended this list to include *F. tularensis* (97, 118, 120, 126, 127).

At the molecular level, p38 favors survival by enhancing MCL-1 abundance, by direct phosphorylation and inhibition of caspase-3 and caspase-8 or by stimulating IL-8 secretion, and in many instances collaborates with PI3K or NF-κB (60, 97, 118, 127, 128). Notably, p38 also has effects on metabolism, and like AKT can phosphorylate glycogen synthase kinase-β (GSK3β) to relieve inhibition of glycogen synthase (129). p38 stimulates glucose uptake via membrane translocation of GLUT1 and phosphorylates MK2 to stimulate PFKFB3 and amplify glycolysis at the level of PFK (130, 131). Precisely how p38 contributes to apoptosis inhibition in our system remains to be determined. Live *F. tularensis* does not trigger secretion of IL-8, but

a role for glucose metabolism is attractive, as expression of *SCL2A1*, which encodes GLUT1, and *PFKFB3* is enhanced (56, 59).

A central finding of this study is our identification of distinct roles for Class IA PI3K isoforms in neutrophil survival in the presence and absence of *F. tularensis* infection. We identified a critical role for PI3Kα in delayed apoptosis of LVS-infected PMN whereas simultaneous inhibition of PI3Kα and PI3Kδ was required to undermine survival of the uninfected controls. Our findings support and extend published data which demonstrate that the roles of PI3K isoforms in cell survival are complex sometimes contradictory. Thus, although deactivation of $PI(3,4,5)P_3$ signaling accompanies constitutive PMN apoptosis, simultaneous inhibition or deletion of at least three Class I PI3K isoforms is required to overcome the pro-survival effects of GM-CSF, and in keeping with this combined loss of PI3Kδ and PI3Kγ is not sufficient to alter resting PMN lifespan (108, 132). On the other hand, the ability of PI3Kβ to accelerate PMN apoptosis under certain circumstances may explain the increased longevity of TGX-221-treated cells shown in **Figure 9C**. Precisely what accounts for the survival-enhancing effect of HS-173 on uninfected PMNs remains to be determined, but this is negated and reversed by GDC-0941 (**Figure 8B**). Although PI3Kδ is generally dispensable for PMN survival (108) (**Figures 9A-**B), a role for p38 and PI3Kδ in IL-8 and MIP-mediated apoptosis inhibition has been described (104). Whether p38 MAPK is directly linked to PI3Kα and/or PI3Kδ in our system remains to be determined.

PIK3CA, which encodes the p110α catalytic subunit of PI3Kα, is mutated and overexpressed in many human cancers, and for this reason isoform-specific inhibitors have been developed as candidate therapeutics (133). HS-173 binds with high affinity to p110α and exhibits antitumor activity *in vivo* and *in vitro* (134). In cancer cell lines, HS-173 causes cell

cycle arrest and apoptosis via the intrinsic pathway which has been linked to disruption of growth factor, insulin and TGFβ receptor signaling (133, 135). Relevant downstream targets and pathways include AKT-dependent phosphorylation of BAD, caspase-9, and GSK3β in addition to effects on mTOR and autophagy (136, 137). Expression of *HIF1A* (HIF-1α) and *VEGFA* (VEGF) are also impaired. Notably, HIF-1α is important for neutrophil survival in normoxia as well as hypoxia, and *VEGFA* and many other HIF-1α target genes, but not *HIF1A* itself, are upregulated following LVS infection including *HK2, LDHA, PDK1* and *SCL2A1* (59, 138). Based on these data and evidence that p38 MAPK is also linked to GLUT1 and GSK3β, as noted above, it is attractive to predict that glycolysis and glucose metabolism may play a role in regulating PMN lifespan during *F. tularensis* infection. Other genes of interest that are differentially expressed in our system and have been linked to PI3K signaling include *GADD45B*, *SOD2*, *BNIP3* and *CDKN1A* (54, 59).

In contrast to the central role of PI3Kα in survival and proliferation of many cell types, PI3Kβ, PI3Kδ, and PI3Kγ are linked to PMN activation (108, 109). PI3Kβ plays a specific role in Fc receptor signaling during phagocytosis and immune complex stimulation in collaboration with PI3Kδ. Accordingly, adhesion, spreading and ROS production are sensitive to inhibition by TGX-221 and IC-87114, but not HS-173. PI3Kγ is required for extravasation, chemotaxis and ROS production triggered by GPCR ligands. PI3Kδ has some influence on polarization and migration but plays a broader role cytokine production and NADPH oxidase activation in PMNs following exposure to a wide range of stimuli of host and microbial origin including LPS, TNFα, IL-8, fMLF and C5a.

AKT is an extensively studied PI3K effector. The fact that AKT phosphorylation was not significantly induced by LVS despite the prominent role of PI3K in infected neutrophil survival

was unexpected, as was the failure of AKT inhibitors to accelerate neutrophil death. However, this latter outcome is not without precedent, as PI3K-dependent/AKT-independent apoptosis inhibition has also been reported following treatment with IGF-1 and after infection by *L. major* (139, 140). Paradoxically, Afuresertib and other AKT inhibitors can also lead to PI3K activation, providing a potential explanation for the ability of Afuresertib to delay neutrophil death in our hands (115). At the same time, redundancy with XIAP and p38 may negate any requirement for AKT with respect to inhibition of caspase-9, BAD or GSK3β (141-144), as noted above. One potential downstream target of PI3Ka signaling during this infection could be the atypical isoform of protein kinase C (PKC) PKC ζ, which has been established as pro-survival factor because of its effects on NF-kB, though its role as a regulator of neutrophil lifespan is unknown (145). PI3K can signal through 3-phoshoinositide dependent protein kinase-1 (PDK1), which subsequently interacts with PKC ζ, but the extent to which this signaling axis regulates neutrophil lifespan, or is modulated during infection with *Francisella tularensis*, is unknown (146).

The ability of NF-κB AI to significantly accelerate apoptosis of *F. tularensis*-infected cells within four hours underscores the central role of this pathway in neutrophil survival. In keeping with this, genes encoding NF-κB subunits p105 (*NFKB1*), p100 (*NFKB2*) and p65 (*RELA*) are upregulated by LVS as are the NF-κB target genes *IL1B, SOD2, GADD45B*, *CFLAR*, *TNFAIP3*, *BCL2A1*, *BIRC3*, and *BIRC4* that encode IL-1β, MnSOD, GADD45β, c-FLIP, A20, A1, cIAP2, and XIAP, respectively, and which act at various points to directly inhibit intrinsic and extrinsic apoptosis pathway activation, detoxify ROS, or promote survival (59). In particular, IL-1β is a PMN survival factor that can act in an autocrine and paracrine manner to stimulate NF-κB signaling (59). Moreover, GADD45β connects p38 MAPK to NF-κB; and MSK1/2, a

downstream target of p38, phosphorylates NF-κB p65 leading to activation of this pathway (59, 147, 148). These data provide critical insight into how the expression of numerous distinct factors involved in cell survival are rapidly and concurrently altered, but precisely how NF-κB is linked to p38 MAPK and/or PI3K activation in *F. tularensis*-infected neutrophils remains to be determined.

Maximal inhibition of neutrophil apoptosis is achieved by the combined effects of intracellular bacteria, as well as bacterial lipoproteins (BLPs) and other factors that are secreted/released by extracellular *F. tularensis* prior to phagocytosis (103, 149). *F. tularensis* PAMPs are detected by TLR2/1 and TLR2/6 but not TLR4, and a specific role for TLR2/1 in BLP-mediated survival signaling has been described (55, 103). In contrast, *F. tularensis* LPS has an atypical structure and is not a TLR4 agonist, and LPS and capsule do not modulate PMN lifespan (56, 103). Based on studies of whole blood, TLR2/1 survival signaling has been linked to PI3K, AKT and NF-κB and is associated with increases in A1 and MCL-1 as well as phosphorylation of BAD. In this case, PI3K is upstream of p38 and ERK, and apoptosis inhibition is sensitive to both PI3K and NF-κB inhibitors (150). The receptors that mediate uptake of unopsonized *F. tularensis* by PMNs are unknown. Nevertheless, we hypothesize that both TLR2 and phagocytic receptor signaling will contribute to apoptosis inhibition in our system. Approximately four hours after uptake, *F. tularensis* escapes the phagosome and replicates in the cytosol (27, 55, 56). As inhibition of NF-κB signaling undermines infected PMN survival as early as four hours after infection (**Figure 11**), it is attractive to predict that TLR2 signaling is critical for this pro-survival response, but additional studies are needed to elucidate the roles of individual PMN receptors and the influence of bacterial localization on p38, PI3Kα and NF-κB and their shared and distinct downstream targets.

In summary, the results of this study provide fundamental insight into the role pro-survival signaling pathways in delayed apoptosis of human neutrophils infected with *F. tularensis*. We identified p38 MAPK, PI3K and NF-κB as essential yet excluded roles for ERK and AKT, results that distinguish *F. tularensis* from other stimuli described to date. In identifying critical roles for PI3Kα and PI3Kδ in resting PMN survival and PI3Kα in longevity of cells infected with *F. tularensis*, our data also fundamentally advance insight into the biology of Class IA PI3K isoforms in this cell type. Overall, our findings also underscore the complexity of the signaling pathways that regulate life and death in this cell type.

CHAPTER 3: METABOLIC REPROGRAMMING MEDIATES DELAYED APOPTOSIS OF HUMAN NEUTROPHILS INFECTED WITH *FRANCISELLA TULARENSIS*

Introduction

Neutrophils comprise the majority of circulating white blood cells within the human body and are produced at a rate of approximately 100 billion per day (33). As one of the first immune cells to be recruited to infection sites, neutrophils are a vital component of the immune system that rapidly identify, engulf, and eradicate invading microbes (33, 35, 151). Neutrophils have a uniquely short lifespan of 18-24 hours in circulation before undergoing constitutive apoptosis, and disruption of this tightly regulated, pre-programmed cell death mechanism disrupts neutrophil function and capacity to resolve infection (36, 37). Mature neutrophils are also metabolically distinctive, as they rely primarily on glycolysis for energy production (82). Although it is known that the idiosyncratic lifespan and metabolism of neutrophils each contribute distinctly to supporting neutrophil function, the extent to which neutrophil metabolism influences lifespan, or vice versa is not well understood (37, 76).

Constitutive apoptosis is tightly regulated and requires global changes in PMN gene expression (37, 42). Overall, cell viability and death are governed by the relative abundance of pro-survival and pro-apoptosis BCL-2 family proteins as well as Inhibitor of Apoptosis Proteins and calpastatin (47). The key event in early apoptosis is permeabilization of the outer mitochondrial membrane by pro-apoptosis BCL-2 proteins BAX and BAK. Thereafter, cytochrome *c* released into the cytosol initiates apoptosome formation for activation of caspsase-9, which in turn activates caspase-3 for execution of cell death. In healthy cells mitochondrial integrity is maintained by pro-survival BCL-2 proteins MCL-1 and BCL2A1 which block

translocation of BAX and BAK. At the same time, Inhibitor of Apoptosis Proteins such as XIAP prevent processing activation of procaspase-9 and procaspase-3 by direct binding. Additional layers of regulation are provided by cIAP1, cIAP2, calpastatin, cyclin-dependent kinases, extrinsic pathway regulators and signaling mediated by growth factor receptors and inflammatory mediators (37, 47). As survival factors are short-lived, continued expression of the encoding genes is critical for PMN viability, but the internal signal that tips the balance toward apoptosis in aging PMNs is unknown (37, 47).

Francisella tularensis is a Gram-negative, facultative, intracellular coccobacillus, the causative agent of the zoonotic disease tularemia, and one of the most infectious pathogens known (1, 12, 19, 64, 65, 152). One of few bacteria capable of parasitizing neutrophils, *F. tularensis* evades elimination via a multifaceted strategy that includes inhibition of NADPH oxidase assembly and activity, followed by phagosome escape and replication in the cytosol (26, 153). At the same time, *F. tularensis* inhibits neutrophil apoptosis and accumulation of dysfunctional neutrophils at the infection site contributes to disease exacerbation rather than resolution (43, 62, 68, 69). These properties are shared by *F. tularensis* subspecies *tularensis* (type A) strains that are exclusive to North America as well as *F. tularensis* subspecies *holarctica* (type B) strains that are found throughout the Northern Hemisphere (55). Although it is unequivocal that *F. tularensis* extends neutrophil lifespan by delaying apoptosis, the mechanisms enabling infected cells to override these highly conserved, tightly regulated apoptosis programs are still incompletely defined (56, 58, 59).

Metabolic regulation of inflammation and immune cell function is a rapidly growing field of study. Although most studies to date have focused on macrophages and T lymphocytes, distinct metabolic states of neutrophils are beginning to be described (75-79, 83, 84). Thus,

recent data demonstrate that neutrophil metabolism can be reprogrammed and that these adaptations contribute directly to elimination of infection or disease progression in a context-specific manner (78, 83, 84, 88, 154). On the other hand, there are limited data regarding potential links between changes in neutrophil behavior elicited by metabolic reprogramming and cell lifespan. In previous work, our laboratory demonstrated that *F. tularensis* significantly extends human neutrophil lifespan via effects on apoptosis pathway signaling and changes in gene expression leading to upregulation of prosurvival factors such as XIAP, calpastatin and BCL2A1 that inhibit caspase activation and sustain mitochondrial integrity (56, 58). We undertook the current study as our transcriptional profiling data suggested that *F. tularensis* may also manipulate neutrophil metabolism. Herein, we demonstrate that *F. tularensis* elicits a distinct metabolic program that is defined by dynamic changes in glycolysis and glycogen abundance that are essential for cell longevity. In addition, we also show that pan-caspase inhibition can alter metabolism in the absence of infection. Collectively, these data advance understanding of PMN metabolic plasticity and support the hypothesis that metabolism and PMN lifespan are intimately linked.

Materials and Methods

Cultivation of bacteria

F. tularensis subspecies *holarctica* live vaccine strain (LVS) or the LVS *fevR* mutant (29) were inoculated onto Difco cysteine heart agar (BD Biosciences, East Rutherford, NJ) supplemented with 9% defibrinated sheep blood (Hemostat Labs, Dixon, CA) and grown at 37˚C in 5% CO_2 for 48-72 hr. Bacteria were transferred from the plate into 1 ml of sterile Hank's Balanced Salt Solution (HBSS) containing divalent cations (Thermo Fisher Scientific, Waltham,

MA) and quantified by measurement of absorbance at 600 nm. Broth cultures were started at an OD_{600} of 0.01 for LVS cultures and an OD_{600} of 0.025 for *fevR* mutant cultures in 5 ml pH 6.8 Bacto brain heart infusion (BHI) broth (BD Biosciences, East Rutherford, NJ) in a 50-ml conical tube. All broth cultures were incubated at 37˚C in 5% CO_2, shaking at 200 RPM and grown to mid-exponential phase either by 1) being incubated for 12 hr, followed by immediate harvest; or 2) by being incubated for 15-17 hr, diluted to an OD_{600} of 0.200 in 5 ml BHI broth and incubated for 2–4 more hr prior to harvest. Mid-exponential growth phase bacteria were pelleted at 12,000 RPM for 2 min, washed once in 1 ml HBSS with divalent cations and quantified by measurement of absorbance at 600 nm.

Ethics Statement

Heparinized, venous blood was obtained from healthy adult volunteers who provided written informed consent according to protocols approved by the Institutional Review Board for Human Subjects at the University of Iowa (#201609850 and #200307026).

Isolation of neutrophils from human blood

Neutrophils were isolated via sequential dextran sedimentation (Pharmacosmos, Holbæk, Denmark), density separation through a Ficoll-Hypaque gradient (GE Healthcare, Chicago, IL) and hypotonic lysis of erythrocytes (99). This method routinely yielded >95% neutrophil purity.

Neutrophil ultrapurification

As indicated, certain experiments utilized ultrapure PMNs. To achieve this, neutrophils, isolated as described above, were counted and centrifuged at 1,100 x g for 5 min. Cells were resuspended to 5 x 10^7/ml in PBS without cations supplemented with 2% fetal bovine serum (Hyclone Laboratories, Pittsburgh, PA) and 1mM EDTA and transferred to 5 ml round-bottomed polypropylene tubes in 0.25-2.5 ml aliquots. Neutrophils were purified using the EasySep™ Human Neutrophil Isolation Kit from Stem Cell Technologies (Vancouver, Canada), according to manufacturer's instructions. Following the ultrapurification process, neutrophil purity was assessed by staining cells (1 x 10^6 cells/staining condition) with CD15-Allophycocyanin (APC) (Invitrogen, Carlsbad, CA) and/or CD16-R-Phycoerythrin (PE) (Biolegend, San Diego, CA) in flow cytometry staining (FACS) buffer (HBSS with cations (Thermo Fisher Scientific, Waltham, MA), 0.2% human serum albumin (Grifols, Los Angeles, CA), 0.2% NaN_3). Approximately 10,000 events per sample were collected using an Accuri C6+ flow cytometer (BD Biosciences, East Rutherford, NJ) and the percentage of CD15+/CD16+ cells was quantified using Accuri C6+ software (BD Biosciences, East Rutherford, NJ). This method routinely yielded >99% neutrophil purity.

Infection of neutrophils with *F. tularensis* wild-type LVS or the isogenic *fevR* mutant

Neutrophils were resuspended in HBSS without divalent cations (Thermo Fisher Scientific, Waltham, MA) for enumeration and diluted to 2x10^7/ml. Unless otherwise stated, neutrophils (5x10^6/ml) were cultured in suspension (1-2 ml) in serum-free HEPES-buffered RPMI-1640 containing L-glutamine and phenol red (Lonza, Walkersville, MD). For lactate supplementation experiments, 4.7 mM sodium lactate (Sigma-Aldrich) was added to serum-free

HEPES-buffered RPMI-1640 at time zero. For pyruvate feeding experiments, neutrophils ($5x10^6$/ml) were cultured in suspension (1 ml) in serum-free HEPES-buffered SILAC RPMI 1640 Flex Media (Thermo Fisher Scientific, Waltham, MA) without glucose or glutamine and supplemented with 2 g/L sodium pyruvate (Sigma Aldrich, Burlington, MA). Cultures were incubated in 14 ml polypropylene tubes at 37˚C with 5% CO_2 in the absence or presence of *F. tularensis* LVS wild-type or the *fevR* mutant as we previously described (103, 155). All experimental replicates were generated using neutrophils from at least three different donors.

RNA isolation and qRT-PCR

Total RNA was isolated from ultrapurified neutrophils at the indicated times using a Qiagen RNeasy kit (Hilden, Germany) according to the manufacturer's instructions. RNA concentrations were measured by Nanodrop ND-1000 spectrophotometry. In an Eppendorf Mastercycler pro (Hamburg, Germany), RNA was reverse transcribed using the Invitrogen Super Script III First Strand Kit (Carlsbad, CA) and cDNA was then amplified with gene-specific primer pairs (Origene, Rockville, MD) (primer sequences are in **Table 2**) using Quanta Biosciences Perfecta SYBR Green Fast Mix (Gaithersburg, MD), all according to the manufacturer's instructions. Melting curve analysis was used to check product specificity. The relative expression level of each transcript was determined using the $2^{-\Delta\Delta Ct}$ method and normalized to β-actin.

Measurement of the extracellular acidification rate (ECAR) using Seahorse analysis

Neutrophils were resuspended in XF assay media (Agilent Technologies, Santa Clara, CA) at a concentration of $1x10^7$/ml and $5x10^6$ cells per condition were plated onto a XF24 cell

Gene	Forward Sequence	Reverse Sequence
SLC2A3	TGCCTTTGGCACTCTCAACCAG	GCCATAGCTCTTCAGACCCAAG
HK2	GAGTTTGACCTGGATGTGGTTGC	CCTCCATGTAGCAGGCATTGCT
PFKFB3	GGCAGGAGAATGTGCTGGTCAT	CATAAGCGACAGGCGTCAGTTTC
PFKL	AAGAAGTAGGCTGGCACGACGT	GCGGATGTTCTCCACAATGGAC
LDHA	GGATCTCCAACATGGCAGCCTT	AGACGGCTTTCTCCCTCTTGCT
GBE1	GCCTTGACTTACCTCATGTTGGC	AGCACAGAGCTGGCATTCCTGA
UGP2	GCAGGAGCAAAATGCCATTGACA	CAGAAAACGGCTCCTTGGCACA
GYS1	CCGCTATGAGTTCTCCAACAAGG	AGAAGGCAACCACTGTCTGCTC

Table 2. Glycolytic and glycolytic enzyme primer-pair sequences.

plate (Agilent Technologies, Santa Clara, CA) pre-coated with 0.1 mg/ml poly-L-lysine (Sigma Aldrich, Burlington, MA). Plates were incubated at 37˚C for 1 hr in the absence of CO_2. ECAR was measured at 8.6-min intervals over a period of 95 min using a Seahorse XF24 analyzer and the Glycolysis Stress Test Kit (both from Agilent Technologies, Santa Clara, CA) according to manufacturer's instructions. All data were analyzed using Seahorse Wave software (Agilent Technologies, Santa Clara, CA).

Measurement of extracellular lactate

Supernatants (1 ml) from neutrophil cultures ($1x10^7$/condition) were deproteinated by adding 1 ml ice-cold 0.5 M metaphosphoric acid, vortexing and placing on ice for 5 min. Supernatants were centrifuged at 10,000 x g at 4˚C for 5 min to pellet proteins. Deproteinated supernatants were transferred to tubes containing 100 µl potassium carbonate to neutralize the acid and centrifuged at 10,000 x g at 4˚C for 5 min to remove any precipitated salts. Lactate concentrations were measured using a luminescence assay kit from Cayman Chemical (Ann Arbor, MI) according to the manufacturer's instructions.

Measurement of intracellular ATP

Neutrophils ($5x10^5$/condition) were transferred directly from culture tubes into a black 96-well plate and ATP concentrations were measured using a luminescence assay kit (Perkin Elmer, Waltham, MA) according to the manufacturer's instructions.

Measurement of pyruvate

Supernatants (0.5 ml) from neutrophil cultures ($5x10^6$/condition) were deproteinated by adding 0.5 ml ice-cold 0.5 M metaphosphoric acid, vortexing and placing on ice for 5 min. Supernatants were centrifuged at 10,000 x g at 4˚C for 5 min to pellet proteins. Deproteinated supernatants were transferred to tubes containing 50 µl potassium carbonate to neutralize the acid and centrifuged at 10,000 x g at 4˚C for 5 min to remove any precipitated salts. Pyruvate concentrations were measured using a luminescence assay kit from Cayman Chemical (Ann Arbor, MI) according to the manufacturer's instructions.

Gas Chromatography-Mass Spectrometry (GC-MS) metabolite analysis

At indicated timepoints, ultrapure neutrophils ($2.5x10^6$/condition) were washed with 1 ml HBSS without cations and pelleted at 1,000 x g for 5 min. Pellets were snap frozen and stored at -80˚C. Data were obtained using a Trace 1310 Gas Chromatograph (Thermo Fisher Scientific, Waltham, MA) coupled with an ISQ LT Singe Quadrupole mass spectrometer (Thermo Fisher Scientific, Waltham, MA) and Xcalibur Software (Thermo Fisher Scientific, Waltham, MA). Metabolite peaks were detected using TraceFinder General Quant (Thermo Fisher Scientific, Waltham, MA) and metabolites were identified using a library of standards developed by the University of Iowa Metabolomics core facility. Metabolomics data were normalized to total ion signal and analyzed by MetaboAnalyst (http://www.metaboanalyst.ca).

Quantitation of apoptosis

At the indicated time points, apoptosis was measured by flow cytometric analysis of phosphatidylserine (PS) externalization using Annexin V-FITC, with addition of propidium

iodide (PI) to detect plasma membrane permeabilization and progression to late apoptosis/secondary necrosis as we described (56, 103). In brief, neutrophils ($5x10^5$/condition) were costained with Annexin V–FITC and PI (both from BioVision, Milpitas, CA) in binding buffer (10 mM HEPES pH 7.4, 140 mM NaCl, 2.5 mM $CaCl_2$) for 5 min, in the dark. Approximately 10,000 events per sample were collected using an Accuri C6+ flow cytometer (BD Biosciences, East Rutherford, NJ) and the data were analyzed using Accuri C6+ software (BD Biosciences, East Rutherford, NJ).

Inhibitor treatments

Inhibitors were added to neutrophils at the following final concentrations 1 hr prior to infection, unless otherwise indicated: 20 μM WZB-117 (20 mM stock in DMSO, Sigma Aldrich, Burlington, MA), 5 mM 2-deoxy-D-glucose (2-DG) (100 mM stock in RPMI-1640, Sigma Aldrich, Burlington, MA), 50-100 μM 3-(3-pyridinyl)-1-(4-pyridinyl)-2-propen-1-one (3PO, 100 mM stock in DMSO, Sigma Aldrich, Burlington, MA), 20 μM CP-91149 (20 mM stock in DMSO, Sigma Aldrich, Burlington, MA), 40 μg/ml chlorogenic acid (40 mg/ml stock in DMSO, Sigma Aldrich, Burlington, MA), 30 μM SB216763 (30 mM stock in DMSO, Sigma Aldrich, Burlington, MA), 25 μM BPTES (25 mM stock in DMSO, Sigma Aldrich, Burlington, MA), or 25 μM 3-Mercaptopicolinic acid (3-MPA) (25 mM stock in DMSO, Cayman Chemical, Ann Arbor, MI). Q-VD-OPh (10 mM stock in DMSO, Cayman Chemical, Ann Arbor, MI) was added to a final concentration of 10 μM, at time zero simultaneously with initiation of infection (no pretreatment).

Immunoblotting

Neutrophils were lysed with 10% NP-40 containing protease and phosphatase inhibitors in Tris-buffered saline (36.76 μg/ml Aprotinin, 43.2 mM Levamisole, 8.65 mM AEBSF, 40.5 μg/ml Leupeptin, 1.76 mM PMSF, 13.2 nM Pepstatin A, 6.76X Protease inhibitor cocktail (all Sigma Aldrich, Burlington, MA) and 6.76X phosphatase inhibitor cocktail (Thermo Fisher Scientific, Waltham, MA). Proteins were separated on NuPAGE 4–12% Bis–Tris gradient gels (Invitrogen, Carlsbad, CA) and transferred to polyvinylidene difluoride membranes (Perkin Elmer, Waltham, MA). Membranes were blocked with 5% bovine serum albumin in Tris-buffered saline with 0.1% Tween 20, then probed with 1:500 rabbit anti-XIAP (23453-1-AP, Proteintech, Rosemont, IL), 1:300 rabbit anti-MCL-1 (16225-1-AP, Proteintech). 1:500 mouse anti-caspase-3 (clone C33, 3004, BioVision), 1:500 rabbit anti-GBE1 (HPA038073, Sigma Aldrich, Burlington, MA), 1:500 rabbit anti-UGP2 (HPA034697, Sigma Aldrich, Burlington, MA), or 1:500 rabbit anti-GYS1 (3893S, Cell Signaling Technology, Danvers, MA). The anti-β-actin (NB600-503SS, Novus Biologicals, Littleton, CO) loading control was used at 1:2,000. Bands were detected using 1:2000 horseradish-peroxidase-conjugated secondary antibodies (Cytiva, Marlborough, MA) and the Pierce SuperSignal West Femto chemiluminescent substrate (Thermo Fisher Scientific, Waltham, MA) and the Odyssey Fc imaging system (LI-COR Biosciences, Lincoln, NE).

Quantitation of glucose uptake

Glucose uptake was measured at indicated times using the zero trans method, as previously described (156). Specifically, neutrophils ($2x10^5$/condition) were centrifuged at 1,400 x g for 5 min, resuspended in glucose-free RPMI 1640 and incubated at 37˚C with 5% CO_2 for 5

minutes. [^{3}H]2-deoxy-D-glucose (1 μCi/ml) was added to a final concentration of 100 μM (0.1 μCi/ml, 1 μCi/sample) and samples were incubated at 37˚C for 3 min. Ice-cold glucose free-RPMl 1640 containing 0.3 mM phloretin (Cayman Chemical, Ann Arbor, MI) was added and samples were placed on ice for 5 min to stop glucose uptake. Samples were centrifuged through a 50 μl cushion of ice-cold 10% (w/v) bovine serum albumin at 8,800 x g for 30 sec and cells were lysed in 100 μl of 1% Triton X-100. Lysates were transferred to scintillation vials along with 5 ml Econo-Safe Economical Biodegradable Counting Cocktail (Research Products International, Mount Prospect, IL) and vials were shaken for 10 sec before counting in a LS6500 Multi-Purpose Liquid Scintillation Counter (Beckman Coulter, Brea, CA).

Measurement of intracellular glycogen stores

Neutrophils (1×10^6 /condition) were lysed with 200 μl ice-cold ddH_2O and boiled at 95˚C for 10 min. Lysates were centrifuged at 18,000 x g at 4˚C for 10 min to remove insoluble material. Glycogen concentrations were measured by colorimetric assay, according to kit instructions (BioVision, Milpitas, CA).

Statistical analyses

All data are plotted as mean ± SEM and represent at least three independent experiments. Data were analyzed using GraphPad Prism version 8 or 9 with $p < 0.05$ dictating statistical significance. Data from experiments with one variable were analyzed via Student's *t*-test. Data from experiments with multiple variables were analyzed via two-way ANOVA and Tukey's multiple-comparisons posttest. Additional details are provided in the figure legends.

Results

Genes encoding glycolytic enzymes and glucose transporters are upregulated by LVS infection

We demonstrated previously that both type B (LVS) and type A (Schu S4) *F. tularensis* strains significantly delay the onset of apoptosis as a means to extend human neutrophil lifespan and this is achieved, at least in part, by transcriptional reprogramming (56, 58, 59). Our prior analysis of the microarray dataset focused on differential expression of genes encoding apoptosis regulators and cell survival factors. However, these data also revealed significant differential expression of ~800 genes linked to metabolism, and glycolysis was among the top pathways identified by KEGG analysis at all timepoints examined 3-24 hours post infection (hpi) (59). Specifically, 10 of 11 genes encoding glycolysis enzymes were induced by LVS along with the two main glucose transporters (GLUTs) that human neutrophils express (**Figure 13A**) (59, 157).

Herein, we validated the microarray data using qRT-PCR and our data demonstrate that expression of genes encoding hexokinase-2 (*HK2*), lactate dehydrogenase (*LDHA*) and GLUT-3 (*SLC2A3*) were significantly increased by 6 hpi (**Figure 13B**). *PFKFB3* (6-phosphofructo-2-kinase/fructose-2,6-bisphosphatase) expression followed a similar trend of upregulation but did not reach statistical significance (**Figure 13B**). Phosphofructokinase (*PFKL*) expression was significantly higher in LVS-infected neutrophils immediately following infection and at 6 hpi (**Figure 13B**). Thus, our current and published data demonstrate upregulation of genes linked to glycolysis during LVS infection.

Francisella infection increases glycolysis and glycolytic capacity

Based on our gene expression data, we hypothesized that glycolytic activity was increased in LVS-infected neutrophils. To address this, we used a Seahorse metabolic analyzer to

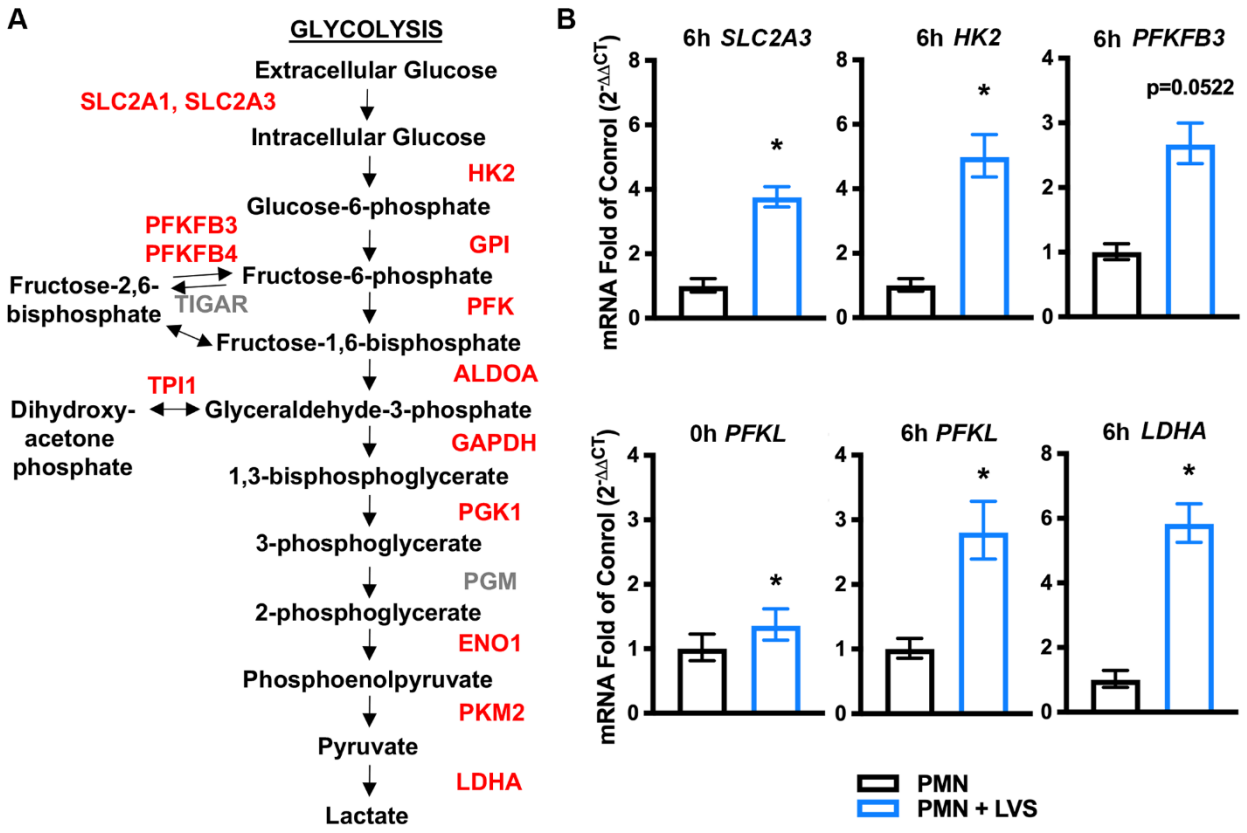

Figure 13. LVS significantly upregulates PMN genes encoding glycolytic enzymes and glucose transporters.

(A) Glycolysis pathway genes shown in red are significantly upregulated relative to uninfected cells by microarray analysis (22). **(B)** Validation of the microarray data by qRT-PCR analysis of *SLC2A3* (6 hpi), *HK2* (6 hpi), *PFKFB3* (6 hpi), *PFKL* (0 hpi and 6 hpi), and *LDHA* (6 hpi), n=3, *$p < 0.05$.

measure glycolysis and glycolytic capacity in neutrophils at various timepoints after infection with comparison to the uninfected controls **(Figure 14)**. Seahorse curves obtained at 12 hr are shown in **Figure 14A**. Pooled data show that in agreement with our microarray data, glycolysis **(Figures 14B-D**) and glycolytic capacity **(Figures 14E-G)** of LVS-infected neutrophils were significantly increased by 12 hpi **(Figures 14C, 14F**) and were sustained thereafter, although overall responses for both infected and control cells were lower at 24 hr **(Figures 14D, 14G)**.

A key outcome of glycolysis is lactate secretion, which drives ECAR detected by Seahorse analysis. Congruent with the data shown in Figure 2, lactate progressively increased in neutrophil extracellular medium and was significantly more abundant following LVS infection than the uninfected controls (**Figure 15A**). Conversely, extracellular pyruvate levels were significantly reduced (**Figure 15B**). In addition, LVS-infected neutrophils contained significantly more intracellular lactate ($p < 0.001$) and a significantly higher ratio of lactate to pyruvate than control neutrophils ($p < 0.01$) at all timepoints examined (**Figure 16**). In agreement with the fact that mature human neutrophils rely primarily on glycolysis for ATP generation (82), we also show that LVS-infected neutrophils contained significantly more ATP than their uninfected counterparts at 24 hpi **(Figure 15C**). LVS lactate, pyruvate, and ATP were also quantified (**Figures 15A-C**), and these data demonstrate that bacterial metabolites cannot account for the differences between control and infected neutrophils. Significant induction of glycolysis was independently confirmed by quantitation of metabolites using GC-MS (**Figure 17**). These data confirm the differential abundance of lactate and pyruvate shown in Figure 3 and extend these data to demonstrate that fructose-6-phosphate and glucose-6-phosphate were also more abundant in the infected PMNs by 9 hpi. In contrast, levels of the TCA cycle intermediates succinate and citrate were unchanged (data not shown).

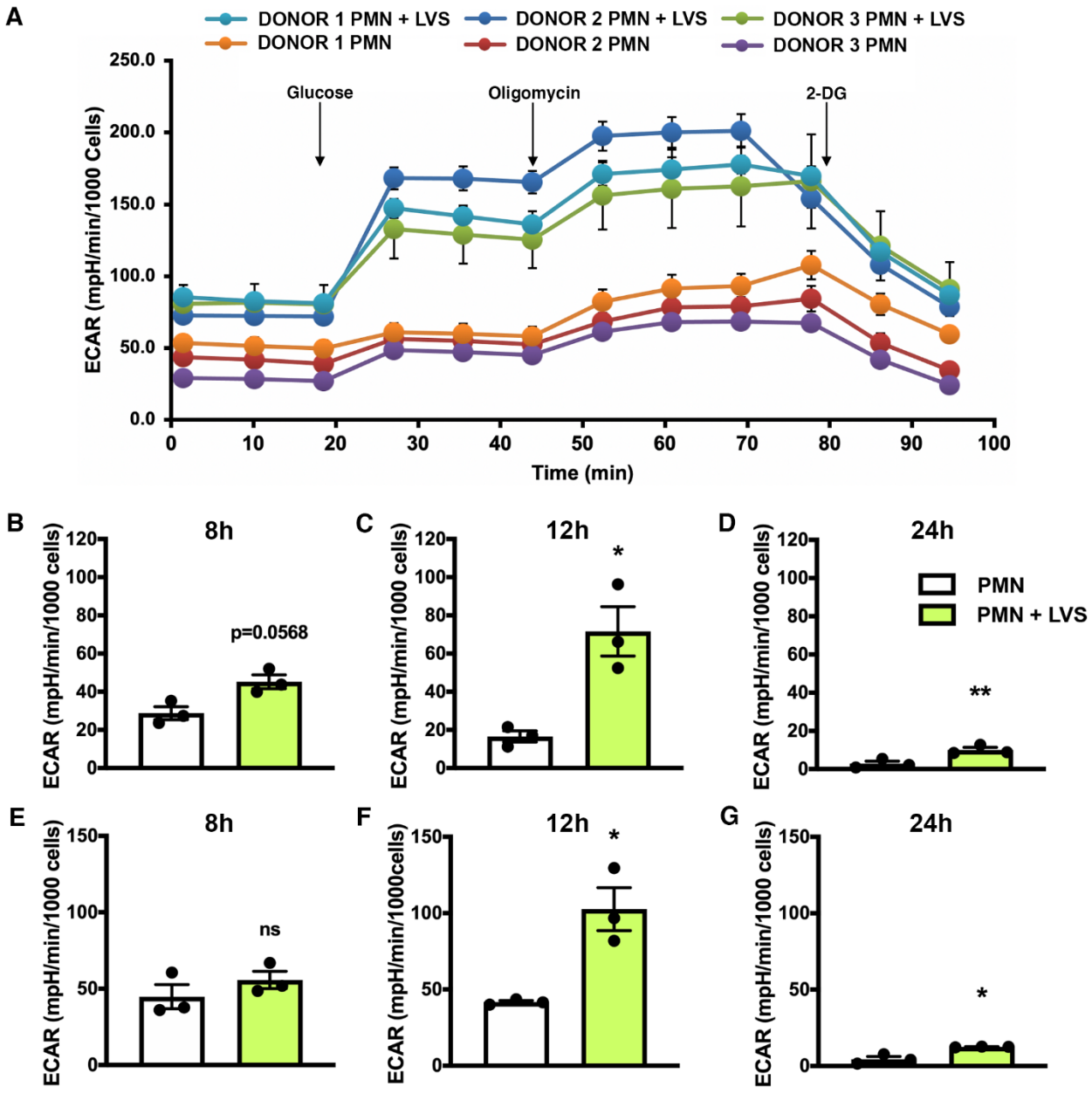
A
DONOR 1 PMN + LVS
DONOR 2 PMN + LVS
DONOR 3 PMN + LVS
DONOR 1 PMN
DONOR 2 PMN
DONOR 3 PMN
Glucose
Oligomycin
2-DG
ECAR (mpH/min/1000 Cells)
Time (min)
B
8h
p=0.0568
C
12h
D
24h
PMN
PMN + LVS
E
8h
ns
F
12h
G
24h
ECAR (mpH/min/1000 cells)

Figure 14. LVS infection upregulates PMN glycolysis.

Glycolytic function measured by Seahorse analysis as extracellular acidification rate (ECAR) in control and LVS-infected PMNs, n=3. **(A)** ECAR curves at 12 hr. Glucose was injected to a final concentration of 10 mM at 20.84 min, oligomycin was injected to a final concentration of 1 μM at 46.78 min and 2-DG was injected to a final concentration of 50 mM at 72.83 min. Where not visible, error bars are smaller than symbols. Quantitation of glycolysis **(B–D)** and glycolytic capacity **(E–G)** in control and LVS-infected PMNs at 8, 12 and 24 hpi. *$p < 0.05$. **$p < 0.01$. ns, not significant.

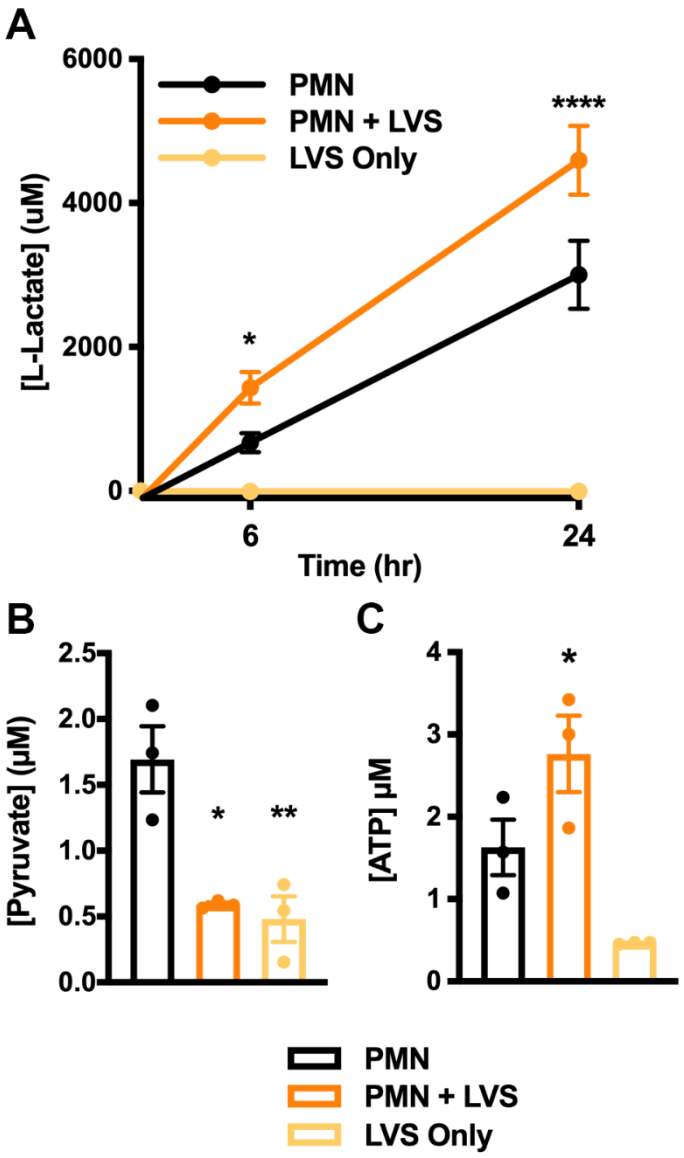

Figure 15. Differential effects of LVS on PMN lactate, ATP, and pyruvate.

(A) Amount of lactate released by control and infected PMNs or LVS alone at 0, 6 and 24 hpi, n=3-4. ****$p < 0.0001$, *$p < 0.05$ vs. uninfected control cells at the indicated time points. **(B, C)** Pyruvate (B) and ATP (C) levels of control and infected PMNs or LVS alone at 24 hr, n=3. *$p < 0.05$, **$p < 0.01$ vs. control PMNs as indicated.

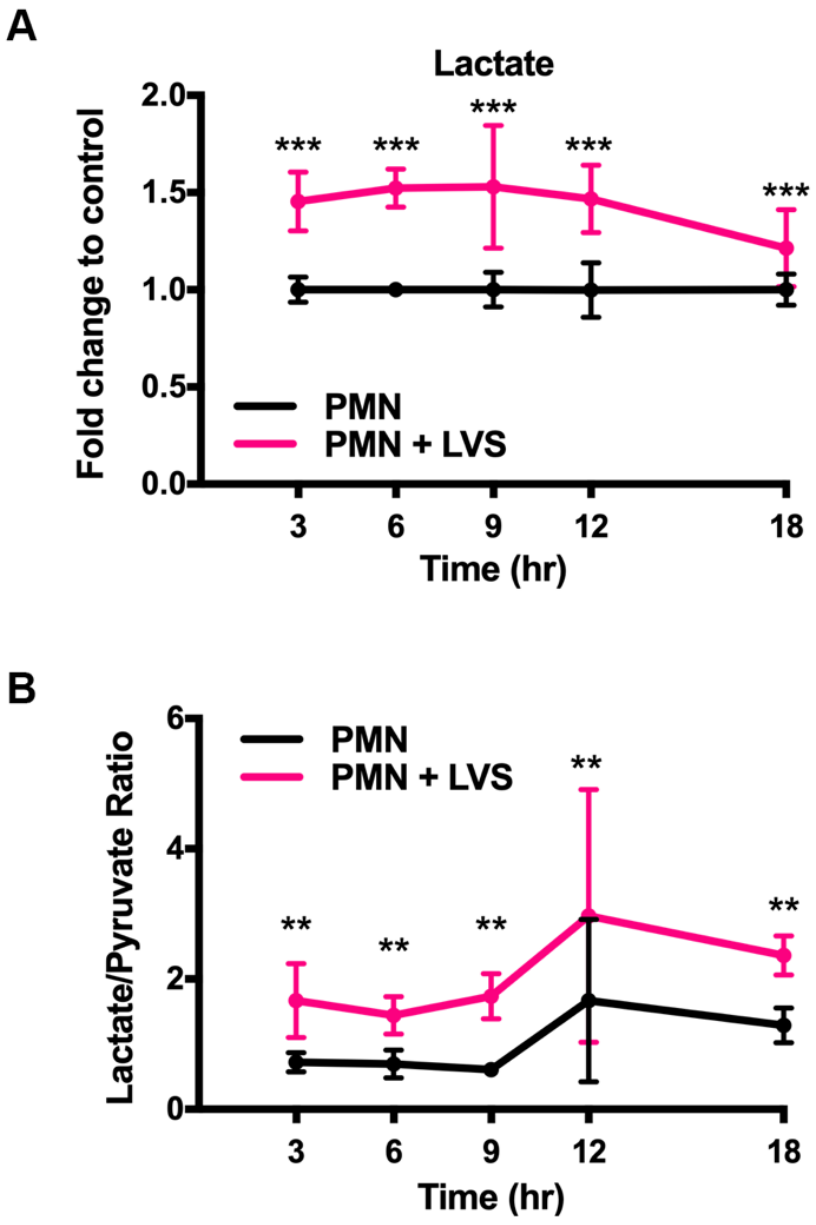

Figure 16. LVS-infected PMNs contain significantly more intracellular lactate.

(A-B) Lactate abundance (A) and lactate/pyruvate ratios (B) measured by GC-MS in control and LVS-infected PMNs at the indicated timepoints, n=3-6. $^{**}p < 0.01$, $^{***}p < 0.001$ compared to control PMNs at each timepoint. Where not visible, error bars are smaller than symbols.

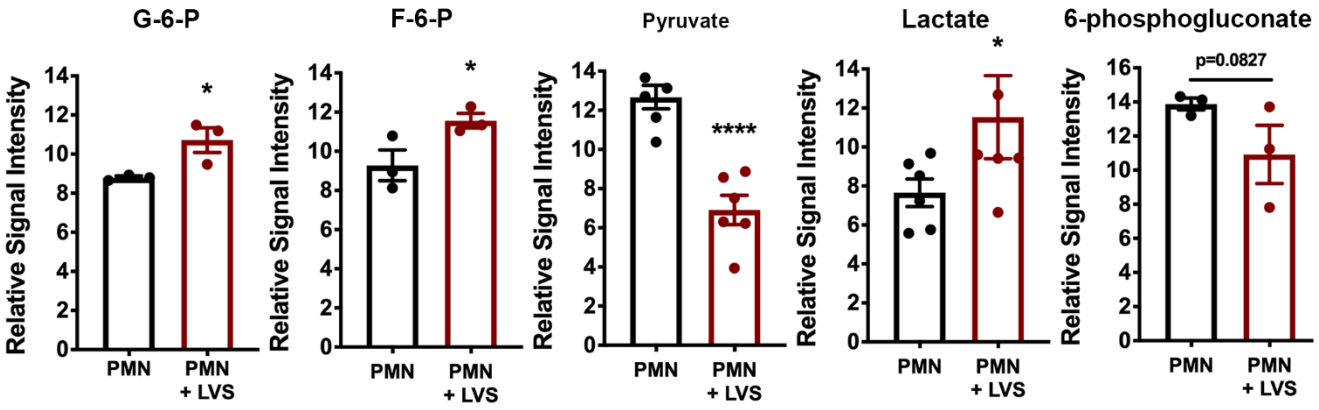

Figure 17. Differential effects of LVS infection on PMN metabolite levels.

The signal intensities of glucose-6-phosphate (G-6-P), fructose-6-phosphate (F-6-P), pyruvate, lactate and 6-phosphogluconate, relative to total ion signal, measured by GC-MS in control and LVS-infected PMNs at 9 hpi, n=3-6. *$p < 0.05$, ****$p < 0.0001$ as indicated.

KEGG analysis of our microarray data also identified the pentose phosphate pathway (PPP)/hexose monophosphate shunt (HMS), but in this case expression of genes encoding pathway enzymes was significantly downregulated rather than induced between 6 and 24 hpi, including glucose-6-phosphate dehydrogenase (*G6PDH*), 6-phosphogluconate dehydrogenase (*PGD*), 6-phosphogluconolactonase (*6PGLS*) and ribose-5-phosphate epimerase (*RPIA*) (59). In agreement with this, 6-phosphogluconate was slightly less abundant in neutrophils after LVS infection by GC-MS (**Figure 17**).

Following phagocytosis, *Francisella* escapes the phagosome and replicates in the cytosol (21-23). To determine whether phagosome egress and bacterial localization in the cytosol were required for the observed glycolytic upregulation, we infected with an isogenic LVS *fevR* mutant, which remains viable but is incapable of phagosome egress (29), and measured glycolysis via lactate release (**Figure 18**). We have previously demonstrated that this mutant retains the ability to extend neutrophil lifespan (103), and in keeping with our hypothesis that neutrophil apoptosis and glycolysis are linked, we observe that these mutant organisms also triggered glycolysis induction (**Figure 18**). These data indicate that localization of the bacteria to the cytosol is not required for glycolysis induction to occur in *F. tularensis*-infected PMNs.

Taken together, our biochemical analyses demonstrate significant induction of glycolysis and glycolytic capacity in LVS-infected PMNs leading to enhanced ATP production, lactate release and extracellular acidification that was not coupled to induction of the PPP.

Glycolysis inhibition blocks the ability of LVS to delay PMN apoptosis

Our next objective was to determine if glycolysis induction contributed to the ability of *F. tularensis* to extend neutrophil lifespan. To interrogate this potential link, we inhibited

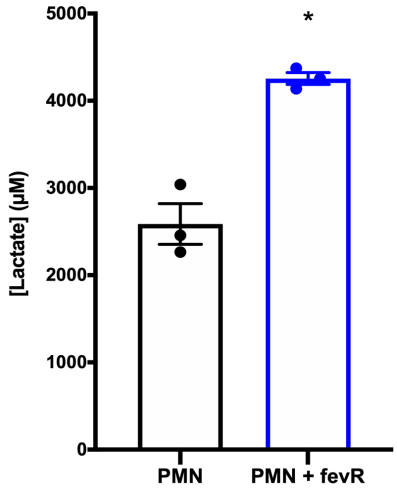

Figure 18. Infection with *F. tularensis* LVS *fevR* significantly increased PMN lactate release.

Amount of lactate released by control or *fevR*-infected PMNs at 12 hpi, n=3. *$p < 0.05$.

hexokinase by treatment with the glucose analog, 2-deoxy-D-glucose (2-DG) (158), and used our established methods to quantify the kinetics of PMN apoptosis using Annexin V-FITC/PI co-staining and flow cytometry (**Figure 19A**) (103, 155). Consistent with our published data, significantly fewer LVS-infected PMNs were apoptotic at 24 hpi as compared with the uninfected controls (45.75 ± 8.9% vs. 82.2 ± 3.8%, $p < 0.0001$, n=4). However, inhibition of PMN glycolysis with 2-DG prior to infection ablated the ability of LVS to extend neutrophil lifespan and at the same time accelerated constitutive apoptosis of uninfected PMNs as indicated by detection of externalized PS by Annexin V-FITC staining at 10 hr ($p < 0.0001$) (**Figure 19A**).

Similarly, the PFK and PFKFB3-inhibitor 3PO (159) undermined PMN survival in a dose-dependent manner and increased the percentage of cells that were PI-positive at 24 hr, indicating progression from early apoptosis to late apoptosis/secondary necrosis (58). Pooled data are shown in **Figure 19B,** and representative flow cytometry dot plots are shown in **Figure 20.** Based on these data, we conclude that glycolysis was essential for PMN survival and the ability of LVS to delay apoptosis.

Pyruvate preferentially accelerates death of LVS-infected neutrophils

As neutrophils have the capacity for gluconeogenesis and can convert pyruvate into glucose-6-phosphate (83), we tested the ability of pyruvate to support PMN survival. To this end, cells were cultured in either in normal RPMI-1640 (which contains 2 g/L glucose) or in medium where glucose was replaced with 2 g/L pyruvate. Under these conditions, apoptosis of LVS-infected PMNs was significantly increased by 6 hpi and glycogen stores and lactate production were significantly diminished (**Figure 21A-C**). At this same time point, lactate production by uninfected PMN was also significantly reduced, but glycogen stores and apoptosis were

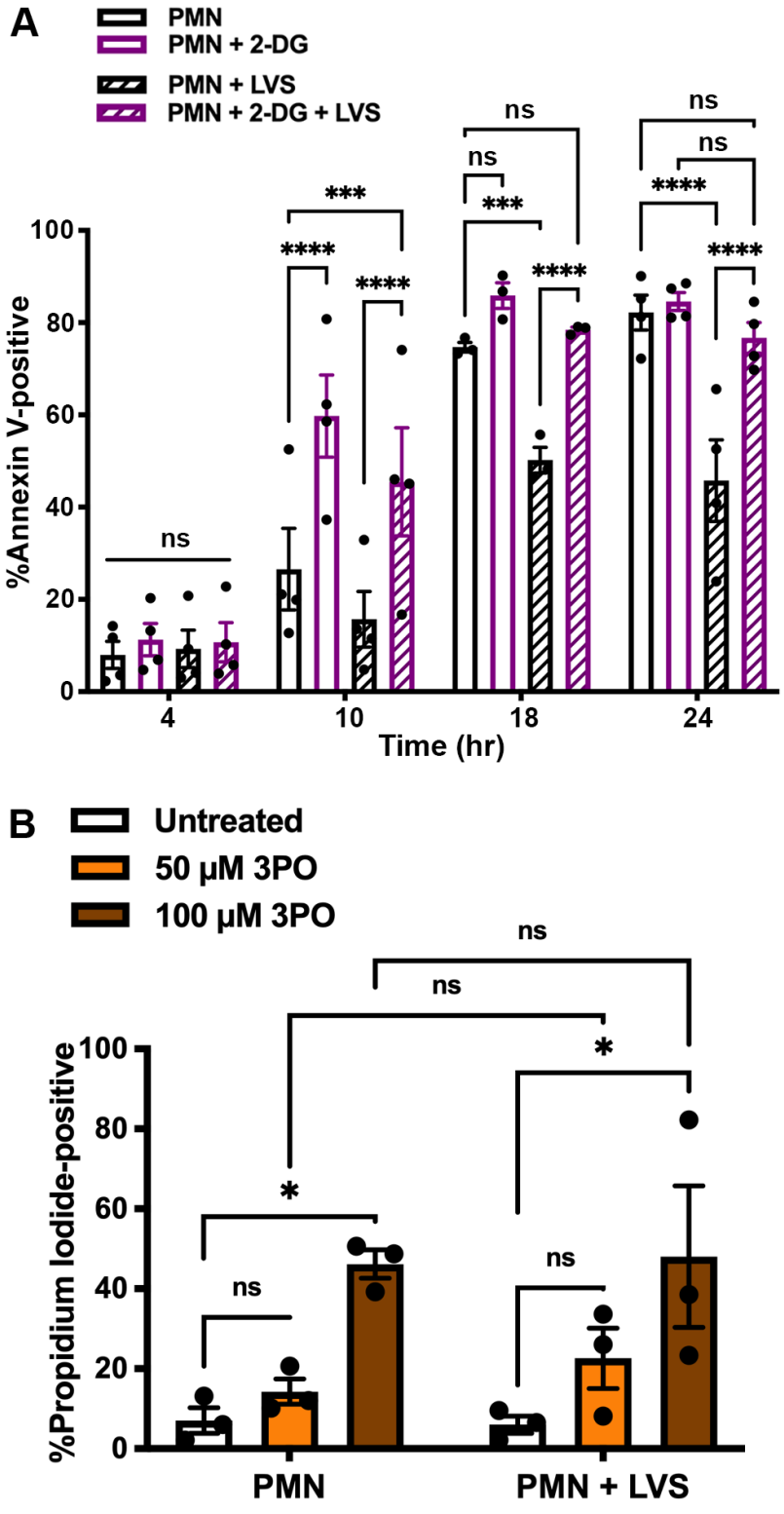
A
PMN
PMN + 2-DG
PMN + LVS
PMN + 2-DG + LVS
%Annexin V-positive
Time (hr)
ns
***
****
B
Untreated
50 µM 3PO
100 µM 3PO
%Propidium Iodide-positive
PMN
PMN + LVS
*

Figure 19. Glycolysis inhibition blocks the ability of LVS to delay PMN apoptosis.

(A) Effects of 2-DG on the kinetics of apoptosis of control and LVS-infected cells were measured using Annexin V-FITC staining and flow cytometry at the indicated time points, n=4. ***$p < 0.001$, ****$p < 0.0001$, ns, not significant, as indicated. **(B)** Effects of 3PO on PMN viability at 24 hr as measured by PI staining and flow cytometry, n=3. *$p < 0.05$, ns = not significant, as indicated.

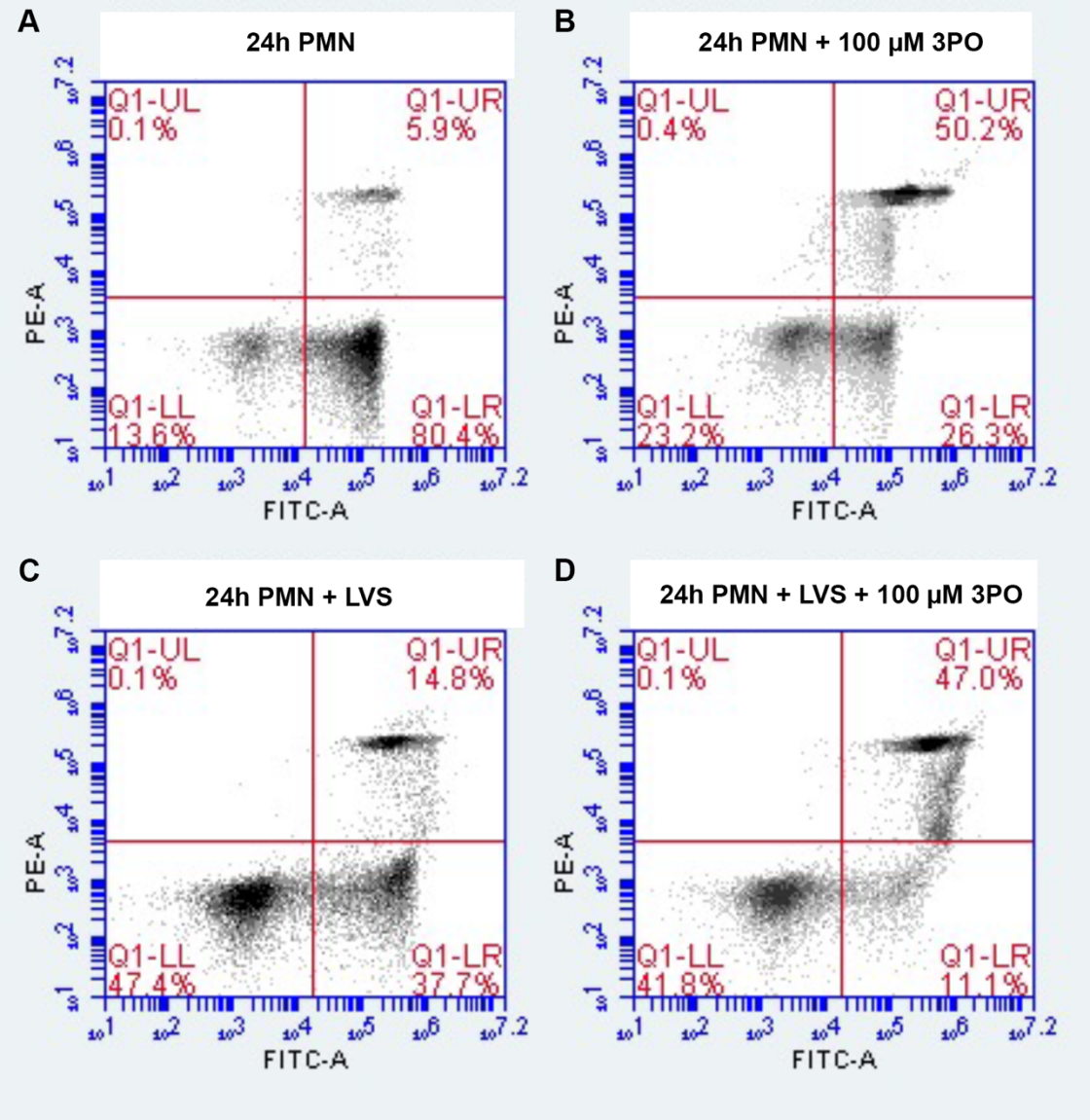

Figure 20. Representative 24 hr 3PO flow plots associated with Figure 19.

Flow cytometry dot plots of PMNs stained with Annexin V-FITC and PI at 24 hr. **(A)** PMNs. **(B)** PMNs treated with 100 µM 3PO. **(C)** LVS-infected PMNs. **(D)** LVS-infected PMNs treated with 100 µM 3PO. Data shown are representative of three independent determinations.

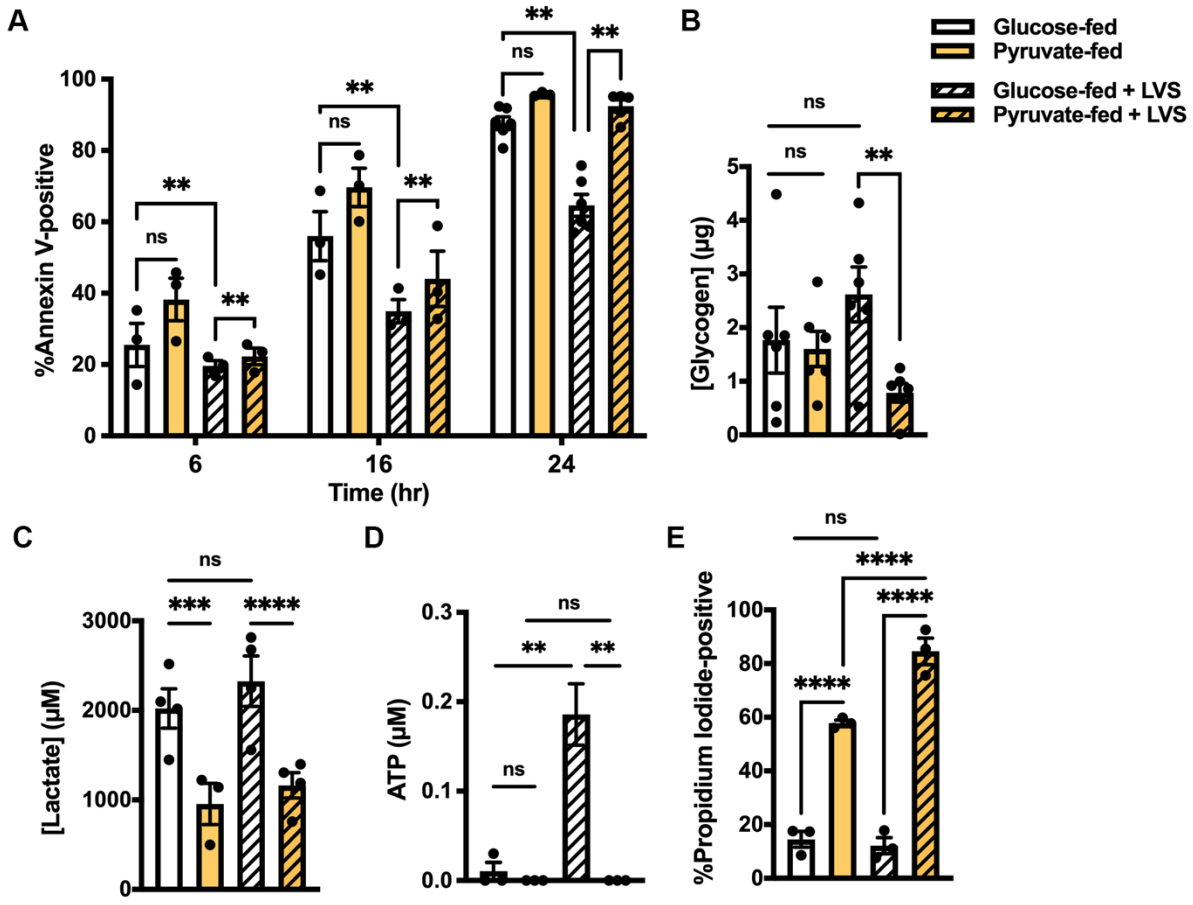

Figure 21. Differential effects of forced pyruvate feeding on apoptosis, glycolysis, and glycogen abundance.

(A) Measurement of apoptotic uninfected and LVS-infected PMNs in the presence of either 2 g/L glucose or 2 g/L pyruvate using Annexin V-FITC/PI staining and flow cytometry at the indicated timepoints, n=3-6. $^{**}p < 0.01$, ns, not significant, as indicated. **(B)** Glycogen abundance in uninfected and LVS-infected PMNs in the presence of either 2 g/L glucose or 2 g/L pyruvate at 6 hr, n=6. $^{**}p < 0.01$, ns, not significant, as indicated. **(C)** Amount of lactate released by control and LVS-infected PMNs in the presence of either 2 g/L glucose or 2 g/L pyruvate at 6 hr, n=3-4. $^{***}p < 0.001$, $^{****}p < 0.0001$, ns, not significant, as indicated. **(D)** ATP levels in uninfected and LVS-infected PMNs in the presence of either 2 g/L glucose or 2 g/L pyruvate at 24 hr, n=3. $^{**}p < 0.01$, ns, not significant, as indicated. **(E)** Percentage of Annexin V-FITC positive cells that are also PI-positive at 24 hr, n=3-6, $^{****}p < 0.0001$.

unchanged relative to the glucose-fed controls. These data suggest that pyruvate can sustain viability of uninfected PMNs for at least 6 hr. By 24 hr, nearly all pyruvate fed cells were Annexin V-positive and ATP depleted (**Figure 21A and 21D**). Moreover, a majority of cells had progressed to late apoptosis/secondary necrosis by 24 hr, but ~80% of infected PMNs were PI-positive as compared with only ~60% of their uninfected counterparts ($p < 0.0001$) (**Figure 21E**). These data identify additional differences between uninfected and infected PMNs and further support the hypothesis that glycolysis was vital for neutrophil survival and extended lifespan after LVS infection.

Glucose uptake is also increased and required for delayed apoptosis

To understand what could be linking apoptosis and glycolysis, we sought to determine what fueled the glycolytic upregulation in LVS-infected neutrophils. As glucose is the substrate of glycolysis, and expression of the genes encoding GLUT-1 (*SLC2A1*) and GLUT-3 (*SLC2A3*) were significantly increased after infection (**Figures 22A-B**) (59), we hypothesized that glucose uptake may also be enhanced. To test this, we used a sensitive and quantitative radiolabeled glucose uptake assay (156), and the data in **Figure 22A** indicate that by 12 hpi, transport of glucose into LVS-infected PMNs was significantly increased relative to the uninfected controls. WBZ-117 inhibits all glucose transporter isoforms that are expressed in PMNs (GLUT-1, GLUT-3 and GLUT-4 (160)) and pretreatment of PMNs with WBZ-117 significantly diminished the ability of LVS to sustain PMN viability at 18 and 24 hpi (**Figure 22B-C**), but unlike 2-DG (**Figure 19A**) did not accelerate constitutive apoptosis of the uninfected controls. Pooled data are shown in **Figures 22B-C** and representative flow cytometry dot plots are shown in **Figure 23**. Neutrophils can also store glucose-6-phosphate in the endoplasmic reticulum for later use, but

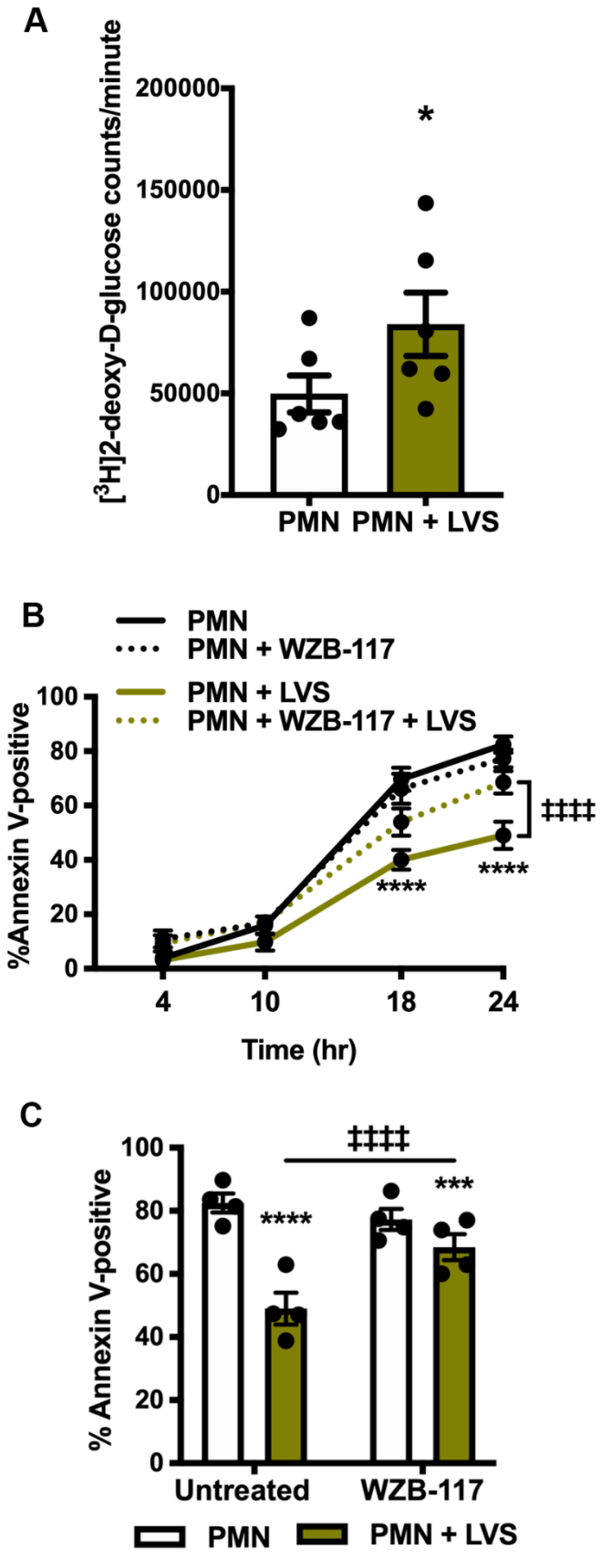
A
[3H]2-deoxy-D-glucose counts/minute
200000
150000
100000
50000
0
*
PMN
PMN + LVS
B
PMN
PMN + WZB-117
PMN + LVS
PMN + WZB-117 + LVS
%Annexin V-positive
100
80
60
40
20
0
‡‡‡‡
****
****
4
10
18
24
Time (hr)
C
% Annexin V-positive
100
80
60
40
20
0
‡‡‡‡
****
***
Untreated
WZB-117
PMN
PMN + LVS

Figure 22. Glucose uptake is increased in LVS-infected PMNs and is required for apoptosis delay.

(A) [^{3}H]2-deoxy-D-glucose uptake was measured at 12 hr. *$p < 0.05$, n=6. **(B, C)** Apoptosis of control and LVS-infected PMNs in the presence or absence of WZB-117 measured by Annexin V-FITC staining and flow cytometry at the indicated timepoints (B) and at 24 h (C). *$p < 0.05$, ***$p < 0.001$, ****$p < 0.0001$ compared to untreated, control PMNs, ‡‡‡‡$p < 0.0001$ compared to untreated, LVS-infected PMNs as indicated, n=4.

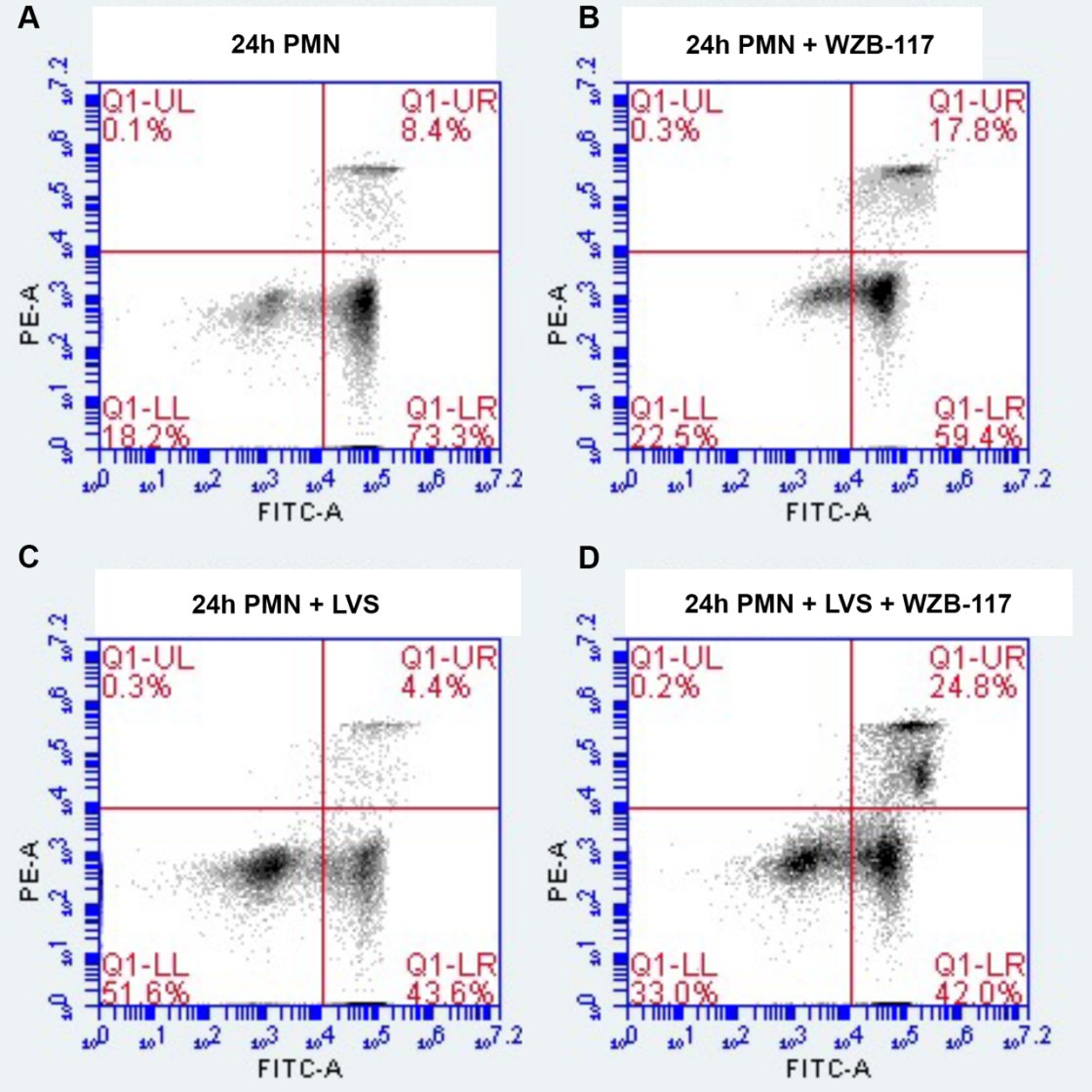

Figure 23. Representative 24 hr WZB-117 flow plots associated with Figure 22.

Flow cytometry dot plots of PMNs stained with Annexin V-FITC and PI at 24 hr. **(A)** PMN. **(B)** PMNs treated with 20 µM WZB-117. **(C)** LVS-infected PMNs. **(D)** LVS-infected PMNs treated with 20 µM WZB-117. Data shown are representative of four independent determinations.

we detected no effects on apoptosis when we treated cells with the glucose-6-phosphate translocase (G6PT) inhibitor, chlorogenic acid (161) (**Figure 24**). These data demonstrate that glucose uptake was significantly increased by LVS and was essential for delayed apoptosis of PMN after infection, whereas glucose-6-phosphate storage in the endoplasmic reticulum did not appear to play a role.

Glycogen dynamics are complex and differ in control and infected neutrophils

To ascertain the role of glycogen as a candidate regulator of PMN lifespan, we first quantified glycogen levels at multiple time points over 48 hr and the data shown in **Figure 25** are noteworthy for several reasons. First, we predicted that LVS-infected neutrophils would consume more glycogen to fuel increased glycolysis, and that glycogen levels would therefore be lower in these cells, but to our surprise LVS-infected neutrophils contained significantly more glycogen than the controls at nearly every assayed timepoint. Second, we show that glycogen was most abundant in all PMNs at 3 hr, the earliest time point examined. Thereafter, glycogen stores of the control PMNs declined progressively. In marked contrast, glycogen stores of LVS-infected PMNs reached a nadir at 9 hpi but were then replenished. Thus, at 12-24 hpi, glycogen stores of LVS-infected PMNs were similar to the control cells at 6 hr and declined significantly only at 32 and 48 hpi. Taken together, these data demonstrate that glycogen stores are dynamically regulated, and that this storage form of glucose was significantly more abundant in LVS-infected PMNs at both early and later stages of infection. Nonetheless, genes encoding the three main enzymes of glycogenesis, UDP-glucose pyrophosphorylase 2 (*UGP2*), glycogen branching enzyme (*GBE1*) and glycogen synthase (*GYS1*) were not differentially expressed as judged by qRT-PCR (**Figure 26A**) and LVS also had no apparent effect on the levels of each

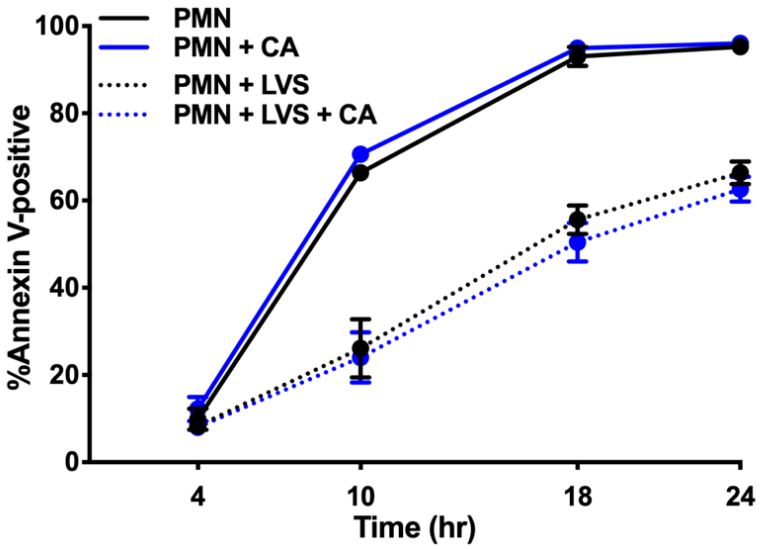

Figure 24. G6PT inhibition does not impact PMN lifespan.

Effect of chlorogenic acid (CA) on apoptosis of control and LVS-infected PMNs was measured using Annexin V-FITC staining and flow cytometry at the indicated time points, n=3-5.

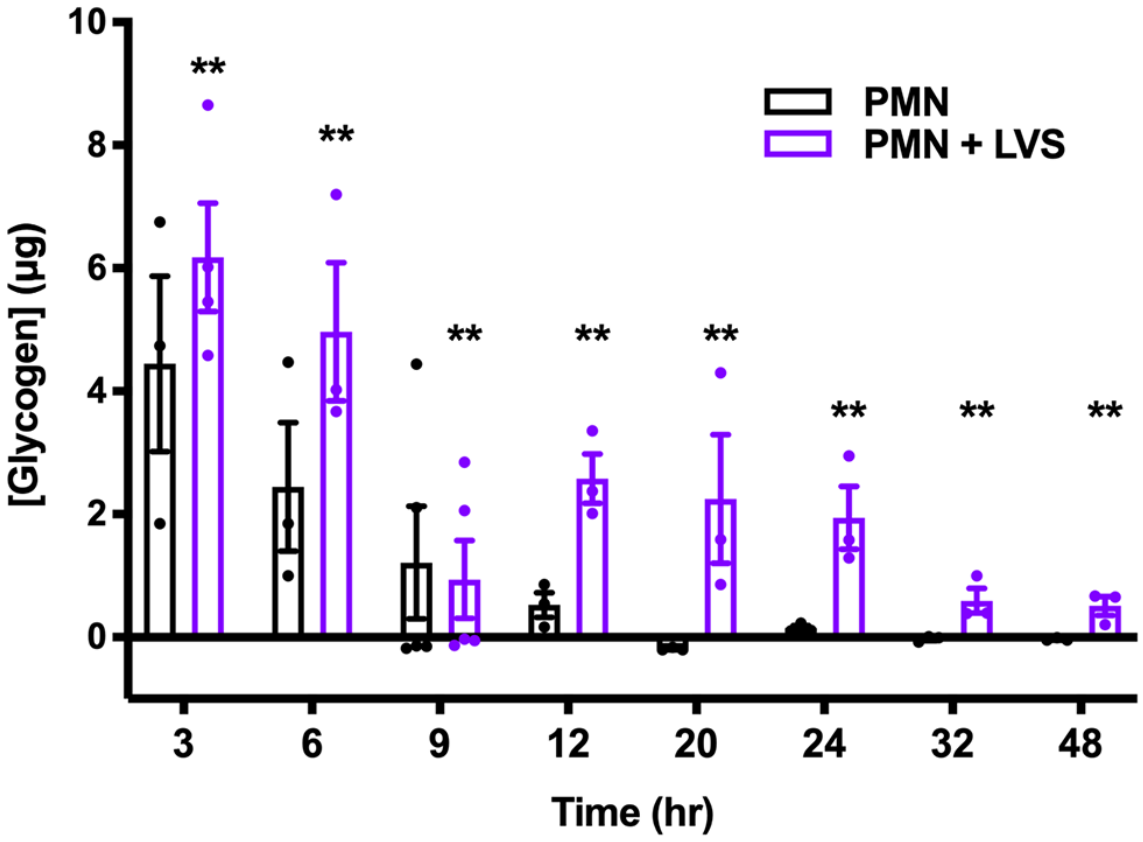

Figure 25. LVS modulates PMN glycogen dynamics and abundance.

Glycogen stores of control and LVS-infected PMNs were quantified at the indicated timepoints, n=3-5. $^{**}p < 0.01$ compared to control PMNs at each timepoint.

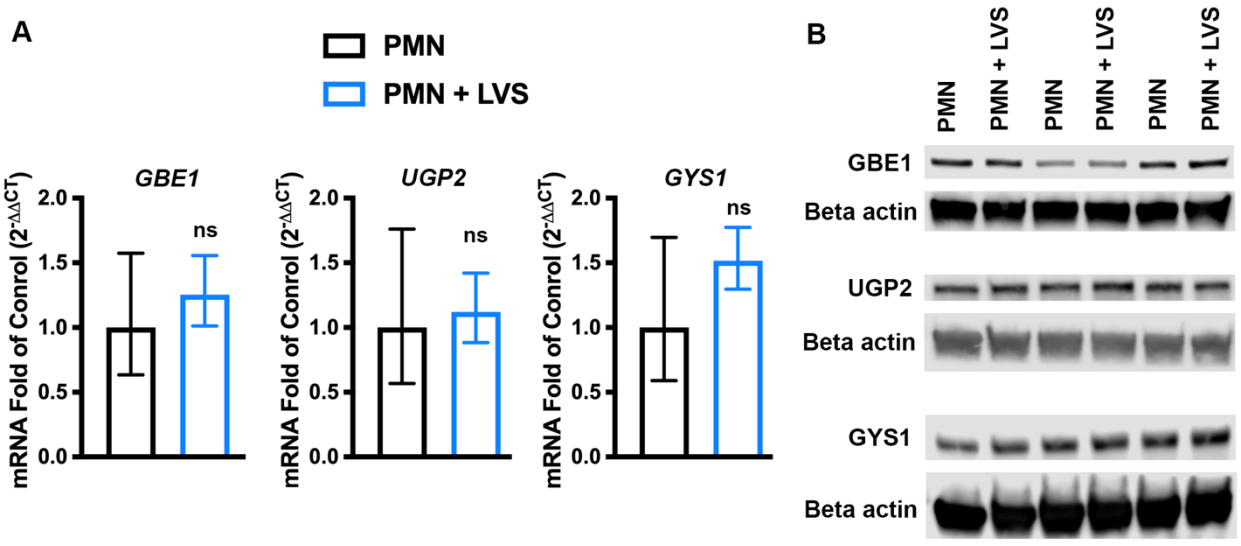

Figure 26. LVS infection does not alter expression of glycogenesis enzyme genes or protein abundance.

(A) qRT-PCR analysis of *GBE1*, *UGP2* and *GYS1* at 12 hr, n=3, ns, not significant. **(B)** Immunoblotting analysis of GBE1, UGP2 and GYS1 in neutrophil lysates from three different donors prepared at 12 hr, with β-actin as the loading control, n=3.

enzyme as judged by immunoblotting of cell lysates (**Figure 26B**). Thus, the ability of LVS-infected PMNs to replenish glycogen stores at 12 hpi cannot be attributed to changes in the abundance of biosynthetic pathway enzymes.

To demonstrate a definitive link between glycogen abundance and cell longevity we assessed the extent to which pharmacologically increasing glycogen affected apoptosis. To this end, we treated cells with CP-91149, a glycogen phosphorylase inhibitor that effectively prevents glycogen breakdown (162). Following CP-91149 treatment we quantified glycogen levels, apoptosis, and lactate release (**Figure 27**). As expected, neutrophils treated with CP-91149 contained significantly more glycogen at 6 hr **(Figure 27A)** and 24 hr **(Figure 27B)** than their untreated counterparts. Specifically, CP-91149 increased glycogen levels ~10-fold at 6 hr in the uninfected PMNs and ~2-fold in the LVS-infected PMNs. At the same time, CP-91149 treatment significantly delayed apoptosis of both control and LVS-infected PMNs as indicated by Annexin V-FITC staining (**Figure 27C**), and significantly increased glycolysis as indicated by quantitation of lactate release (**Figure 27D**). We also treated cells with the GSK3β inhibitor, SB216763, which relieves inhibition of glycogen synthesis, and observed that SB216763 treatment is sufficient to extend lifespan in control and LVS-infected neutrophils (**Figure 28**). We therefore conclude that pharmacologically increasing glycogen was sufficient to delay constitutive apoptosis and increase glycolysis of uninfected control PMNs and further enhanced the ability of LVS to extend PMN lifespan and upregulate glycolysis.

<u>Glutaminolysis and gluconeogenesis are not required for apoptosis delay of LVS-infected PMNs</u>

It was recently demonstrated that gluconeogenesis and glutaminolysis are key metabolic pathways for fueling antimicrobial responses and maintaining glycogen levels in neutrophils

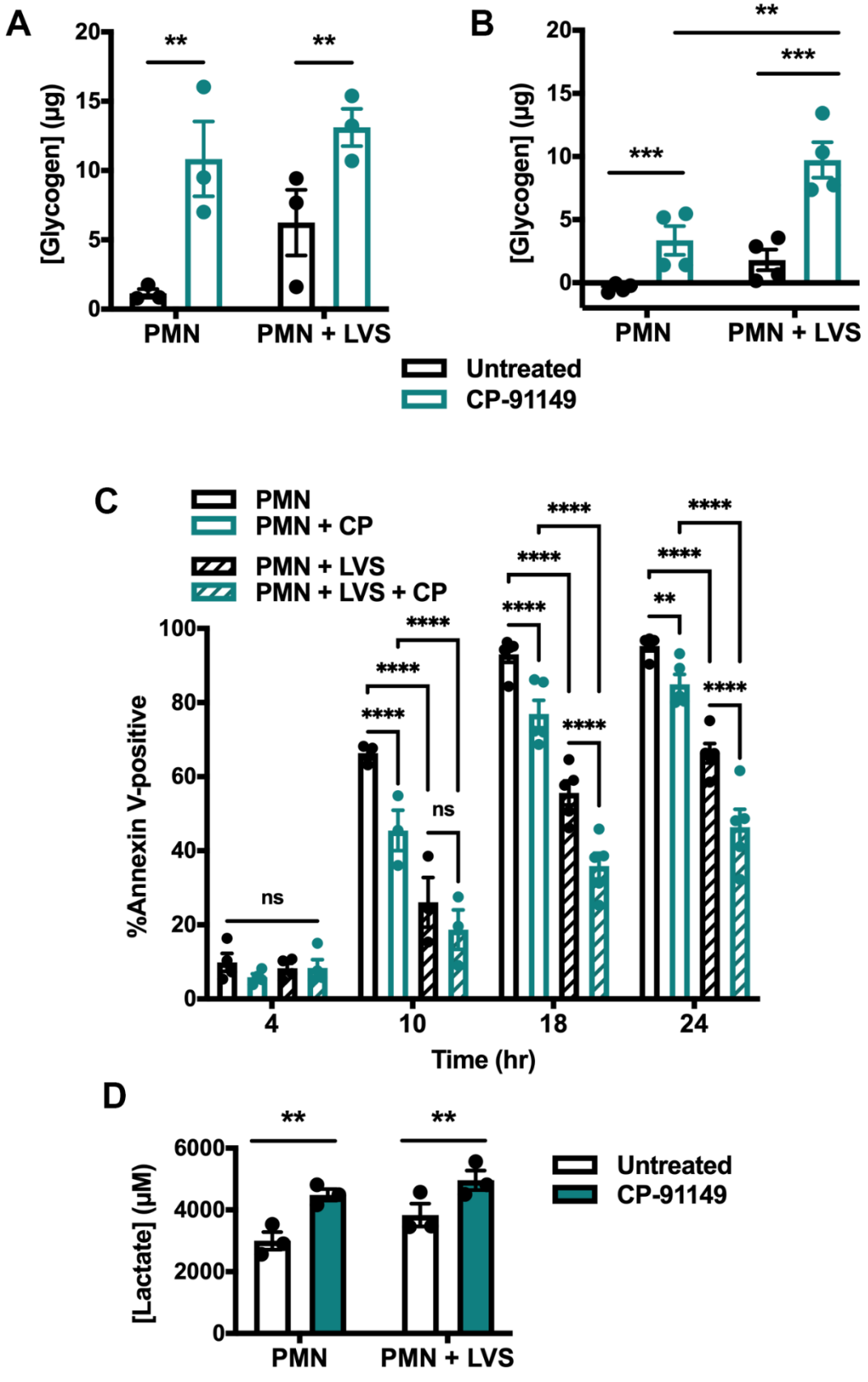
A
[Glycogen] (µg)
20
15
10
5
0
**
**
PMN
PMN + LVS
B
[Glycogen] (µg)
**
***
***
PMN
PMN + LVS
Untreated
CP-91149
C
PMN
PMN + CP
PMN + LVS
PMN + LVS + CP
%Annexin V-positive
100
80
60
40
20
0
ns
****
****
****
ns
****
****
****
**
****
****
4
10
18
24
Time (hr)
D
[Lactate] (µM)
6000
4000
2000
0
**
**
PMN
PMN + LVS
Untreated
CP-91149

Figure 27. Glycogen abundance correlates with delayed apoptosis.

(A, B) Glycogen abundance in uninfected and LVS-infected PMNs in the presence or absence of CP-91149 at 6 hr (A) and 24 hr (B), n=3-4. $^{**}p < 0.01$, $^{***}p < 0.001$ as indicated. **(C)** Apoptosis of uninfected and LVS-infected PMNs in the presence or absence of CP-91149 quantified using Annexin V-FITC staining and flow cytometry at the indicated timepoints, n=3-5. $^{**}p < 0.01$, $^{****}p < 0.0001$, ns, not significant, as indicated. **(D)** Amount of lactate released by control and LVS-infected PMNs in the presence or absence of CP-91149 at 12 hr, n=3. $^{**}p < 0.01$ as indicated.

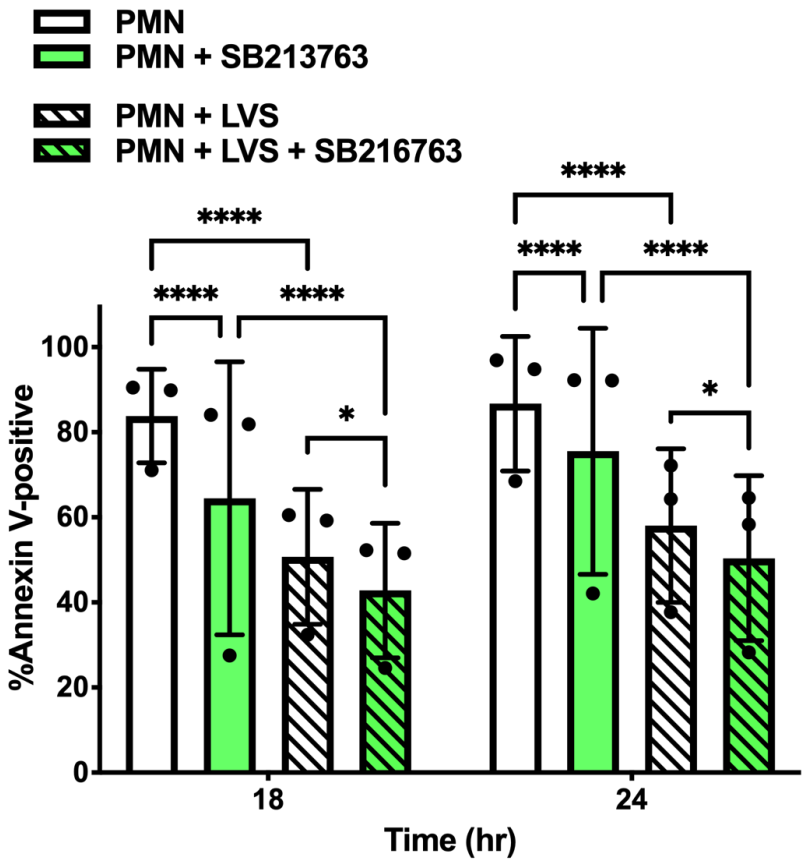

Figure 28. GSK3β inhibition extends neutrophil lifespan.

Effect of SB216763 treatment on apoptosis of control and LVS-infected PMNs was measured using Annexin V-FITC staining and flow cytometry at the indicated time points, n=3, *$p < 0.05$, ****$p < 0.0001$ as indicated.

(83). To determine the involvement of these pathways in the delayed apoptosis of LVS-infected PMNs we treated PMNs with the glutaminolysis inhibitor, BPTES, or the gluconeogenesis inhibitor, 3-Mercaptopicolinic acid (3-MPA), measured apoptosis (**Figure 29**) and glycogen levels (**Figure 30**). Interestingly, loss of glutaminolysis or gluconeogenesis had no discernible effect on apoptosis of control neutrophils and only modestly decreased apoptosis in LVS-infected cells (**Figure 29**). Similarly, BPTES or 3-MPA treatment did not significantly alter glycogen levels, regardless of infection (**Figure 30**). However, culturing cells in media that lack glutamine modestly increased necrosis, as measured by propidium iodide staining, compared to cells cultured in glutamine-containing media (**Figure 31**). These data demonstrate that glutaminolysis and gluconeogenesis play little, if any, role in increasing glycogen levels or extending lifespan in neutrophils during LVS infection.

Caspase inhibition increases PMN glycolysis, glycolytic capacity, and glycogen stores

To further examine the link between neutrophil metabolism and apoptosis, we asked if inhibiting caspases pharmacologically with the pan-caspase inhibitor Q-VD-OPh (163) would phenocopy the increased glycolysis and glycogen abundance observed in LVS-infected neutrophils. As shown in **Figure 32**, Q-VD-OPh treatment nearly ablated PMN apoptosis over the time course examined, as 94.13 ± 1.7% of drug-treated cells remained viable at 24 hr (**Figure 32A**). We next measured glycolytic function using Seahorse analysis and show that this pan-caspase inhibitor increased neutrophil glycolysis and glycolytic capacity ~7-fold at 12 hr (**Figure 32B**). Finally, we demonstrate that Q-VD-OPh-treated cells also contained significantly more glycogen at 24 hr (**Figure 32C**). These data further support the hypothesis that neutrophil survival and glycolysis are fundamentally linked and reinforce the notion that glycogen

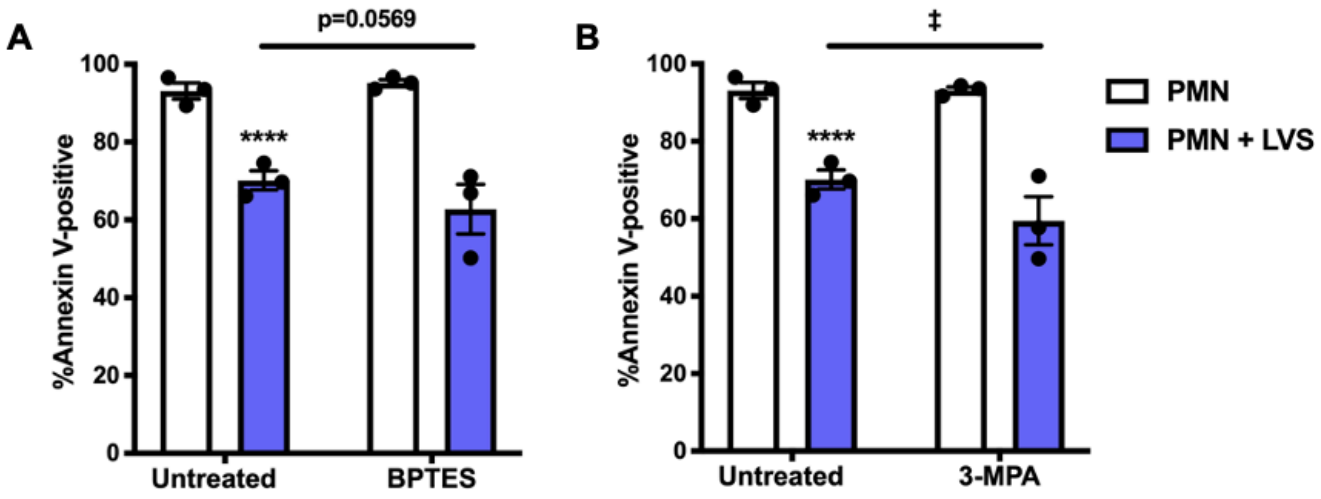

Figure 29. Inhibition of glutaminolysis or gluconeogenesis does not impact neutrophil lifespan.

Effect of **(A)** BPTES or **(B)** 3-Mercaptopicolinic acid (3-MPA) treatment on apoptosis of control and LVS-infected PMNs was measured using Annexin V-FITC staining and flow cytometry at 24 hr, n=3, ****$p < 0.0001$ compared to untreated control PMNs, ‡$p < 0.05$ compared to untreated LVS-infected PMNs.

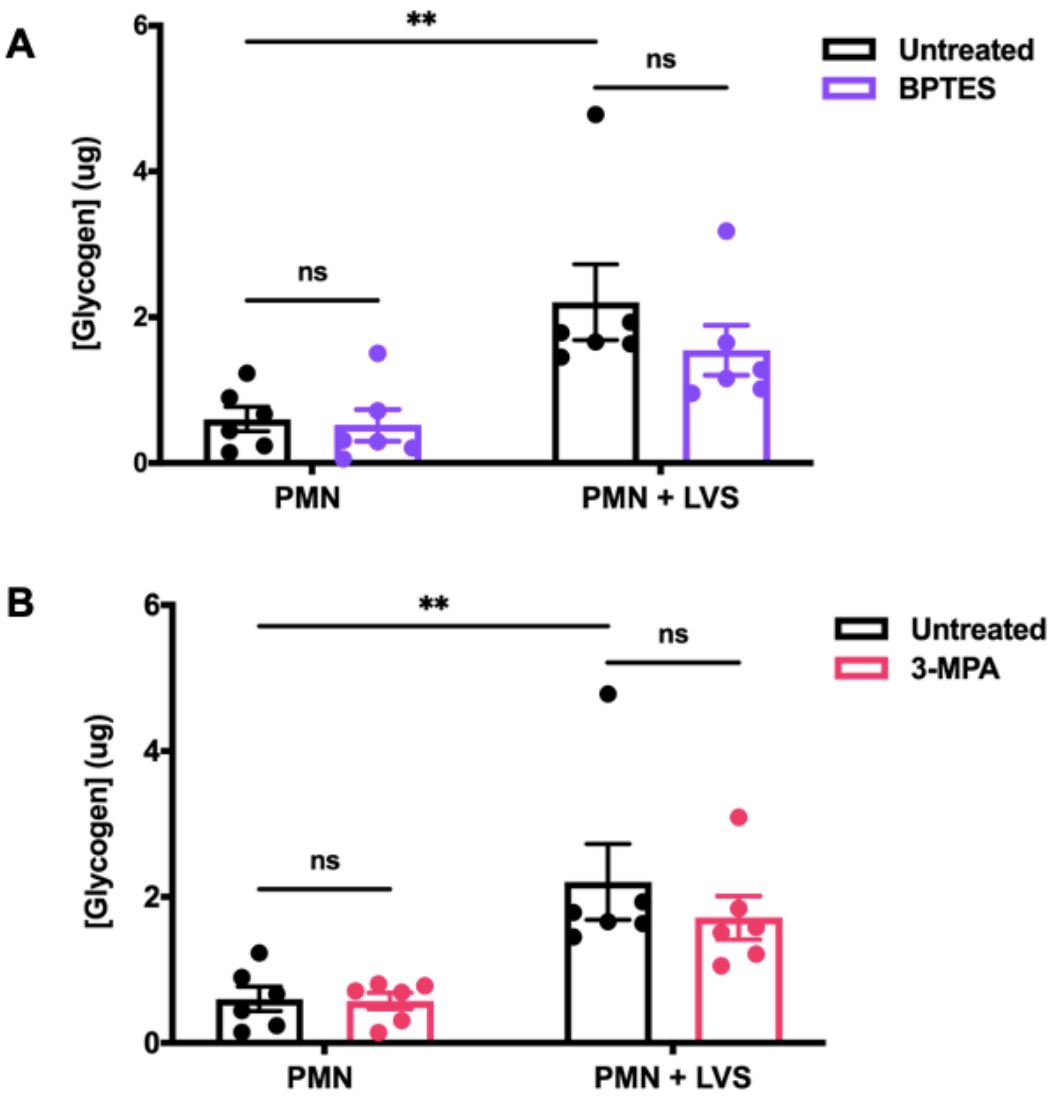

Figure 30. Inhibition of glutaminolysis or gluconeogenesis does not impact neutrophil glycogen levels.

Glycogen abundance in uninfected and LVS-infected PMNs in the presence or absence of **(A)** BPTES or **(B)** 3-Mercaptopicolinic acid (3-MPA) at 7 hr, n=6. $^{**}p < 0.01$, ns = not significant, as indicated.

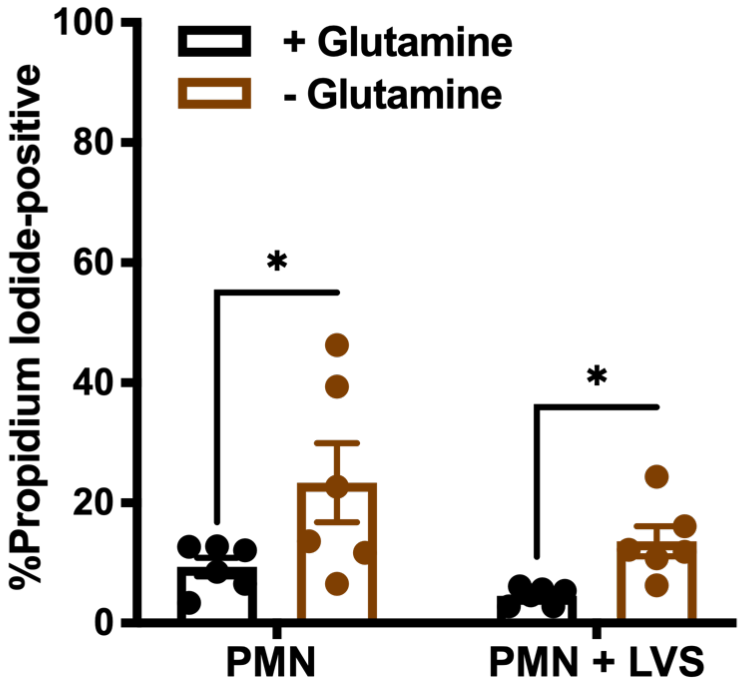

Figure 31. Glutamine starvation modestly increases neutrophil necrosis.

Measurement of apoptotic uninfected and LVS-infected PMNs cultured in either RPMI containing glutamine (+ glutamine) or RPMI lacking glutamine (- glutamine) using PI staining and flow cytometry at 24 hr, n=6. *$p < 0.05$, as indicated.

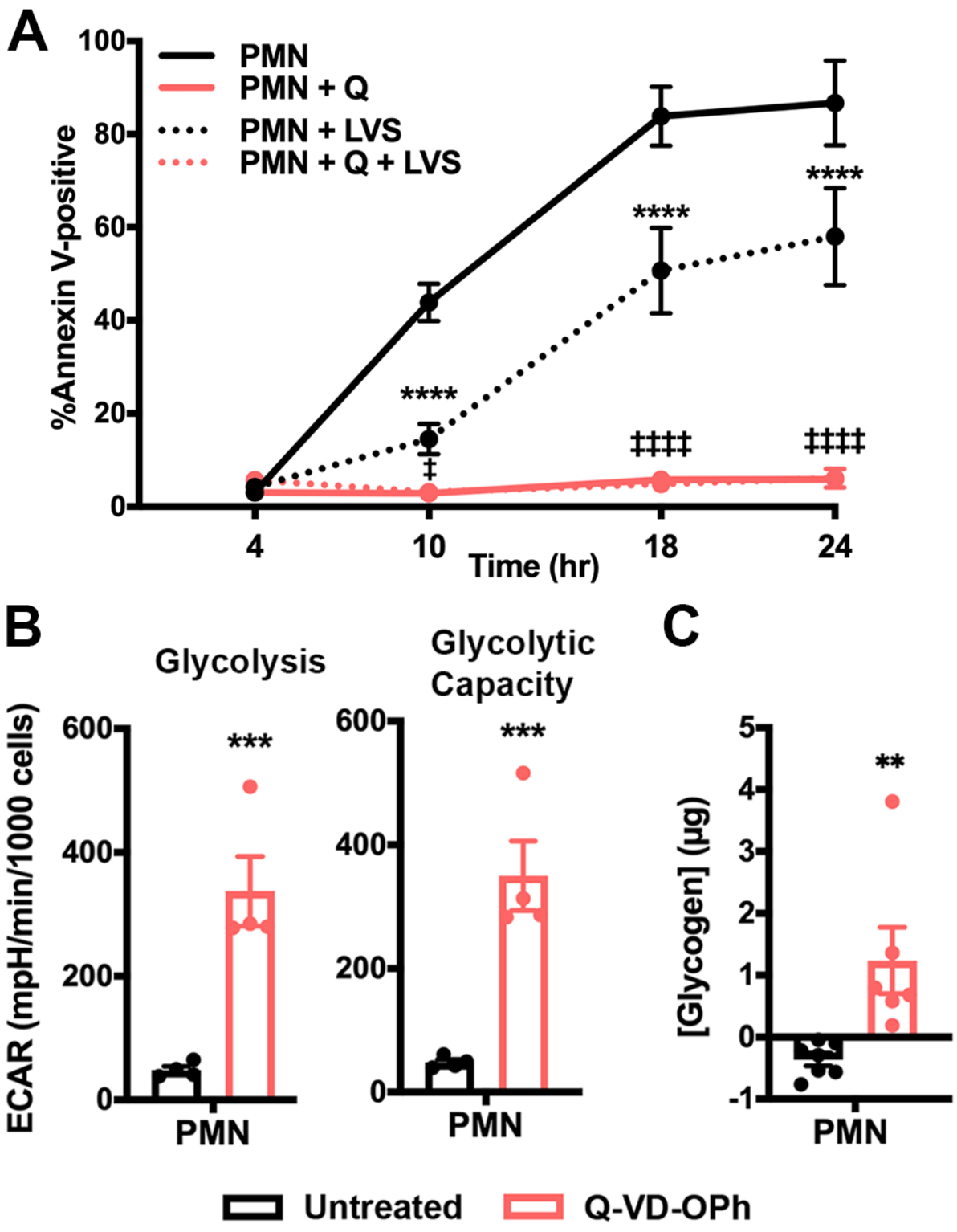
A
100
80
60
40
20
0
%Annexin V-positive
PMN
PMN + Q
PMN + LVS
PMN + Q + LVS
****
****
****
‡
‡‡‡‡
‡‡‡‡
4
10
18
24
Time (hr)
B
Glycolysis
Glycolytic Capacity
ECAR (mpH/min/1000 cells)
600
400
200
0
***
***
PMN
PMN
C
[Glycogen] (µg)
5
4
3
2
1
0
-1
**
PMN
Untreated
Q-VD-OPh

Figure 32. Caspase inhibition increases PMN glycolysis, glycolytic capacity, and glycogen abundance.

(A) Kinetics of apoptosis of control and Q-VD-OPh-treated PMNs were measured using Annexin V-FITC staining and flow cytometry. Data are the mean ± SEM, n=3. ****$p < 0.0001$ compared to untreated, uninfected PMNs, ‡$p < 0.05$ and ‡‡‡‡$p < 0.0001$ compared to untreated, LVS-infected PMNs at the indicated time points. **(B)** Quantitation of glycolysis and glycolytic capacity measured by Seahorse analysis as extracellular acidification rate (ECAR) in PMNs in the presence or absence of Q-VD-OPh at 12 hr, n=4. ***$p < 0.001$. **(C)** Measurement of glycogen abundance in PMNs in the presence or absence of Q-VD-OPh at 24 hr, n=6-7. **$p < 0.01$.

abundance correlates with delayed apoptosis.

Effects of lactate and 2-DG on apoptosis and apoptosis regulatory factors

Precisely how glycolysis is linked to PMN longevity in our system is unknown. Thus, we tested whether the amount of lactate secreted by LVS-infected PMNs (4.7 mM) was sufficient to alter constitutive apoptosis. Specifically, lactate was added to uninfected PMNs at time zero, and the rate of apoptosis was determined using Annexin V-FITC/PI staining over 24 hr. By this assay, lactate had no discernible effect on constitutive PMN death (**Figure 33**).

To interrogate the effects of 2-DG, we used western blotting. As shown in **Figure 34A**, 2-DG treatment increased processing of procaspase-3 to its cleaved, disappearance of XIAP from control PMNs by 24 hr and its sustained abundance in cells infected with LVS, but to our surprise, 2-DG did not cause XIAP to disappear from infected PMNs.

However, XIAP expression does appear to decrease with 2-DG treatment, compared to untreated, LVS-infected cells (**Figure 34B**). On the other, 2-DG had no apparent effect on levels MCL-1, regardless of infection (**Figure 34C**).

Discussion

Neutrophils are key mediators of infection resolution that are inherently short-lived and undergo constitutive apoptosis approximately 24 hours after release into circulation (37). This tightly regulated lifespan is intimately linked to cell function, as disruption of neutrophil turnover can lead to exacerbated disease and tissue destruction (43, 62, 69). Published data from our group demonstrate that infection with *F. tularensis* strains, including LVS and Schu S4,

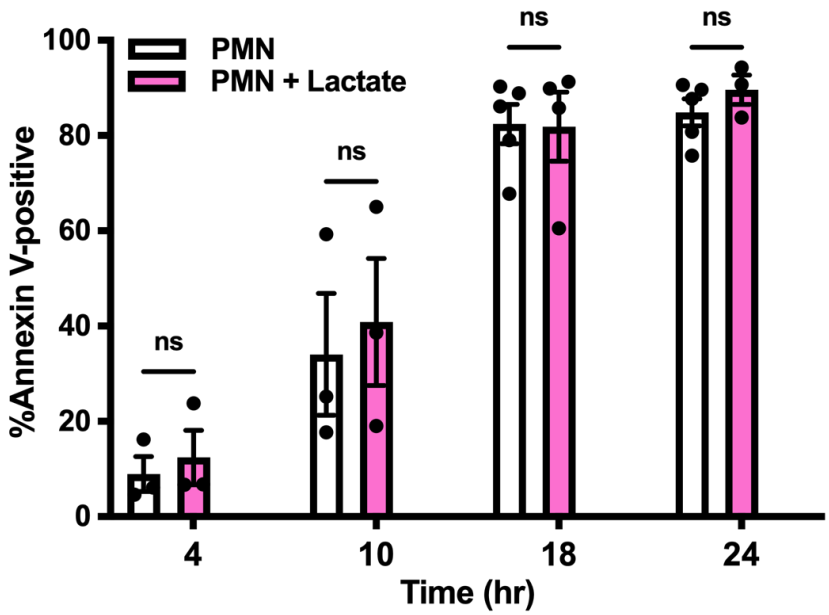

Figure 33. Exogenous lactate does not alter PMN apoptosis kinetics.

Neutrophils were incubated in medium with or without 4.7 mM sodium lactate supplementation, and the rate of apoptosis was quantified using Annexin V-FITC staining and flow cytometry. Data shown are the mean ± SEM, n=3. ns, not significant.

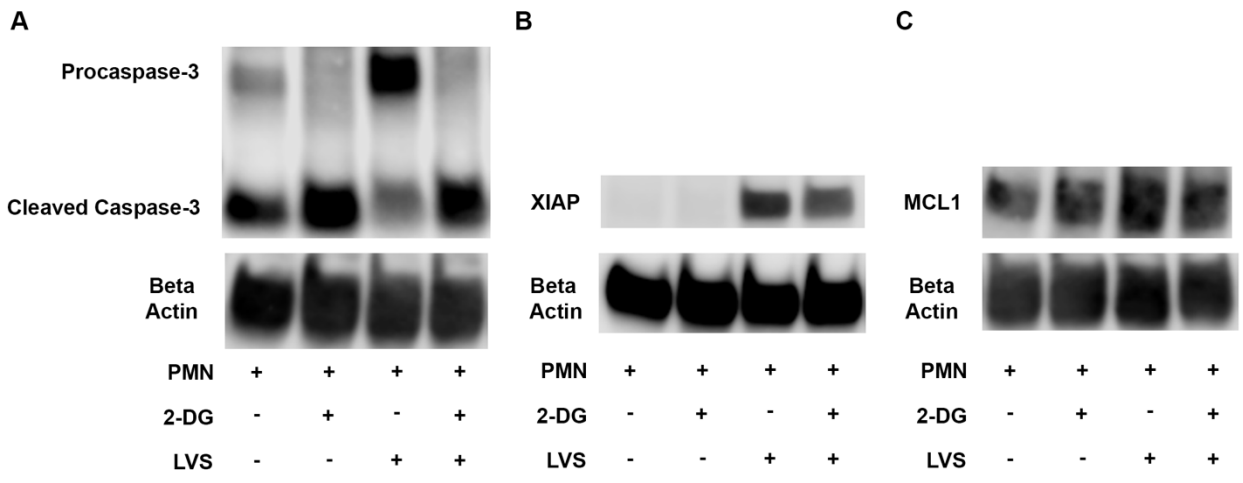

Figure 34. Effects of 2-DG on caspase-3 processing and abundance of XIAP and MCL-1.

Neutrophils were left untreated or infected with LVS in the presence or absence of 2-DG for 24 hr. Immunoblots of cell lysates were probed to detect caspase-3 (pro and mature forms) (A), XIAP (B), and MCL-1 (C). b-actin was used as the loading control. Data shown are representative of three independent determinations.

significantly extends neutrophil lifespan (56, 59, 153), but the mechanisms enabling infected neutrophils to override this strictly regulated cell death program are not fully understood.

The realization that metabolism can directly regulate inflammation and immune cell function has significant implications for our understanding of the molecular mechanisms associated with control or exacerbation of infection as well as cancer, obesity, autoimmunity and atherosclerosis. A majority of studies in the rapidly advancing field of immunometabolism have focused on macrophages and T lymphocytes, and relatively few have included or focused on neutrophils or other leukocyte types (75-78, 83, 88). The central finding of this study is that *F. tularensis* elicits a metabolic program in human neutrophils that is distinct from other stimuli described to date and is essential for cell longevity and delayed apoptosis.

Our published data establish that LVS infection significantly dysregulates over 800 neutrophil genes associated with metabolism, including upregulation of genes encoding nearly every glycolytic enzyme and the two main glucose transporters used by neutrophils (59). PFKL and HK2 are the two most prominent regulatory enzymes of glycolysis, and we confirm that in LVS-infected neutrophils *HK2* expression increased nearly 6-fold and *PFKL* expression increased ~3-fold by 6 hpi (**Figure 13**). Notably, significant induction of *PFKL* expression was apparent within minutes of LVS addition (0 hpi), reinforcing the notion that *F. tularensis* can act at a distance and begin to alter neutrophil function at the earliest stages of infection prior to bacterial binding and phagocytosis (149). At the biochemical level, changes in PMN gene expression led to increases in glucose uptake (**Figure 22A**) as well as glycolysis and glycolytic flux (**Figure 14**) that peaked at 12 hpi and were accompanied by accumulation of pathway intermediates as well as ATP and lactate (**Figures 15-17**). The LDHA isoform of lactate dehydrogenase catalyzes the conversion of pyruvate to lactate (164), and following LVS

infection, *LDHA* expression increased ~6-fold by 6 hpi (**Figure 13**). Furthermore, increases in lactate and the lactate/pyruvate ratio and reduction of pyruvate were apparent by GC-MS as early as 3 hpi and were sustained to at least 24 hpi (**Figures 15, 16B and 17**), and lactate also accumulated in the extracellular medium (**Figure 15A**). The opposing effects of LVS on lactate and pyruvate abundance contrasts with simultaneous increases in both metabolites that typically accompany PMN activation and microbe killing, and it has been proposed that changes in the ratio of these metabolites may be a hallmark of metabolic reprogramming (84, 154).

PMNs store glucose as glycogen, a branched glucose polymer that surrounds a glycogenin core. ^{14}C-glucose pulse-chase experiments demonstrated that glycogen stores are highly dynamic and are constantly adding and removing glucose units even at steady state (165). Accordingly, glycogenolysis ensues immediately in glucose free medium, reducing stores by up to 38% in 60 min, and glycogen is rapidly resynthesized when exogenous glucose is restored. As little as 5.3 μg glucose /10^6 cells/60 min is sufficient to maintain glycogen stores and 74 μg/10^6 cells supports maximum resynthesis (165). Enzymes that mediate glycogen synthesis and their encoding mRNAs are long-lived, and both glycogen synthase and glycogen phosphorylase bind glycogen (165). It has long been believed that neutrophils use glycogen for fuel only during phagocytosis and when extracellular glucose is scarce (76, 82, 89). However, recent reports (83) and the results of this study (**Figure 25**) contest this model. We show here that glycogen levels in uninfected neutrophils declined progressively as cells aged despite being cultured in glucose-replete medium. On the other hand, glycogen dynamics of LVS-infected cells were characterized by waves of net glycogenolysis and glycogenesis. Glycogen stores were highest at 3 hr and were more abundant in LVS-infected cells than the uninfected controls. Although glycogen stores declined to a nadir at 9 hpi, they were replenished in the infected cells by 12 hpi and then

maintained at a distinct intermediate level, before declining again at 32-48 hpi. To our knowledge, changes in glycogen stores of aging PMNs have not previously been reported. As near total glycogen depletion in control PMNs at 9-12 hr coincides with the onset of caspase-3 activation and progression to apoptosis (**Figures 25 and 27C**) (56), our data suggest that the ability of LVS-infected cells to replenish their glycogen stores 12-24 hpi is critical to their longevity, and as such suggests that glycogen abundance may be a key determinant that dictates PMN lifespan.

The results of this study demonstrate that glucose metabolism and glycolysis are critical for PMN survival. We extend prior results of Healy *et al*. (166) to show that blockade of glycolysis with 2-DG and replacement of glucose with pyruvate significantly accelerated apoptosis of both control and LVS-infected cells. At the same time, the dynamic changes in glycogen stores reported here and the survival-enhancing effects of CP-91149 confirm that glycogen is critical for PMN viability (83), which contrasts markedly with the ability of CP-91149 to cause death of hepatocellular carcinomas (167). Finally, the fact that Q-VD-OPh-mediated caspase inhibition was sufficient to profoundly enhance glycolysis and glycolytic capacity and markedly increased glycogen stores in parallel with ablation of apoptosis at 24 hr (**Figure 32**) is additional definitive evidence that PMN metabolism and lifespan are intimately linked. These data are summarized in **Figure 35**.

Thus far, two direct links between glycolysis and apoptosis have been described. First, HK2 translocates to mitochondria and binds VDAC which enhances mitochondrial integrity, diminishes cytochrome *c* release and reduces sensitivity to BAX and other pro-apoptosis BCL-2 proteins (168, 169). Mitochondrial association of HK correlates directly with increased glycolytic flux and this may be regulated by phosphoinositide 3-kinase and Akt pro-survival

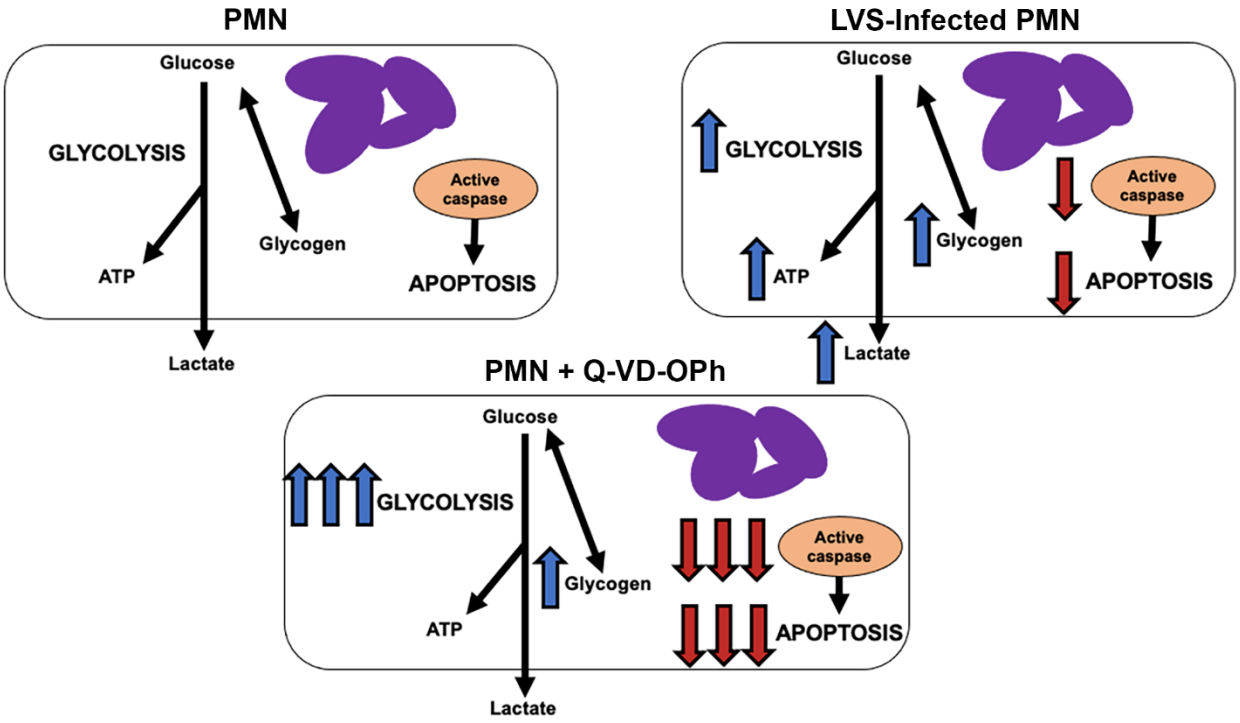

Figure 35. Model. Effects of *F. tularensis* and Q-VD-OPh on neutrophil metabolism.

See Discussion for details.

signaling (168). Second, PKM2 has been linked to apoptosis resistance via its ability to phosphorylate and stabilize pro-survival BCL-2 family proteins (170, 171). PKM2 also translocates into the nucleus to modulate NF-κB-dependent gene expression and may inhibit caspase-3 indirectly via effects on miR-143 (170, 172). Our published data show that mitochondrial integrity is significantly prolonged by LVS infection, and in keeping with this, BAX mRNA and protein are diminished and BAX translocation to mitochondria is significantly delayed (58, 59), but whether this is attributable to HK2-VDAC interactions at mitochondrial surfaces and/or phosphoinositide 3- kinase signaling remains to be determined. In addition, several anti-apoptosis genes of PMNs are regulated by NF-κB including *BCL2A1, A20, XIAP* and *MCL1* (47). Caspase activation is inhibited in LVS infection by the concerted actions of XIAP, cIAPs and calpastatin (58, 59). *PKM2* expression is induced by LVS, but its specific role in our system is currently unknown. Conversely, *HK* expression is downregulated during apoptosis and caspases inhibit PFK and pyruvate kinase to block glycolysis during cell death (42, 173). To gain further insight into links between glycolysis and apoptosis we utilized western blotting to elucidate the effects of 2-DG on caspase-3 processing and the abundance of XIAP and MCL-1. Although procaspase-3 processing was enhanced, XIAP and MCL-1 were unchanged (**Figure 34**). Thus, another possibility that must be considered is the ability of 2-DG to trigger cell death by inducting oxidative stress (56). Addressing this question in greater detail is of interest but is beyond the scope of this study.

Lactate is a major end-product of PMN glycolysis and is emerging as a key regulator of metabolism (174). Similar to pyruvate, lactate can be used for gluconeogenesis, but its major established role is as a signaling intermediate that functions inside and between cells to alter function and activation state. For example, in monocytes, macrophages and T lymphocytes,

elevated levels of lactate inhibit glycolysis and have been linked to immunosuppression as indicated by impaired production of proinflammatory cytokines by monocytes, changes in macrophage gene expression leading to M2 polarization, and impaired CD8+ T cell proliferation and toxicity (58, 59). In contrast, lactate signaling in tumor cells increases glucose uptake, enhances expression and activity of glycolysis enzymes, and reduces mitochondrial function via mechanisms linked to HIF-1α and *PIK3CA* (57). Regarding neutrophils, 10 mM exogenous lactate is sufficient to induce NETosis, but its effects on other aspects of cell function are unknown (57, 60). Our data indicate that the average amount of lactate released by LVS-infected PMNs over 24 hr (4.7 mM) had no discernible effect on the rate of constitutive apoptosis in the absence of infection (**Figure 33**) and did not induce NETs (data not shown).

Although the apoptosis differentiation program of neutrophils has been extensively studied, the intracellular trigger that initiates changes in gene expression that lead to cell death is unknown. Recently, Sadiku *et al*. showed that the capacity to synthesize glycogen is required for neutrophil survival in mice and that blockade of glycogen breakdown with CP-91149 in glucose-free medium causes PMN death within 12 hr (83). The notion that glycogen levels directly control neutrophil longevity is also supported by our data which demonstrate that inhibition of glycogen breakdown by CP-91149 expanded glycogen stores and extend neutrophil lifespan (**Figure 25A-C**). At the same time, the data in Figure 20 lead us to speculate that depletion of glycogen stores may trigger constitutive PMN death. Precisely what accounts for this remains to be determined, as GYS1, UGP2 and GBE1 enzymes and mRNA are unchanged (**Figure 26**). A comparison of the data in Figure 25 and Figure 21 confirms that although pyruvate can be used for gluconeogenesis it is less able to sustain glycogen stores, ATP production and PMN viability than glucose (83).

Glucose-6-phosphate that is not used for glycolysis or stored as glycogen can be transported into the endoplasmic reticulum. Mutations in *G6PT* prevent glucose-6-phosphate uptake into the endoplasmic reticulum that is associated with apoptosis and neutropenia in patients and can be mimicked by treating wild-type cells with the G6PT inhibitor chlorogenic acid (175). However, Veiga-da-Cunha *et al*. demonstrated that PMN death is not due to impaired G6P transport, as has long been believed (176). Rather, toxicity is due to a long-lived common dietary glucose analog, 1,5-anhydroglucitol (1,5AG), that is abundant in blood and serum and is converted to 1,5AG6P by HK after uptake. In the absence of functional G6PT, 1,5AG6P cannot be further metabolized and accumulates, leading to inhibition of HK and PMN death. The lack of effect of chlorogenic acid on PMN viability in our hands (**Figure 24**) supports this model as all our studies of *F. tularensis* and PMNs are performed using serum-free RPMI-1640 that is devoid of 1,5AG (56-58, 103).

The major metabolic pathways of neutrophils are aerobic and anaerobic glycolysis, TCA cycle, PPP, fatty acid biosynthesis and oxidation, glycogenolysis, glycogenesis, glutaminolysis, and in immature cells oxidative phosphorylation (76, 77, 83). These pathways are differentially utilized by PMNs under different conditions, and at least seven metabolic states have been described that distinguish 1) immature and tumor-associated neutrophils, 2) resting, mature PMNs, 3) cells undergoing chemotaxis, 4) phagocytosis, 5) canonical activation and ROS production, 6) elaboration of NETs or 7) apoptosis (42, 77, 78, 88, 89). Although additional studies are needed, the metabolic profile of LVS-infected PMNs described here is distinct from other metabolic profiles described to date. Specifically, the major metabolic pathways used by immature and tumor-associated PMNs are fatty acid oxidation, TCA cycle and oxidative phosphorylation, whereas resting mature cells rely on glycolysis and phagocytosis selectively

stimulates glycogenolysis. Chemotaxis is driven by glycolysis and mitochondrial purinergic signaling, NET formation requires glycolysis and PPP, and canonical activation is notable for glycolysis, glycogenolysis, PPP, TCA and glutaminolysis, and glycolysis and glycogenin synthesis are downregulated during apoptosis (42, 77, 78). In contrast, LVS-infected PMNs are notable for sequential glycogenolysis and glycogenesis, as well as induction of glycolysis and glucose uptake and downregulation of the PPP. As the PPP supplies NADPH that is essential for production of superoxide during the respiratory burst, downregulation of PPP enzymes and intermediates (**Figure 17**) (59) is in keeping with the ability of *F. tularensis* to elicit rapid, global inhibition of superoxide production via effects on NADPH oxidase assembly and activation (26, 153).

Metabolic reprogramming does not occur during or following every phagocytic event or infection, despite phagocytosis consuming half of a neutrophil's total ATP (82). Kobayashi et al., demonstrated that although glycolysis genes are expressed in PMNs at rest, most are not differentially expressed during constitutive or phagocytosis-induced apoptosis, though expression of *HK* and genes linked to glycogen synthesis declined (42). Among other bacterial pathogens that persist or replicate in neutrophils, there are relatively little data regarding their effects on glycolysis or other aspects of host cell metabolism. Like *F. tularensis*, *Anaplasma phagocytophilum*, *Chlamydia pneumoniae* and *Neisseria gonorrhoeae* replicate intracellularly and modulate apoptosis (94, 177, 178). However, effects of *C. pneumoniae* and *N. gonorrhoeae* on expression of genes linked to glycolysis have not been reported, and although *A. phagocytophilum* elicits upregulation of *PFKFB3* and downregulation *LDHA*, consequences for cell metabolism, if any, remain to be determined (177). On the other hand, the periodontal pathogen *Filofactor alocis* modulates cholesterol homeostasis and selectively increases

expression of genes linked to glycogen synthesis and glycosphingolipid metabolism rather than glycolysis (179). Upregulation of glycolysis has been observed in the context of infection with *Legionella pneumophila* or *Leishmania donovani* (84, 180) and LPS stimulation *in vitro* (83), but in these models glycolysis is coupled to PMN activation and bacterial clearance which contrasts sharply with the ability of *F. tularensis* to evade oxidative host defense, escape the phagosome and replicate in PMN cytosol (26, 56, 153).

The bacterial factors that mediate PMN metabolic reprogramming remain to be determined. Our published data demonstrate that maximum extension of neutrophil lifespan is independent of capsule and LPS and is mediated by the combined effects of intracellular bacteria along with *F. tularensis* lipoproteins and other factors that are rapidly released into conditioned media (56, 57, 103). Thus, it is tempting to speculate that bacterial lipoproteins and other secreted factors may begin to influence PMN metabolism, including *PFKL* expression, at the earliest stages of infection as noted above. Addressing this knowledge gap is the focus of on-going studies by our group.

In summary, neutrophil turnover is disrupted during *F. tularensis* infection and, consequently, neutrophils contribute distinctly to tularemia pathogenesis by exacerbating host tissue destruction. Herein, we extended our previous studies of apoptosis inhibition to demonstrate neutrophil metabolic reprogramming by *F. tularensis*. We show that this bacterium elicits a distinct metabolic signature in human neutrophils that differs from other stimuli studied date. At the molecular level, this response is notable for induction of glycolysis, elevated lactate/pyruvate ratios, and complex glycogen dynamics. Although many questions remain unanswered, and other pathways and intermediates need to be explored, our findings reinforce

links between metabolism and PMN longevity and set the stage for additional studies that may include other infections and disease states.

CHAPTER 4: SYNTHESIS

Introduction

Francisella tularensis is a Gram-negative, facultative, intracellular coccobacillus, and the etiological agent of the disease tularemia (1). The high infectivity, low infectious dose, and ability to aerosolize and enter the respiratory route make this organism a potential bioterrorism threat, for which no vaccine is currently available. For this reason, tularemia research has largely focused on vaccine development, however our understanding of the modulation of the host immune system by *Francisella tularensis* infection is lacking. Our laboratory has established that infection with this organism aberrantly extends neutrophil lifespan, and while this phenotype has been partially characterized, the complex mechanisms enabling *Francisella*-infected neutrophils to live longer are not fully understood (55, 59). Addressing this gap in knowledge could provide avenues for development of novel tularemia therapeutics, as well as inform studies of other disease models which are characterized by aberrant extension of neutrophil lifespan.

The research described in this thesis endeavored to characterize the mechanisms by which *Francisella tularensis*-infected neutrophils survive longer by determining how neutrophil signaling and metabolism were modulated in these cells. This work identified several neutrophil signaling pathways that exhibit increased activation in *Francisella*-infected neutrophils, and are required for these cells to live longer (see Chapter 2). Furthermore, we determined the metabolic signature of neutrophils infected with *Francisella tularensis* and defined the kinetics of metabolic reprogramming in these cells. We also established a link between neutrophil apoptosis and metabolism (see Chapter 3). These data significantly further our understanding of neutrophil biology, establish that neutrophil lifespan is regulated by metabolism, and vice versa, and

provide a foundation for future studies exploring metabolism as a regulator of neutrophil function.

Neutrophil survival signaling during *Francisella tularensis* infection

As the most abundant leukocyte in circulation and one of the first responders to infection sites, neutrophils are a vital component of the innate immune system (33, 34, 151). Uniquely, neutrophils undergo constitutive apoptosis ~24 hours after entering circulation and tight regulation of neutrophil lifespan and turnover is required for maintenance of host homeostasis, as well as inflammation resolution (36, 37). Due to their short lifespan, neutrophils have long been understudied and discounted as incapable of contributing consequentially to a disease's progression. However, it is now evident that aberrant extension of neutrophil lifespan underlies the pathogenesis of many inflammatory diseases, affirming that tight regulation of neutrophil apoptosis is crucial for resolution of disease. *Francisella tularensis* disrupts neutrophil turnover by delaying apoptosis, which elicits a dysfunctional immune response that is incapable of eradicating the pathogen (55, 59). Furthermore, delay of neutrophil apoptosis distinctly contributes to tularemia pathogenesis, as it leads to a profound accumulation of neutrophils in host tissues, which favors aberrant release of histotoxic components and enhanced host tissue destruction (62). We have previously demonstrated that *Francisella tularensis* infection inhibits the three main death mechanisms in neutrophils, PICD, the extrinsic apoptosis pathway, and the intrinsic apoptosis pathway (26, 55, 58, 59). This is mediated, in part, by delayed caspase processing and activation, assembly of a dysfunctional NADPH oxidase, which culminates in a severely weakened respiratory burst that is ineffective at killing the pathogen, sustained mitochondrial integrity, global transcriptional reprogramming, which includes dysregulation of

365 genes linked to apoptosis and survival, and manipulation of key apoptosis regulators including XIAP, cIAP2, BAX, MCL-1, calpastatin, and others (55, 59). However, the mechanisms by which *Francisella*-infected neutrophils overcome the strict regulation of these pathways in order to live longer require further characterization.

Neutrophil survival is also regulated by signaling pathways that are not strictly relegated to control of apoptosis, and indeed we identified p38 MAPK, PI3Kα and NF-κB as being more highly activated and/or required for apoptosis delay in neutrophils infected with *Francisella tularensis*. p38 MAPK specifically is more highly activated in *Francisella*-infected neutrophils and required for these cells to live longer. p38 MAPK has context-dependent effects on neutrophil apoptosis and can function to promote either apoptosis or survival (54, 60, 124). The apoptosis-promoting effect of p38 MAPK in neutrophils is often attributed to phosphorylation of priming sites in $p47^{phox}$, which promotes NADPH oxidase activation and ROS production, though constitutive apoptosis of resting neutrophils does not require p38 MAPK (60, 120, 124, 125). Thus, it is advantageous for *Francisella tularensis* to commandeer p38 MAPK signaling as further means to disrupt NADPH oxidase activation, but the pro-survival function of p38 MAPK signaling during infection by this organism requires further exploration.

We also established a role for PI3Kα signaling, though AKT activation was surprisingly not induced or required for the extended lifespan of these cells. This suggests that PI3Kα must signal outside of the PI3K/AKT signaling axis to regulate neutrophil lifespan, and one downstream candidate could be isoform PKCζ. It has been demonstrated that PI3Kα can activate PKCζ by signaling through PDK1, but this has not been directly demonstrated in human neutrophils, and the role of this signaling axis during infection with *Francisella tularensis* is not known (146).

Finally, we determined the requirement of NF-*k*B signaling for apoptosis delay of *Francisella*-infected neutrophils. This result was unsurprising as NF-*k*B is a well-established regulator of neutrophil apoptosis that transcriptionally controls an extensive list of key anti-apoptotic factors (59). Though the exact means by which NF-*k*B is modulated in *Francisella*-infected neutrophils is not known, a number of pro-survival NF-κB target genes are upregulated following infection, and warrant further study (59). These genes include *IL1B, SOD2, GADD45B*, *CFLAR*, *TNFAIP3*, *BCL2A1*, *BIRC3*, and *BIRC4* that encode IL-1β, MnSOD, GADD45β, c-FLIP, A20, A1, cIAP2, and XIAP, respectively (59).

The requirement and modulation of these signaling pathways during apoptosis delay of *Francisella*-infected neutrophils have further interesting implications as these signaling pathways also regulate glycolysis, though the extent to which these signaling pathways regulate neutrophil glycolysis has not been explored.

Neutrophil metabolism and lifespan are linked

The emerging field of immunometabolism has highlighted metabolism as a key regulator of immune cell function, but only a handful of studies have investigated neutrophil metabolism to date (75-80). It has long been known that the idiosyncratic lifespan of neutrophils is tightly linked to their functional capacity, and it is beginning to be appreciated that neutrophil metabolism influences function, but the extent to which metabolism regulates lifespan, or vice versa, in these cells has not been explored. This research establishes that metabolic reprogramming of neutrophils, specifically glycolysis induction, is a key and previously unappreciated feature of prolonged neutrophil lifespan. Further support for the link between neutrophil metabolism and lifespan was provided by the results of our experiments with the pan-

caspase inhibitor, Q-VD-OPh, wherein pharmacological inhibition of caspases also induced glycolysis.

Following infection with *Francisella tularensis*, neutrophils exhibit transcriptional reprogramming which includes dysregulation of over 800 metabolism-associated genes, and this research highlighted the importance of glycolysis specifically. This work defines the kinetics of glycolytic upregulation in neutrophils infected with *Francisella tularensis*. In short, metabolic reprogramming of *Francisella*-infected PMNs begins at the transcriptional level immediately following infection (0-6 hpi), glycolytic upregulation reaches its peak in infected neutrophils at 12 hpi, and glycolysis induction is sustained in infected neutrophils at 24 hpi, though at a much lower level overall than earlier timepoints. This contrasts with *Francisella* infection of macrophages, wherein *Francisella* prevents macrophages from shifting to aerobic glycolysis, effectively impairing inflammatory cytokine production and promoting bacterial replication (181).

Glycolytic upregulation does not occur during or following every phagocytic event, despite phagocytosis consuming half of a neutrophil's total ATP (82), and it is not a hallmark of all infections. *Anaplasma phagocytophilum* and *Neisseria gonorrhoeae* also delay neutrophil apoptosis (177, 182), but glycolysis enzyme genes are not upregulated in these infection models. Furthermore, transcriptome analysis of neutrophils isolated from human volunteers 3-6 hr after *Escherichia coli* LPS injection to induce transient endotoxemia demonstrates that *HK2* expression decreases, suggesting glycolysis is downregulated in these cells (183). Neutrophil glycolytic upregulation has been observed in the context of *Legionella* infection (180), *Leishmania* infection (84) and *E. coli* LPS stimulation *in vitro* (83). However, the observed glycolytic upregulation in these infection models occurs within the first 6 hr following infection

and is reported as key to mediating neutrophil function and bacterial clearance (83). Sadiku et al also report that stimulation with *E. coli* LPS *in vitro* significantly increased neutrophil glycogen stores, and this is also key for maintaining neutrophil antimicrobial activities (83). While *Francisella*-infected neutrophils also displayed increases in glycogen and glycolysis, glycolytic upregulation occurred much later, at 12 hpi. Furthermore, we have previously demonstrated that neutrophils infected with *Francisella tularensis* are highly dysfunctional, exhibit diminished antimicrobial activity and fail to clear the infection (55, 59), indicating that the metabolic reprogramming elicited by *Francisella tularensis* is distinct from what occurs following LPS stimulation.

Glycolysis is the main ATP-generating pathway in human neutrophils, but the role of glycolysis in regulation of neutrophil lifespan is not well understood. Neutrophil apoptosis that is triggered by phagocytosis requires downregulation of *HK2* mRNA and correlates precisely with increased mRNA expression of *UQCRB* (encodes Ubiquinol-cytochrome c reductase binding protein), which is a marker of oxidative phosphorylation activation (42). It has also been reported that increasing extracellular glucose and glucose metabolism protects against spontaneous and anti-Fas antibody-induced apoptosis in human neutrophils (166). The work presented here are congruent with these studies and support the notion that neutrophil glycolysis promotes neutrophil longevity. However, it has also been reported that TANs revert to an immature phenotype, which includes a shift back to mitochondrial metabolism, and TANs are able to survive this metabolic adaptation, even in a low-glucose environment (88). The role of neutrophil metabolic reprogramming during various disease contexts is a realm of study that is still in its infancy, but the work that has been done to date has revealed that alterations in neutrophil metabolism are complex, distinct, and highly context dependent. However, it is

notable that Q-VD-OPh treatment phenocopied *Francisella* infection with regard to glycolytic upregulation. This suggests that the mechanism connecting neutrophil apoptosis and glycolysis may be specifically linked via caspase inhibition, though further research is required to explore this mechanism.

Potential signaling mediators of neutrophil glycolysis and apoptosis

The signaling pathways identified by this research as being more highly activated and required for apoptosis delay of *Francisella*-infected neutrophils are also notable for their ability to regulate metabolism. Specifically, p38 MAPK has been shown to phosphorylate GSK3β to encourage glycogenesis (129), stimulate glucose uptake via membrane translocation of GLUT1 and phosphorylate MK2 to stimulate PFKFB3 and amplify glycolysis at the level of PFK (130, 131). PI3Kα is also capable of upregulating glycolysis in an AKT-independent mechanism, which involves Rac-dependent mobilization of glycolytic enzymes from the actin cytoskeleton, but the ability of neutrophil metabolism to be regulated in this way is unknown (184). As *Francisella*-infected neutrophils require the activity of the PI3Kα isoform specifically, independently of AKT activity, in order to delay apoptosis, it is attractive to predict that PI3Kα could also be functioning to induce glycolysis in our system.

TLR signaling is upstream of both p38 MAPK and PI3Kα, and our data demonstrate a role for TLR2/1 signaling in the prolonged lifespan of *Francisella*-infected neutrophils (103). Specifically, we have identified *Francisella tularensis* BLPs as an anti-apoptotic factor that achieves neutrophil apoptosis delay by binding and activating TLR2/1 (103). Thus, it is possible that TLR is signaling upstream of either or both p38 MAPK and PI3Kα to effectively prolong neutrophil lifespan and upregulate glycolysis. This proposed model is summarized in **Figure 36**.

Additional support for the notion that TLR signaling contributes to the *Francisella tularensis* infection strategy is provided by the determination that neutrophils infected with *Francisella tularensis fevR* live even longer than WT LVS (103). This is notable because it is established that TLR2 accumulates on phagosomes and *fevR* mutants are unable to escape the phagosome, thus highlighting a potentially important role for intraphagosomal signaling (185). Indeed, it is possible that the enhanced apoptosis delay exhibited by *fevR*-infected neutrophils is due to sustained or amplified signaling through TLR2 from the phagosomal compartment, however, the contributions of TLR signaling to apoptosis inhibition or glycolysis induction in *Francisella*-infected neutrophils requires further investigation.

Glycogen as a candidate regulator of neutrophil lifespan

This research uncovered a surprising role for glycogen as a regulator of neutrophil apoptosis and metabolism. We have revealed that glycogen is much more functionally dynamic than previously thought and is not simply an inert fuel. Specifically, we demonstrate that prolongation of neutrophil lifespan, whether via *Francisella tularensis* infection or Q-VD-OPh treatment, elicited increases in glycogen content. Further interrogation of this phenotype established that neutrophil glycogen levels progressively decrease as the cells age, but sustenance of glycogen levels with CP-91149 treatment was sufficient to extend neutrophil lifespan and induce glycolysis, highlighting glycogen as a pro-survival factor that could mediate crosstalk between metabolism and apoptosis.

Although neutrophil apoptosis has been extensively studied and characterized, the intracellular trigger that initiates changes in gene expression ultimately leading to cell death is unknown. This research and the recent work from the Walmsley group support the notion that

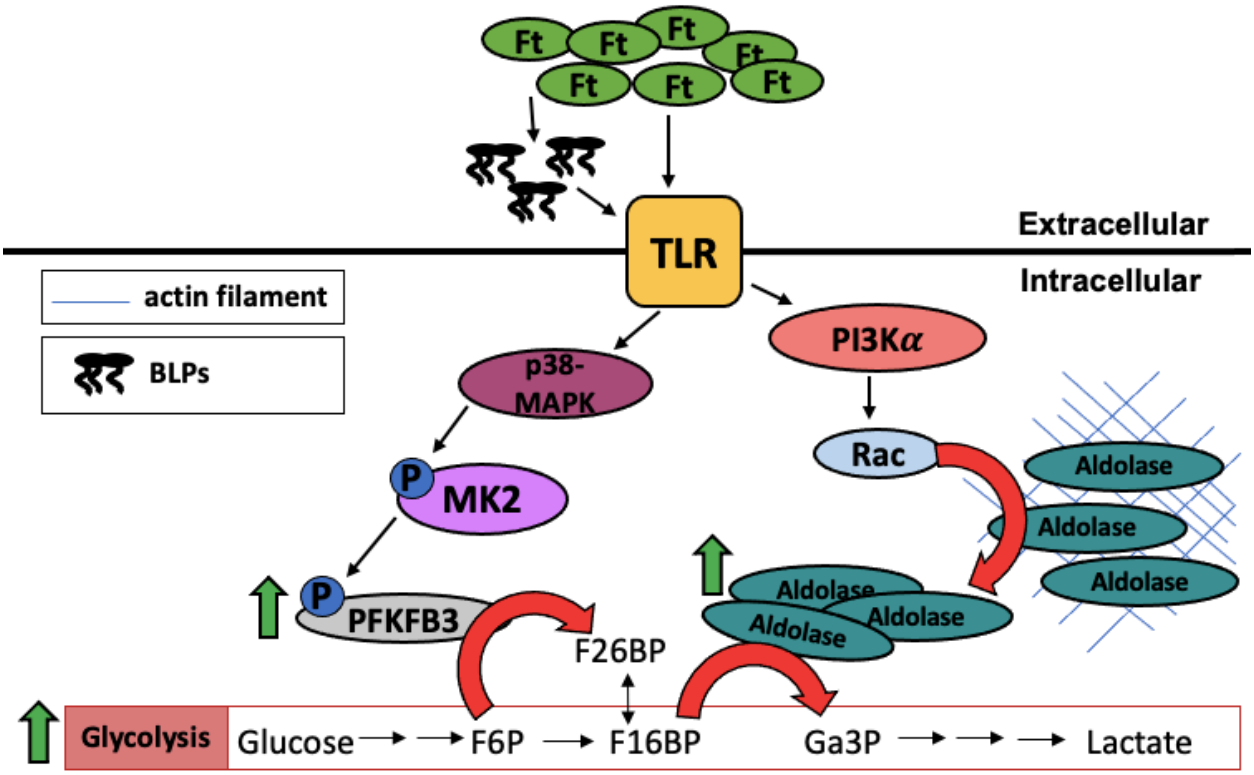

Figure 36. <u>Hypothetical</u> model for glycolytic upregulation.

During Ft infection, p38 MAPK could phosphorylate MK2, thereby promoting phosphorylation of PFKFB3 and increasing glycolytic flux. PI3Ka could be signaling via Rac to release glycolytic enzymes, such as aldolase, from the actin cytoskeleton to further enhance glycolysis induction.

glycogen levels directly control neutrophil longevity (83).

As the timing of near total glycogen depletion correlates with the onset of caspase-3 activation (~9-12 hr) in control neutrophils, it is attractive to predict that the ability of *Francisella*-infected neutrophils to replenish and sustain their glycogen stores are critical for their prolonged lifespan. This research has revealed glycogen as a candidate regulator of apoptosis, and in fact loss of glycogen may be the intracellular trigger that initiates neutrophil apoptosis. Future studies will endeavor to understand the mechanism by which glycogen levels regulate neutrophil lifespan and it would be interesting to investigate if glycogen metabolism enzymes are able to interact with caspases or other apoptosis regulators.

Future directions

Neutrophil turnover is disrupted during *Francisella* infection and, as a direct consequence, neutrophils contribute distinctly to tularemia pathogenesis by exacerbating host tissue destruction. Our data provide new insight into this phenomenon by demonstrating that neutrophil metabolism and apoptosis are fundamentally linked. We determined that glycolysis induction and glycogen abundance are directly linked to neutrophil lifespan, as both are increased during apoptosis delay, either via infection with *Francisella tularensis* or pan-caspase inhibition with Q-VD-OPh.

Our data provide a basis for additional studies to investigate the role of neutrophil metabolism in the context of other disease states that feature dysregulated neutrophil lifespan. As our laboratory has also identified a role for *Francisella tularensis* conditioned media (CM) and BLPs in neutrophil apoptosis delay, future studies are needed to ascertain the contributions of CM or BLPs to glycolysis induction or increased glycogen abundance. Further work must also

be done to identify which bacterial factors mediate glycolytic upregulation and glycogen maintenance. It would also be important to understand how bacterial metabolism is changing, if at all, following engulfment by the neutrophil. What is the metabolic crosstalk between host and pathogen, and what is the impact of this cross talk on our observed phenotypes?

The timing of glycolytic upregulation correlates with the timing of glycogen replenishment in *Francisella*-infected neutrophils (~12 hpi), but whether the glycolytic upregulation and glycogen replenishment are directly linked is not known and warrants further exploration. One possibility is that neutrophil glycolysis and glycogen dynamics are linked to an internal checkpoint wherein the status of either or both glycolysis and glycogen at the 12 hr timepoint dictates whether the cell proceeds towards apoptosis or survival.

Another interesting avenue of investigation would be to further interrogate the metabolomic changes that occur in neutrophils following infection with *Francisella tularensis*. Specifically, we observe increases in the ketone body β-hydroxybutyrate and the TCA metabolite malate (data not shown). β-hydroxybutyrate would be interesting to investigate because there are almost no data on the contribution of this metabolite to neutrophil biology, though it has been shown to increase viability in neurons by increasing flux through autophagy. Is β-hydroxybutyrate contributing to or required for prolonged neutrophil lifespan during infection with *Francisella tularensis*? Is β-hydroxybutyrate also modulating autophagy in neutrophils? Finally, it is intriguing that we observe increases in malate in *Francisella*-infected neutrophils, and indeed it is reproducibly the most highly upregulated metabolite following infection, but as we see no change in the other TCA metabolites, the significance of this finding is unclear and requires further examination.

Summary

This work endeavored to understand how neutrophil metabolism is reprogrammed following infection with *Francisella tularensis*. We identified glycolysis and glycogen as key components of the metabolic program and established a link between neutrophil metabolism and apoptosis. This research contributed not only to our understanding of the *Francisella tularensis* infection strategy, but also to our comprehension of the basic biology and metabolic processes that control neutrophil function. Immunometabolism is a new, rapidly evolving scientific frontier, and the notion that neutrophil function is influenced by metabolism is an intriguing one that deserves further exploration.

REFERENCES

1. Francis, E. 1983. Landmark article April 25, 1925: Tularemia. By Edward Francis. *JAMA* 250: 3216-3224.
2. McCoy, G. W., and C. W. Chapin. 1911. Tuberculosis among Ground Squirrels (Citellus Beecheyi, Richardson). *J Med Res* 25: 189-198.
3. McCoy, G. W. 1911. Some Features of the Squirrel Plague Problem. *Cal State J Med* 9: 105-109.
4. Wherry, W. B., and B. H. Lamb. 2004. Infection of man with Bacterium tularense. 1914. *J Infect Dis* 189: 1321-1329.
5. Olsufjev, N. G. 1970. Taxonomy and characteristic of the genus Francisella Dorofeev, 1947. *J Hyg Epidemiol Microbiol Immunol* 14: 67-74.
6. Keim, P., A. Johansson, and D. M. Wagner. 2007. Molecular epidemiology, evolution, and ecology of Francisella. *Ann N Y Acad Sci* 1105: 30-66.
7. Olsufiev, N. G., O. S. Emelyanova, and T. N. Dunayeva. 1959. Comparative study of strains of B. tularense in the old and new world and their taxonomy. *J Hyg Epidemiol Microbiol Immunol* 3: 138-149.
8. Sandstrom, G., A. Sjostedt, M. Forsman, N. V. Pavlovich, and B. N. Mishankin. 1992. Characterization and classification of strains of Francisella tularensis isolated in the central Asian focus of the Soviet Union and in Japan. *J Clin Microbiol* 30: 172-175.
9. Pechous, R. D., T. R. McCarthy, and T. C. Zahrt. 2009. Working toward the future: insights into Francisella tularensis pathogenesis and vaccine development. *Microbiol Mol Biol Rev* 73: 684-711.
10. McLendon, M. K., M. A. Apicella, and L. A. Allen. 2006. Francisella tularensis: taxonomy, genetics, and Immunopathogenesis of a potential agent of biowarfare. *Annu Rev Microbiol* 60: 167-185.
11. McCaffrey, R. L., and L. A. Allen. 2006. Francisella tularensis LVS evades killing by human neutrophils via inhibition of the respiratory burst and phagosome escape. *J Leukoc Biol* 80: 1224-1230.
12. Hestvik, G., E. Warns-Petit, L. A. Smith, N. J. Fox, H. Uhlhorn, M. Artois, D. Hannant, M. R. Hutchings, R. Mattsson, L. Yon, and D. Gavier-Widen. 2015. The status of tularemia in Europe in a one-health context: a review. *Epidemiol Infect* 143: 2137-2160.
13. Oyston, P. C., A. Sjostedt, and R. W. Titball. 2004. Tularaemia: bioterrorism defence renews interest in Francisella tularensis. *Nat Rev Microbiol* 2: 967-978.
14. Hopla, C. E. 1974. The ecology of tularemia. *Adv Vet Sci Comp Med* 18: 25-53.
15. Tarnvik, A., and L. Berglund. 2003. Tularaemia. *Eur Respir J* 21: 361-373.
16. Tarnvik, A., G. Sandstrom, and A. Sjostedt. 1996. Epidemiological analysis of tularemia in Sweden 1931-1993. *FEMS Immunol Med Microbiol* 13: 201-204.
17. Ellis, J., P. C. Oyston, M. Green, and R. W. Titball. 2002. Tularemia. *Clin Microbiol Rev* 15: 631-646.
18. McCrumb, F. R. 1961. Aerosol Infection of Man with Pasteurella Tularensis. *Bacteriol Rev* 25: 262-267.
19. Saslaw, S., H. T. Eigelsbach, J. A. Prior, H. E. Wilson, and S. Carhart. 1961. Tularemia vaccine study. II. Respiratory challenge. *Arch Intern Med* 107: 702-714.

20. McLendon, M. K., M. A. Apicella, and L.-A. H. Allen. 2006. Francisella tularensis: taxonomy, genetics, and Immunopathogenesis of a potential agent of biowarfare. *Annu Rev Microbiol* 60: 167-185.
21. Checroun, C., T. D. Wehrly, E. R. Fischer, S. F. Hayes, and J. Celli. 2006. Autophagy-mediated reentry of Francisella tularensis into the endocytic compartment after cytoplasmic replication. *Proc Natl Acad Sci U S A* 103: 14578-14583.
22. Clemens, D. L., B. Y. Lee, and M. A. Horwitz. 2004. Virulent and avirulent strains of Francisella tularensis prevent acidification and maturation of their phagosomes and escape into the cytoplasm in human macrophages. *Infect Immun* 72: 3204-3217.
23. Clemens, D. L., B. Y. Lee, and M. A. Horwitz. 2009. Francisella tularensis phagosomal escape does not require acidification of the phagosome. *Infect Immun* 77: 1757-1773.
24. Craven, R. R., J. D. Hall, J. R. Fuller, S. Taft-Benz, and T. H. Kawula. 2008. Francisella tularensis invasion of lung epithelial cells. *Infect Immun* 76: 2833-2842.
25. Golovliov, I., V. Baranov, Z. Krocova, H. Kovarova, and A. Sjostedt. 2003. An attenuated strain of the facultative intracellular bacterium Francisella tularensis can escape the phagosome of monocytic cells. *Infect Immun* 71: 5940-5950.
26. McCaffrey, R. L., J. T. Schwartz, S. R. Lindemann, J. G. Moreland, B. W. Buchan, B. D. Jones, and L.-A. H. Allen. 2010. Multiple mechanisms of NADPH oxidase inhibition by type A and type B Francisella tularensis. *J Leukoc Biol* 88: 791-805.
27. McCaffrey, R. L., and L.-A. H. Allen. 2006. Pivotal Advance: *Francisella tularensis* evades killing by human neutrophils via inhibition of the respiratory burst and phagosome escape. *J. Leukoc. Biol.* 80: 1224-1230.
28. Brotcke, A., and D. M. Monack. 2008. Identification of fevR, a novel regulator of virulence gene expression in Francisella novicida. *Infect Immun* 76: 3473-3480.
29. Buchan, B. W., R. L. McCaffrey, S. R. Lindemann, L. A. Allen, and B. D. Jones. 2009. Identification of migR, a regulatory element of the Francisella tularensis live vaccine strain iglABCD virulence operon required for normal replication and trafficking in macrophages. *Infect Immun* 77: 2517-2529.
30. Long, M. E., S. R. Lindemann, J. A. Rasmussen, B. D. Jones, and L. A. Allen. 2013. Disruption of Francisella tularensis Schu S4 iglI, iglJ, and pdpC genes results in attenuation for growth in human macrophages and in vivo virulence in mice and reveals a unique phenotype for pdpC. *Infect Immun* 81: 850-861.
31. Meibom, K. L., M. Barel, and A. Charbit. 2009. Loops and networks in control of Francisella tularensis virulence. *Future Microbiol* 4: 713-729.
32. Nano, F. E., N. Zhang, S. C. Cowley, K. E. Klose, K. K. Cheung, M. J. Roberts, J. S. Ludu, G. W. Letendre, A. I. Meierovics, G. Stephens, and K. L. Elkins. 2004. A Francisella tularensis pathogenicity island required for intramacrophage growth. *J Bacteriol* 186: 6430-6436.
33. Borregaard, N. 2010. Neutrophils, from marrow to microbes. *Immunity* 33: 657-670.
34. Athens, J. W., O. P. Haab, S. O. Raab, A. M. Mauer, H. Ashenbrucker, G. E. Cartwright, and M. M. Wintrobe. 1961. Leukokinetic studies. IV. The total blood, circulating and marginal granulocyte pools and the granulocyte turnover rate in normal subjects. *J Clin Invest* 40: 989-995.
35. Nauseef, W. M. 2007. How human neutrophils kill and degrade microbes: an integrated view. *Immunol Rev* 219: 88-102.

36. Kobayashi, S. D., and F. R. Deleo. 2004. An apoptosis differentiation programme in human polymorphonuclear leucocytes. *Biochem Soc Trans* 32: 474-476.
37. Kennedy, A. D., and F. R. DeLeo. 2009. Neutrophil apoptosis and the resolution of infection. *Immunol Res* 43: 25-61.
38. Kobayashi, S. D., and F. R. DeLeo. 2009. Role of neutrophils in innate immunity: a systems biology-level approach. *Wiley Interdiscip Rev Syst Biol Med* 1: 309-333.
39. Watson, R. W., H. P. Redmond, J. H. Wang, C. Condron, and D. Bouchier-Hayes. 1996. Neutrophils undergo apoptosis following ingestion of Escherichia coli. *J Immunol* 156: 3986-3992.
40. Kobayashi, S. D., J. M. Voyich, C. L. Buhl, R. M. Stahl, and F. R. DeLeo. 2002. Global changes in gene expression by human polymorphonuclear leukocytes during receptor-mediated phagocytosis: cell fate is regulated at the level of gene expression. *Proc Natl Acad Sci U S A* 99: 6901-6906.
41. Kobayashi, S. D., K. R. Braughton, A. R. Whitney, J. M. Voyich, T. G. Schwan, J. M. Musser, and F. R. DeLeo. 2003. Bacterial pathogens modulate an apoptosis differentiation program in human neutrophils. *Proc Natl Acad Sci U S A* 100: 10948-10953.
42. Kobayashi, S. D., J. M. Voyich, G. A. Somerville, K. R. Braughton, H. L. Malech, J. M. Musser, and F. R. DeLeo. 2003. An apoptosis-differentiation program in human polymorphonuclear leukocytes facilitates resolution of inflammation. *J Leukoc Biol* 73: 315-322.
43. Kobayashi, S. D., J. M. Voyich, K. R. Braughton, A. R. Whitney, W. M. Nauseef, H. L. Malech, and F. R. DeLeo. 2004. Gene expression profiling provides insight into the pathophysiology of chronic granulomatous disease. *J Immunol* 172: 636-643.
44. Conus, S., R. Perozzo, T. Reinheckel, C. Peters, L. Scapozza, S. Yousefi, and H. U. Simon. 2008. Caspase-8 is activated by cathepsin D initiating neutrophil apoptosis during the resolution of inflammation. *J Exp Med* 205: 685-698.
45. Conus, S., C. Pop, S. J. Snipas, G. S. Salvesen, and H. U. Simon. 2012. Cathepsin D primes caspase-8 activation by multiple intra-chain proteolysis. *J Biol Chem* 287: 21142-21151.
46. Witko-Sarsat, V., M. Pederzoli-Ribeil, E. Hirsch, S. Sozzani, and M. A. Cassatella. 2011. Regulating neutrophil apoptosis: new players enter the game. *Trends Immunol* 32: 117-124.
47. McCracken, J. M., and L.-A. H. Allen. 2014. Regulation of human neutrophil apoptosis and lifespan in health and disease. *J. Cell Death* 7: 15-23.
48. Maianski, N. A., J. Geissler, S. M. Srinivasula, E. S. Alnemri, D. Roos, and T. W. Kuijpers. 2004. Functional characterization of mitochondria in neutrophils: a role restricted to apoptosis. *Cell Death Differ* 11: 143-153.
49. Akgul, C., D. A. Moulding, and S. W. Edwards. 2001. Molecular control of neutrophil apoptosis. *FEBS Lett* 487: 318-322.
50. Fox, S., A. E. Leitch, R. Duffin, C. Haslett, and A. G. Rossi. 2010. Neutrophil apoptosis: relevance to the innate immune response and inflammatory disease. *J Innate Immun* 2: 216-227.
51. Kobayashi, S. D., J. M. Voyich, K. R. Braughton, and F. R. DeLeo. 2003. Down-regulation of proinflammatory capacity during apoptosis in human polymorphonuclear leukocytes. *J Immunol* 170: 3357-3368.

52. Rigby, K. M., and F. R. DeLeo. 2012. Neutrophils in innate host defense against Staphylococcus aureus infections. *Semin Immunopathol* 34: 237-259.
53. DeLeo, F. R. 2004. Modulation of phagocyte apoptosis by bacterial pathogens. *Apoptosis* 9: 399-413.
54. McCracken, J. M., and L.-A. H. Allen. 2014. Regulation of human neutrophil apoptosis and lifespan in health and disease. *J Cell Death* 7: 15-23.
55. Kinkead, L. C., and L.-A. H. Allen. 2016. Multifaceted effects of Francisella tularensis on human neutrophil function and lifespan. *Immunol Rev* 273: 266-281.
56. Schwartz, J. T., J. H. Barker, J. Kaufman, D. C. Fayram, J. M. McCracken, and L.-A. H. Allen. 2012. Francisella tularensis inhibits the intrinsic and extrinsic pathways to delay constitutive apoptosis and prolong human neutrophil lifespan. *J Immunol* 188: 3351-3363.
57. Schwartz, J. T., S. Bandyopadhyay, S. D. Kobayashi, J. McCracken, A. R. Whitney, F. R. Deleo, and L. A. Allen. 2013. Francisella tularensis alters human neutrophil gene expression: insights into the molecular basis of delayed neutrophil apoptosis. *J Innate Immun* 5: 124-136.
58. McCracken, J. M., L. C. Kinkead, R. L. McCaffrey, and L.-A. H. Allen. 2016. Francisella tularensis Modulates a Distinct Subset of Regulatory Factors and Sustains Mitochondrial Integrity to Impair Human Neutrophil Apoptosis. *J Innate Immun* 8: 299-313.
59. Schwartz, J. T., S. Bandyopadhyay, S. D. Kobayashi, J. McCracken, A. R. Whitney, F. R. Deleo, and L.-A. H. Allen. 2013. Francisella tularensis alters human neutrophil gene expression: insights into the molecular basis of delayed neutrophil apoptosis. *J Innate Immun* 5: 124-136.
60. Geering, B., and H. U. Simon. 2011. Peculiarities of cell death mechanisms in neutrophils. *Cell Death Differ* 18: 1457-1469.
61. McCracken, J. M., and L. A. Allen. 2014. Regulation of human neutrophil apoptosis and lifespan in health and disease. *J Cell Death* 7: 15-23.
62. Malik, M., C. S. Bakshi, K. McCabe, S. V. Catlett, A. Shah, R. Singh, P. L. Jackson, A. Gaggar, D. W. Metzger, J. A. Melendez, J. E. Blalock, and T. J. Sellati. 2007. Matrix metalloproteinase 9 activity enhances host susceptibility to pulmonary infection with type A and B strains of Francisella tularensis. *J Immunol* 178: 1013-1020.
63. Hall, W. C., R. M. Kovatch, and R. L. Schricker. 1973. Tularaemic pneumonia: pathogenesis of the aerosol-induced disease in monkeys. *J Pathol* 110: 193-201.
64. Schricker, R. L., H. T. Eigelsbach, J. Q. Mitten, and W. C. Hall. 1972. Pathogenesis of tularemia in monkeys aerogenically exposed to Francisella tularensis 425. *Infect Immun* 5: 734-744.
65. Tulis, J. J., H. T. Eigelsbach, and R. W. Kerpsack. 1970. Host-parasite relationship in monkeys administered live tularemia vaccine. *Am J Pathol* 58: 329-336.
66. Tulis, J. J., H. T. Eigelsbach, and R. B. Hornick. 1969. Oral vaccination against tularemia in the monkeys. *Proc Soc Exp Biol Med* 132: 893-897.
67. Eigelsbach, H. T., J. J. Tulis, M. H. McGavran, and J. D. White. 1962. LIVE TULAREMIA VACCINE I. : Host-Parasite Relationship in Monkeys Vaccinated Intracutaneously or Aerogenically. *J Bacteriol* 84: 1020-1027.
68. Hall, J. D., M. D. Woolard, B. M. Gunn, R. R. Craven, S. Taft-Benz, J. A. Frelinger, and T. H. Kawula. 2008. Infected-host-cell repertoire and cellular response in the lung

following inhalation of Francisella tularensis Schu S4, LVS, or U112. *Infect Immun* 76: 5843-5852.
69. Bosio, C. M., H. Bielefeldt-Ohmann, and J. T. Belisle. 2007. Active suppression of the pulmonary immune response by Francisella tularensis Schu4. *J Immunol* 178: 4538-4547.
70. Bosio, C. M., and K. L. Elkins. 2001. Susceptibility to secondary Francisella tularensis live vaccine strain infection in B-cell-deficient mice is associated with neutrophilia but not with defects in specific T-cell-mediated immunity. *Infect Immun* 69: 194-203.
71. Melillo, A. A., O. Foreman, and K. L. Elkins. 2013. IL-12Rbeta2 is critical for survival of primary Francisella tularensis LVS infection. *J Leukoc Biol* 93: 657-667.
72. Dunaeva, T. N., and K. N. Shlygina. 1975. [Phagocytic activity of the neutrophils in tularemia in animals with varying infective sensitivity]. *Zh Mikrobiol Epidemiol Immunobiol*: 22-26.
73. Conlan, J. W., W. Chen, H. Shen, A. Webb, and R. KuoLee. 2003. Experimental tularemia in mice challenged by aerosol or intradermally with virulent strains of Francisella tularensis: bacteriologic and histopathologic studies. *Microb Pathog* 34: 239-248.
74. Lamps, L. W., J. M. Havens, A. Sjostedt, D. L. Page, and M. A. Scott. 2004. Histologic and molecular diagnosis of tularemia: a potential bioterrorism agent endemic to North America. *Mod Pathol* 17: 489-495.
75. Corcoran, S. E., and L. A. O'Neill. 2016. HIF1alpha and metabolic reprogramming in inflammation. *J Clin Invest* 126: 3699-3707.
76. Curi, R., A. C. Levada-Pires, E. B. D. Silva, S. O. Poma, R. F. Zambonatto, P. Domenech, M. M. Almeida, R. B. Gritte, T. Souza-Siqueira, R. Gorjao, P. Newsholme, and T. C. Pithon-Curi. 2020. The Critical Role of Cell Metabolism for Essential Neutrophil Functions. *Cell Physiol Biochem* 54: 629-647.
77. Jeon, J. H., C. W. Hong, E. Y. Kim, and J. M. Lee. 2020. Current Understanding on the Metabolism of Neutrophils. *Immune Netw* 20: e46.
78. Kumar, S., and M. Dikshit. 2019. Metabolic Insight of Neutrophils in Health and Disease. *Front Immunol* 10: 2099.
79. Sadiku, P., and S. R. Walmsley. 2019. Hypoxia and the regulation of myeloid cell metabolic imprinting: consequences for the inflammatory response. *EMBO Rep* 20:e47388.
80. Sadiku, P., J. A. Willson, R. S. Dickinson, F. Murphy, A. J. Harris, A. Lewis, D. Sammut, A. S. Mirchandani, E. Ryan, E. R. Watts, A. A. R. Thompson, H. M. Marriott, D. H. Dockrell, C. T. Taylor, M. Schneider, P. H. Maxwell, E. R. Chilvers, M. Mazzone, V. Moral, C. W. Pugh, P. J. Ratcliffe, C. J. Schofield, B. Ghesquiere, P. Carmeliet, M. K. Whyte, and S. R. Walmsley. 2017. Prolyl hydroxylase 2 inactivation enhances glycogen storage and promotes excessive neutrophilic responses. *J Clin Invest* 127: 3407-3420.
81. Mestas, J., and C. C. Hughes. 2004. Of mice and not men: differences between mouse and human immunology. *J Immunol* 172: 2731-2738.
82. Borregaard, N., and T. Herlin. 1982. Energy metabolism of human neutrophils during phagocytosis. *J Clin Invest* 70: 550-557.
83. Sadiku, P., J. A. Willson, E. M. Ryan, D. Sammut, P. Coelho, E. R. Watts, R. Grecian, J. M. Young, M. Bewley, S. Arienti, A. S. Mirchandani, M. A. Sanchez Garcia, T. Morrison, A. Zhang, L. Reyes, T. Griessler, P. Jheeta, G. G. Paterson, C. J. Graham, J. P. Thomson, K. Baillie, A. A. R. Thompson, J. M. Morgan, A. Acosta-Sanchez, V. M.

Darde, J. Duran, J. J. Guinovart, G. Rodriguez-Blanco, A. Von Kriegsheim, R. R. Meehan, M. Mazzone, D. H. Dockrell, B. Ghesquiere, P. Carmeliet, M. K. B. Whyte, and S. R. Walmsley. 2021. Neutrophils fuel effective immune responses through gluconeogenesis and glycogenesis. *Cell Metab* 33: 1062-1064.

84. Ohms, M., C. Ferreira, H. Busch, I. Wohlers, A. C. Guerra de Souza, R. Silvestre, and T. Laskay. 2021. Enhanced Glycolysis Is Required for Antileishmanial Functions of Neutrophils Upon Infection With Leishmania donovani. *Front Immunol* 12: 632512.
85. Pfeiffer, T., S. Schuster, and S. Bonhoeffer. 2001. Cooperation and competition in the evolution of ATP-producing pathways. *Science* 292: 504-507.
86. Peek, C. B., D. C. Levine, J. Cedernaes, A. Taguchi, Y. Kobayashi, S. J. Tsai, N. A. Bonar, M. R. McNulty, K. M. Ramsey, and J. Bass. 2017. Circadian Clock Interaction with HIF1alpha Mediates Oxygenic Metabolism and Anaerobic Glycolysis in Skeletal Muscle. *Cell Metab* 25: 86-92.
87. Bartrons, R., A. Rodriguez-Garcia, H. Simon-Molas, E. Castano, A. Manzano, and A. Navarro-Sabate. 2018. The potential utility of PFKFB3 as a therapeutic target. *Expert Opin Ther Targets* 22: 659-674.
88. Rice, C. M., L. C. Davies, J. J. Subleski, N. Maio, M. Gonzalez-Cotto, C. Andrews, N. L. Patel, E. M. Palmieri, J. M. Weiss, J. M. Lee, C. M. Annunziata, T. A. Rouault, S. K. Durum, and D. W. McVicar. 2018. Tumour-elicited neutrophils engage mitochondrial metabolism to circumvent nutrient limitations and maintain immune suppression. *Nat Commun* 9: 5099.
89. Injarabian, L., A. Devin, S. Ransac, and B. S. Marteyn. 2019. Neutrophil Metabolic Shift during their Lifecycle: Impact on their Survival and Activation. *Int J Mol Sci* 21.
90. Luo, H. R., and F. Loison. 2008. Constitutive neutrophil apoptosis: mechanisms and regulation. *Am J Hematol* 83: 288-295.
91. Edwards, S. W., M. Derouet, M. Howse, and R. J. Moots. 2004. Regulation of neutrophil apoptosis by Mcl-1. *Biochem Soc Trans* 32: 489-492.
92. McCracken, J. M., and L.-A. H. Allen. 2014. Regulation of human neutrophil apoptosis and lifespan in health and disease. *J. Cell Death* 7: 15-23.
93. Du, K., Q. Zheng, M. Zhou, L. Zhu, B. Ai, and L. Zhou. 2011. Chlamydial antiapoptotic activity involves activation of the Raf/MEK/ERK survival pathway. *Curr Microbiol* 63: 341-346.
94. Sarkar, A., S. Moller, A. Bhattacharyya, M. Behnen, J. Rupp, G. van Zandbergen, W. Solbach, and T. Laskay. 2015. Mechanisms of apoptosis inhibition in Chlamydia pneumoniae-infected neutrophils. *Int J Med Microbiol* 305: 493-500.
95. Kim, H. Y., and Y. Rikihisa. 2002. Roles of p38 mitogen-activated protein kinase, NF-kappaB, and protein kinase C in proinflammatory cytokine mRNA expression by human peripheral blood leukocytes, monocytes, and neutrophils in response to Anaplasma phagocytophila. *Infect Immun* 70: 4132-4141.
96. Lee, H. C., and J. L. Goodman. 2006. *Anaplasma phagocytophilum* causes global induction of antiapoptosis in human neutrophils. *Genomics* 88: 496-503.
97. Cherla, R., Y. Zhang, L. Ledbetter, and G. Zhang. 2018. Coxiella burnetii inhibits neutrophil apoptosis by exploiting survival pathways and antiapoptotic protein Mcl-1. *Infect. Immun.* 86: e00504-e00517.
98. Dennis, D. T., T. V. Inglesby, D. A. Henderson, J. G. Bartlett, M. S. Ascher, E. Eitzen, A. D. Fine, A. M. Friedlander, J. Hauer, M. Layton, S. R. Lillibridge, J. E. McDade, M. T.

Osterholm, T. O'Toole, G. Parker, T. M. Perl, P. K. Russell, K. Tonat, and B. Working Group on Civilian. 2001. Tularemia as a biological weapon: medical and public health management. *JAMA* 285: 2763-2773.
99. Nauseef, W. M. 2007. Isolation of human neutrophils from venous blood. *Methods Mol Biol* 412: 15-20.
100. Klein, J. B., A. Buridi, P. Y. Coxon, M. J. Rane, T. Manning, R. Kettritz, and K. R. McLeish. 2001. Role of extracellular signal-regulated kinase and phosphatidylinositol 3-kinase in chemoattractant and LPS delay of constitutive neutrophil apoptosis. *Cell Signal* 13: 335-343.
101. Klein, J. B., M. J. Rane, J. A. Scherzer, P. Y. Coxon, R. Kettritz, J. M. Mathiesen, A. Buridi, and K. R. McLeish. 2000. Granulocyte-macrophage colony-stimulating factor delays neutrophil constitutive apoptosis through phosphoinositide 3-kinase and extracellular signal-regulated kinase pathways. *J Immunol* 164: 4286-4291.
102. Tsai, Y. R., Y. J. Wang, M. R. Lee, M. F. Hsu, and J. P. Wang. 2013. p38 Mitogen-activated protein kinase and extracellular signal-regulated kinase signaling pathways are not essential regulators of formyl peptide-stimulated p47(phox) activation in neutrophils. *Eur J Pharmacol* 701: 96-105.
103. Kinkead, L. C., L. C. Whitmore, J. M. McCracken, J. R. Fletcher, B. B. Ketelsen, J. W. Kaufman, B. D. Jones, D. S. Weiss, J. H. Barker, and L.-A. H. Allen. 2018. Bacterial lipoproteins and other factors released by Francisella tularensis modulate human neutrophil lifespan: Effects of a TLR1 SNP on apoptosis inhibition. *Cell Microbiol* 20: e12795.
104. Fortin, C. F., A. Cloutier, T. Ear, S. Sylvain-Prevost, T. Z. Mayer, R. Bouchelaghem, and P. P. McDonald. 2011. A class IA PI3K controls inflammatory cytokine production in human neutrophils. *Eur J Immunol* 41: 1709-1719.
105. Hawkins, P. T., L. R. Stephens, S. Suire, and M. Wilson. 2010. PI3K signaling in neutrophils. *Curr Top Microbiol Immunol* 346: 183-202.
106. Chen, D., X. Lin, C. Zhang, Z. Liu, Z. Chen, Z. Li, J. Wang, B. Li, Y. Hu, B. Dong, L. Shen, J. Ji, J. Gao, and X. Zhang. 2018. Dual PI3K/mTOR inhibitor BEZ235 as a promising therapeutic strategy against paclitaxel-resistant gastric cancer via targeting PI3K/Akt/mTOR pathway. *Cell Death Dis* 9: 123.
107. Vanhaesebroeck, B., S. J. Leevers, G. Panayotou, and M. D. Waterfield. 1997. Phosphoinositide 3-kinases: a conserved family of signal transducers. *Trends Biochem Sci* 22: 267-272.
108. Juss, J. K., R. P. Hayhoe, C. E. Owen, I. Bruce, S. R. Walmsley, A. S. Cowburn, S. Kulkarni, K. B. Boyle, L. Stephens, P. T. Hawkins, E. R. Chilvers, and A. M. Condliffe. 2012. Functional redundancy of class I phosphoinositide 3-kinase (PI3K) isoforms in signaling growth factor-mediated human neutrophil survival. *PLoS One* 7: e45933.
109. Zillikens, H., A. Kasprick, C. Osterloh, N. Gross, M. Radziewitz, C. Hass, V. Hartmann, M. Behnen-Harer, N. Ernst, K. Boch, G. Vidarsson, R. Visser, T. Laskay, X. Yu, F. Petersen, R. J. Ludwig, and K. Bieber. 2021. Topical Application of the PI3Kbeta-Selective Small Molecule Inhibitor TGX-221 Is an Effective Treatment Option for Experimental Epidermolysis Bullosa Acquisita. *Front Med* 8: 713312.
110. Sarker, D., J. E. Ang, R. Baird, R. Kristeleit, K. Shah, V. Moreno, P. A. Clarke, F. I. Raynaud, G. Levy, J. A. Ware, K. Mazina, R. Lin, J. Wu, J. Fredrickson, J. M. Spoerke, M. R. Lackner, Y. Yan, L. S. Friedman, S. B. Kaye, M. K. Derynck, P. Workman, and J.

S. de Bono. 2015. First-in-human phase I study of pictilisib (GDC-0941), a potent pan-class I phosphatidylinositol-3-kinase (PI3K) inhibitor, in patients with advanced solid tumors. *Clin Cancer Res* 21: 77-86.
111. Setti, A., M. J. Kumar, K. R. Babu, A. Rasagna, M. G. Prasanna, T. A. Devi, and S. C. Pawar. 2016. Potency and pharmacokinetics of broad spectrum and isoform-specific p110gamma and delta inhibitors in cancers. *J Recept Signal Transduct Res* 36: 26-36.
112. Chen, J., H. Tang, N. Hay, J. Xu, and R. D. Ye. 2010. Akt isoforms differentially regulate neutrophil functions. *Blood* 115: 4237-4246.
113. Yamaji, M., A. Ota, M. Wahiduzzaman, S. Karnan, T. Hyodo, H. Konishi, S. Tsuzuki, Y. Hosokawa, and M. Haniuda. 2017. Novel ATP-competitive Akt inhibitor afuresertib suppresses the proliferation of malignant pleural mesothelioma cells. *Cancer Med* 6: 2646-2659.
114. Johnson, J., Z. Chow, E. Lee, H. L. Weiss, B. M. Evers, and P. Rychahou. 2021. Role of AMPK and Akt in triple negative breast cancer lung colonization. *Neoplasia* 23: 429-438.
115. Will, M., A. C. Qin, W. Toy, Z. Yao, V. Rodrik-Outmezguine, C. Schneider, X. Huang, P. Monian, X. Jiang, E. de Stanchina, J. Baselga, N. Liu, S. Chandarlapaty, and N. Rosen. 2014. Rapid induction of apoptosis by PI3K inhibitors is dependent upon their transient inhibition of RAS-ERK signaling. *Cancer Discov* 4: 334-347.
116. Lawrence, T. 2009. The nuclear factor NF-kappaB pathway in inflammation. *Cold Spring Harb Perspect Biol* 1: a001651.
117. Tsai, J. J., P. J. Pan, and F. T. Hsu. 2017. Regorafenib induces extrinsic and intrinsic apoptosis through inhibition of ERK/NF-kappaB activation in hepatocellular carcinoma cells. *Oncol Rep* 37: 1036-1044.
118. Dyugovskaya, L., A. Polyakov, D. Ginsberg, P. Lavie, and L. Lavie. 2011. Molecular pathways of spontaneous and TNF-{alpha}-mediated neutrophil apoptosis under intermittent hypoxia. *Am J Respir Cell Mol Biol* 45: 154-162.
119. Klein, J. B., M. J. Rane, J. A. Scherzer, P. Y. Coxon, R. Kettriz, J. M. Mathiesen, P. VBirdid, and K. R. McLeish. 2000. Granulocyte-Macrophage Colony Stimulating Factor delays neutrophil constitutive apoptosis through phosphoinositide3-kinase and extracellular signal-regulated kinase pathways. *J Immunol* 164: 4286-4291.
120. Klein, J. B., A. Buridi, P. Y. Coxon, M. J. Rane, T. Manning, R. Kettriz, and K. R. McLeish. 2001. Role of extracellular signal-regulatd kinase and phosphatidylinositol 3-kinase in chemoattractant and LPS delay of constitutive neutrophil apoptosis. *Cell Signal* 13: 335-343.
121. Perianayagam, M. C., V. S. Balakrishnan, B. J. G. Pereira, and B. L. Jaber. 2004. C5a delays apoptosis of human neutrophils via an extracellular signal-regualted kinase and Bad-medicated signaling pathway. *Eur J Clin Invest* 34:50-56.
122. Allan, L. A., N. Morrice, S. Brady, G. Magee, S. Pathak, and P. R. Clarke. 2003. Inhibition of caspase-9 through phosphorylation at Thr 125 by ERK MAPK. *Nat Cell Biol* 5: 647-654.
123. Yan, B., M. Zemskova, S. Holder, V. Chin, A. Kraft, P. J. Koskinen, and M. Lilly. 2003. The PIM-2 kinase phosphorylates BAD on serine 112 and reverses BAD-induced cell death. *J Biol Chem* 278: 45358-45367.
124. Luo, H. R., and F. Loison. 2008. Constitutive neutrophil apoptosis: Mechanisms and regulation. *Am. J. Hematol.* 83: 288-295.

125. Frasch, S. C., J. A. Nick, V. A. Fadok, D. B. Bratton, G. S. Worthen, and P. M. Henson. 1998. p38 mitogen-activated protein kinase-dependent and independent intracellular signal transduction pathways leading to apoptosis in human neutrophils. . *J Biol Chem* 273: 8389-8397.
126. Allaeys, I., I. Gymninova, C. Canet-Jourdan, and P. E. Poubelle. 2014. IL-32gamma delays spontaneous apoptosis of human neutrophils through MCL-1, regulated primarily by the p38 MAPK pathway. *PLoS One* 9: e109256.
127. Saffar, A. S., S. Dragon, P. Ezzati, L. Shan, and A. S. Gounni. 2008. Phosphatidylinositol 3-kinase and p38 mitogen-activated protein kinase regulate induction of Mcl-1 and survival in glucocorticoid-treated human neutrophils. *J Allergy Clin Immunol* 121: 492-498 e410.
128. Alvarado-Kristensson, M., F. Melander, K. Leandersson, L. Ronnstrand, C. Wernstedt, and T. Andersson. 2004. p38-MAPK signals survival by phosphorylation of caspase-8 and caspase-3 in human neutrophils. *J Exp Med* 199: 449-458.
129. Rayasam, G. V., V. K. Tulasi, R. Sodhi, J. A. Davis, and A. Ray. 2009. Glycogen synthase kinase 3: more than a namesake. *Br J Pharmacol* 156: 885-898.
130. Schuster, D. P., S. L. Brody, Z. Zhou, M. Bernstein, R. Arch, D. Link, and M. Mueckler. 2007. Regulation of lipopolysaccharide-induced increases in neutrophil glucose uptake. *Am J Physiol Lung Cell Mol Physiol* 292: L845-L851.
131. Novellasdemunt, L., L. Bultot, A. Manzano, F. Ventura, J. L. Rosa, D. Vertommen, M. H. Rider, A. Navarro-Sabate, and R. Bartrons. 2013. PFKFB3 activation in cancer cells by the p38/MK2 pathway in response to stress stimuli. *Biochem J* 452: 531-543.
132. Zhu, D., H. Hattori, H. Jo, Y. Jia, K. K. Subramanian, F. Loison, J. You, Y. Le, M. Honczarenko, L. Silberstein, and H. R. Luo. 2006. Deactivation of phosphatidylinositol 3,4,5-trisphosphate/Akt signaling mediates neutrophil spontaneous death. *Proc Natl Acad Sci U S A* 103: 14836-14841.
133. Runman, M., K. H. Jung, Z. Fang, Y. H.H., M. K. Son, S. J. Kim, J. Kim, J. H. Park, J. H. Sim, S. Hong, and A.-S. Hong. 2016. HS-173, a novel PI3K inhibitor suppresses EMT and metastasis in pancreatic cancer. *Oncotarget* 7: 78029-78047.
134. Landry, M. R., A. N. DuRoss, M. J. Neufeld, L. Hahn, G. Sahay, R. Luxenhofer, and C. Sun. 2020. Low dose novel PARP-PI3K inhibition via nanoformulation improves colorectal cancer immunoradiotherapy. *Mater Today Bio* 8: 100082.
135. Lee, H., K. H. Jung, Y. Jeong, S. Hong, and S. S. Hong. 2013. HS-173, a novel phosphatidylinositol 3-kinase (PI3K) inhibitor, has anti-tumor activity through promoting apoptosis and inhibiting angiogenesis. *Cancer Lett* 328: 152-159.
136. Rane, M. J., and J. B. Klein. 2009. Regulatio of neutropil apoptosis by modulation of PKB/Akt activation. *Front. Biosci.* 14: 2400-2412.
137. Fan, Y. H., W. Li, D. D. Liu, M. X. Bai, H. R. Song, Y. N. Xu, S. Lee, Z. P. Zhou, J. Wang, and H. W. Ding. 2017. Design, synthesis, and biological evaluation of novel 3-substituted imidazo[1,2-a]pyridine and quinazolin-4(3H)-one derivatives as PI3Kalpha inhibitors. *Eur J Med Chem* 139: 95-106.
138. Cramer, T., Y. Yamanishi, B. E. Clausen, I. Forster, R. Pawlinski, N. Machkman, V. H. Haase, R. Jaenisch, M. Corr, V. Nizet, G. S. Firestein, H.-P. Gerber, N. Ferrara, and R. S. Johnson. 2003. HIF-1alpha is essential for myeloid cell-mediated inflammation. *Cell* 112: 645-657.

139. Sarkar, A., E. Aga, U. Bussmeyer, A. Bhattacharyya, S. Moller, L. Hellberg, M. Behnen, W. Solbach, and T. Laskay. 2013. Infection of neutrophil granulocytes with Leishmania major activates ERK 1/2 and modulates multiple apoptotic pathways to inhibit apoptosis. *Med Microbiol Immunol* 202: 25-35.
140. Himpe, E., C. Degaillier, A. Coppens, and R. Kooijman. 2008. Insulin-like growth factor-1 delays Fas-mediated apoptosis in human neutrophils through the phosphatidylinositol-3 kinase pathway. *J Endocrinol* 199: 69-80.
141. Dan, H. C., M. Sun, S. Kaneko, R. I. Feldman, S. V. Nicosia, H. G. Wang, B. K. Tsang, and J. Q. Cheng. 2004. Akt phosphorylation and stabilization of X-linked inhibitor of apoptosis protein (XIAP). *J Biol Chem* 279: 5405-5412.
142. Datta, S. R., H. Dudek, X. Tao, S. Masters, H. Fu, Y. Gotoh, and M. E. Greenberg. 1997. Akt phosphorylation of BAD couples survival signals to the cell-intrinsic death machinery. *Cell* 91: 231-241.
143. Gardai, S. J., D. A. Hildeman, S. K. Frankel, B. B. Whitlock, S. C. Frasch, N. Borregaard, P. Marrack, D. L. Bratton, and P. M. Henson. 2004. Phosphorylation of Bax Ser184 by Akt regulates its activity and apoptosis in neutrophils. *J Biol Chem* 279: 21085-21095.
144. Takahashi, R., Q. Deveraux, I. Tamm, K. Welsh, N. Assa-Munt, G. S. Salvesen, and J. C. Reed. 1998. A single BIR domain of XIAP sufficient for inhibiting caspases. *J Biol Chem* 273: 7787-7790.
145. Diaz-Meco, M. T., and J. Moscat. 2012. The atypical PKCs in inflammation: NF-kappaB and beyond. *Immunol Rev* 246: 154-167.
146. Park, J. W., H. P. Kim, S. J. Lee, X. Wang, Y. Wang, E. Ifedigbo, S. C. Watkins, M. Ohba, S. W. Ryter, Y. M. Vyas, and A. M. Choi. 2008. Protein kinase C alpha and zeta differentially regulate death-inducing signaling complex formation in cigarette smoke extract-induced apoptosis. *J Immunol* 180: 4668-4678.
147. Christian, F., E. L. Smith, and R. J. Carmody. 2016. The Regulation of NF-kappaB Subunits by Phosphorylation. *Cells* 5:1-12.
148. Hoffman, B., and D. A. Liebermann. 2009. Gadd45 modulation of intrinsic and extrinsic stress responses in myeloid cells. *J Cell Physiol* 218: 26-31.
149. Allen, L.-A. H. 2013. Neutrophils: potential therapeutic targets in tularemia? *Frontiers in cellular and infection microbiology* 3: 109.
150. Francois, S., J. El Benna, P. M. C. Dang, E. Pedruzzi, M.-A. Gougerot-Pocidalo, and C. Elbim. 2005. Inhibition of Neutrophil Apoptosis by TLR Agonists in Whole Blood: Involvement of the Phosphoinositide 3-Kinase/Akt and NF-{kappa}B Signaling Pathways, Leading to Increased Levels of Mcl-1, A1, and Phosphorylated Bad. *J. Immunol.* 174: 3633-3642.
151. Nauseef, W. M., and N. Borregaard. 2014. Neutrophils at work. *Nat Immunol* 15: 602-611.
152. Morner, T. 1992. The ecology of tularaemia. *Rev Sci Tech* 11: 1123-1130.
153. Kinkead, L. C., and L. A. Allen. 2016. Multifaceted effects of Francisella tularensis on human neutrophil function and lifespan. *Immunol Rev* 273: 266-281.
154. McElvaney, O. J., N. L. McEvoy, O. F. McElvaney, T. P. Carroll, M. P. Murphy, D. M. Dunlea, O. Ni Choileain, J. Clarke, E. O'Connor, G. Hogan, D. Ryan, I. Sulaiman, C. Gunaratnam, P. Branagan, M. E. O'Brien, R. K. Morgan, R. W. Costello, K. Hurley, S. Walsh, E. de Barra, C. McNally, S. McConkey, F. Boland, S. Galvin, F. Kiernan, J.

O'Rourke, R. Dwyer, M. Power, P. Geoghegan, C. Larkin, R. A. O'Leary, J. Freeman, A. Gaffney, B. Marsh, G. F. Curley, and N. G. McElvaney. 2020. Characterization of the Inflammatory Response to Severe COVID-19 Illness. *Am J Respir Crit Care Med* 202: 812-821.

155. McCracken, J. M., L. C. Kinkead, R. L. McCaffrey, and L. A. Allen. 2016. Francisella tularensis Modulates a Distinct Subset of Regulatory Factors and Sustains Mitochondrial Integrity to Impair Human Neutrophil Apoptosis. *J Innate Immun* 8: 299-313.
156. Berridge, M. V., and A. S. Tan. 1995. Interleukin-3 facilitates glucose transport in a myeloid cell line by regulating the affinity of the glucose transporter for glucose: involvement of protein phosphorylation in transporter activation. *Biochem J* 305 (Pt 3): 843-851.
157. Maratou, E., G. Dimitriadis, A. Kollias, E. Boutati, V. Lambadiari, P. Mitrou, and S. A. Raptis. 2007. Glucose transporter expression on the plasma membrane of resting and activated white blood cells. *Eur J Clin Invest* 37: 282-290.
158. Wick, A. N., D. R. Drury, H. I. Nakada, and J. B. Wolfe. 1957. Localization of the primary metabolic block produced by 2-deoxyglucose. *J Biol Chem* 224: 963-969.
159. Xintaropoulou, C., C. Ward, A. Wise, H. Marston, A. Turnbull, and S. P. Langdon. 2015. A comparative analysis of inhibitors of the glycolysis pathway in breast and ovarian cancer cell line models. *Oncotarget* 6: 25677-25695.
160. Liu, Y., Y. Cao, W. Zhang, S. Bergmeier, Y. Qian, H. Akbar, R. Colvin, J. Ding, L. Tong, S. Wu, J. Hines, and X. Chen. 2012. A small-molecule inhibitor of glucose transporter 1 downregulates glycolysis, induces cell-cycle arrest, and inhibits cancer cell growth in vitro and in vivo. *Mol Cancer Ther* 11: 1672-1682.
161. Arion, W. J., W. K. Canfield, F. C. Ramos, P. W. Schindler, H. J. Burger, H. Hemmerle, G. Schubert, P. Below, and A. W. Herling. 1997. Chlorogenic acid and hydroxynitrobenzaldehyde: new inhibitors of hepatic glucose 6-phosphatase. *Arch Biochem Biophys* 339: 315-322.
162. Martin, W. H., D. J. Hoover, S. J. Armento, I. A. Stock, R. K. McPherson, D. E. Danley, R. W. Stevenson, E. J. Barrett, and J. L. Treadway. 1998. Discovery of a human liver glycogen phosphorylase inhibitor that lowers blood glucose in vivo. *Proc Natl Acad Sci U S A* 95: 1776-1781.
163. Keoni, C. L., and T. L. Brown. 2015. Inhibition of Apoptosis and Efficacy of Pan Caspase Inhibitor, Q-VD-OPh, in Models of Human Disease. *J Cell Death* 8: 1-7.
164. Ratter, J. M., H. M. M. Rooijackers, G. J. Hooiveld, A. G. M. Hijmans, B. E. de Galan, C. J. Tack, and R. Stienstra. 2018. In vitro and in vivo Effects of Lactate on Metabolism and Cytokine Production of Human Primary PBMCs and Monocytes. *Front. Immunol.* 9: 2564.
165. Scott, R. B. 1968. Glycogen in human peripheral blood leukocytes. I. Characteristics of the synthesis and turnover of glycogen in vitro. *J. Clin. Invest.* 47: 344-352.
166. Healy, D. A., R. W. Watson, and P. Newsholme. 2002. Glucose, but not glutamine, protects against spontaneous and anti-Fas antibody-induced apoptosis in human neutrophils. *Clin Sci (Lond)* 103: 179-189.
167. Barot, S., E. M. Abo-Ali, D. L. Zhou, C. Palaguachi, and V. V. Dukhande. 2019. Inhibition of glycogen catabolism induces intrinsic apoptosis and augments multikinase inhibitors in hepatocellular carcinoma cells. *Exp Cell Res* 381: 288-300.

168. Pastorino, J. G., and J. B. Hoek. 2008. Regulation of hexokinase binding to VDAC. *J. Bioenerg. Biomembr.* 40: 171-182.
169. Lauterwasser, J., F. Fimm-Todt, A. Oelgeklaus, A. Schreiner, K. Funk, H. Falquez-Medina, R. Klesse, G. Jahreis, R. M. Zerbes, K. O'Neill, M. van der Laan, X. Luo, and F. Edlich. 2021. Hexokinases inhibit death receptor-dependent apoptosis on the mitochondria. *Proc. Natl. Acad. Sci. USA* 118: e2021175118.
170. Puckett, D. L., M. Alquraishi, W. Chowanadisai, and A. Bettaieb. 2021. The Role of PKM2 in Metabolic Reprogramming: Insights into the Regulatory Roles of Non-Coding RNAs. *Int. J. Mol. Sci.* 22: 1171.
171. Liang, J., R. Cao, X. Wang, Y. Zhang, P. Wang, H. Gao, C. Li, F. Yang, R. Zeng, P. Wei, D. Li, W. Li, and W. Yang. 2017. Mitochondrial PKM2 regulates oxidative stress-induced apoptosis by stabilizing Bcl2. *Cell Res.* 27: 329-351.
172. Gu, J., X. Li, L. Zhao, Y. Yang, C. Xue, Y. Gao, J. Li, Q. Han, Z. Sun, C. Bai, and R. C. Zhao. 2021. The role of PKM2 nuclear translocation in the constant activation of the NF-kappaB signaling pathway in cancer-associated fibroblasts. *Cell Death Dis.* 12: 291.
173. Pradelli, L. A., E. Villa, B. Zunino, S. Marchetti, and J. E. Ricci. 2014. Glucose metabolism is inhibited by caspases upon the induction of apoptosis. *Cell Death Dis.* 5: e1406.
174. Brooks, G. A. 2020. Lactate as a fulcrum of metabolism. *Redox Biol.* 35: 101454.
175. Leuzzi, R., G. Banhegyi, T. Kardon, P. Marcolongo, P. L. Capecchi, H. J. Burger, A. Benedetti, and R. Fulceri. 2003. Inhibition of microsomal glucose-6-phosphate transport in human neutrophils results in apoptosis: a potential explanation for neutrophil dysfunction in glycogen storage disease type 1b. *Blood* 101: 2381-2387.
176. Veiga-da-Cunha, M., N. Chevalier, X. Stephenne, J. P. Defour, N. Paczia, A. Ferster, Y. Achouri, J. P. Dewulf, C. L. Linster, G. T. Bommer, and E. Van Schaftingen. 2019. Failure to eliminate a phosphorylated glucose analog leads to neutropenia in patients with G6PT and G6PC3 deficiency. *Proc. Natl. Acad. Sci., USA* 116: 1241-1250.
177. Borjesson, D. L., S. D. Kobayashi, A. R. Whitney, J. M. Voyich, C. M. Argue, and F. R. Deleo. 2005. Insights into pathogen immune evasion mechanisms: Anaplasma phagocytophilum fails to induce an apoptosis differentiation program in human neutrophils. *J Immunol* 174: 6364-6372.
178. Simons, M. P., W. M. Nauseef, T. S. Griffith, and M. A. Apicella. 2006. Neisseria gonorrhoeae delays the onset of apoptosis in polymorphonuclear leukocytes. *Cell Microbiol* 8: 1780-1790.
179. Miralda, I., A. Vashishta, M. N. Rogers, E. C. Rouchka, X. Li, S. Waigel, R. J. Lamont, and S. M. Uriarte. 2020. Whole Transcriptome Analysis Reveals That Filifactor alocis Modulates TNFalpha-Stimulated MAPK Activation in Human Neutrophils. *Front Immunol* 11: 497.
180. Price, C. T. D., H. E. Hanford, A. Vashishta, M. Ozanic, M. Santic, S. Uriarte, and Y. A. Kwaik. 2021. Dot/Icm-Dependent Restriction of Legionella pneumophila within Neutrophils. *mBio* 12: e0100821.
181. Wyatt, E. V., K. Diaz, A. J. Griffin, J. A. Rasmussen, D. D. Crane, B. D. Jones, and C. M. Bosio. 2016. Metabolic Reprogramming of Host Cells by Virulent Francisella tularensis for Optimal Replication and Modulation of Inflammation. *J Immunol* 196: 4227-4236.

182. Cho, C., A. Teghanemt, M. A. Apicella, and W. M. Nauseef. 2020. Modulation of phagocytosis-induced cell death of human neutrophils by Neisseria gonorrhoeae. *J Leukoc Biol* 108: 1543-1553.
183. de Kleijn, S., M. Kox, I. E. Sama, J. Pillay, A. van Diepen, M. A. Huijnen, J. G. van der Hoeven, G. Ferwerda, P. W. Hermans, and P. Pickkers. 2012. Transcriptome kinetics of circulating neutrophils during human experimental endotoxemia. *PLoS One* 7: e38255.
184. Hu, H., A. Juvekar, C. A. Lyssiotis, E. C. Lien, J. G. Albeck, D. Oh, G. Varma, Y. P. Hung, S. Ullas, J. Lauring, P. Seth, M. R. Lundquist, D. R. Tolan, A. K. Grant, D. J. Needleman, J. M. Asara, L. C. Cantley, and G. M. Wulf. 2016. Phosphoinositide 3-Kinase Regulates Glycolysis through Mobilization of Aldolase from the Actin Cytoskeleton. *Cell* 164: 433-446.
185. Ozinsky, A., D. M. Underhill, J. D. Fontenot, A. M. Hajjar, K. D. Smith, C. B. Wilson, L. Schroeder, and A. Aderem. 2000. The repertoire for pattern recognition of pathogens by the innate immune system is defined by cooperation between toll-like receptors. *Proc Natl Acad Sci U S A* 97: 13766-13771.